# Divergence in polymerization induced by conjugate substitution of α-(substituted methyl)acrylates

Doctoral Dissertation

(Shinshu University)

March 2021

**Keito Hagiwara**

# Contents

*Chapter 1*

# General Introduction

## *Prolegomenon*

Polymerization is a repeat of elemental reactions in numerous times. If an elemental reaction contains some side reactions, propagation of polymer chains should be terminated to lead low degree of polymerization; even if the propagation was not interrupted, side reactions should cause structural errors in repeating units. Therefore, quantitative, selective and robust reactions are necessary as an elemental reaction in polymerization. In fact, typical polymerizations are composed of well-controlled reactions, e.g., addition to vinyl group, acyl substitution, nucleophilic aromatic substitution, ring-opening of epoxides, and addition of cumulated double bond.

Since the first practical polycondensation have been developed by Carothers,[1a] polymerizations, particularly step-growth polymerizations, are performed so as to afford one distinct polymer from one monomer or one pair of monomers. In other words, monomer design unambiguously means polymer design. On the other hand, nature give a variety of polymers from a single monomer; for example, amylose, pullulan and dextran are derived from α-glucose.[2] Such diversity in the resulting polymers is provided by the controls of reacting points of α-glucose by enzymes. This natural molecular strategy, *i.e.* polymerization design from single monomer to various polymer, seems more efficient than that in current typical polymer engineering. Thus, such molecular strategy has been investigated in the past decades, and some examples in certain chain polymerizations achieved it, e.g., stereospecific polymerization of vinyl monomers,[3] cyclopolymerization/asymmetric polymerization of divinyl monomers,[4] and polymerization of bifunctional cyclic monomers in multiple modes.[5] However, the molecular strategy has been scarcely applied to step-growth polymerizations, although they are common reaction in nature.

Therefore, step-growth polymerizations leading to a diversity of resulting polymers are expected to open a new field of polymer chemistry as that found in nature. In order to study this concept, exploring of new elemental reaction is an issue to be addressed; as mentioned at the front, common elemental reactions in step-growth polymerization have been selected to avoid any side reactions yielding a single product. Thus, these elemental reactions are not suitable to develop the diversity in step-growth polymerizations. For this

reason, this thesis has focused on conjugate substitution reaction of α-(substituted methyl)acrylate.

In this chapter, the background of this thesis on ***elemental reaction of step-growth polymerization*** and ***conjugate substitution reaction*** are described. Then, the concept and purpose of the research is presented.

# 1. Elemental Reactions of Step-Growth Polymerization

## *1.1 Demands for Elemental Reactions*

In polycondensation, a typical example of step-growth polymerization, two monomer molecules react each other to provide dimers in the initial stage of the reaction; the dimers grow up to trimer or tetramer, and further coupling reaction of the resulting oligomers follows to afford macromolecules. Flory–Carothers theory[1] statistically explains polycondensation on the hypothesis that all reactive groups in monomers, oligomers and polymers have equal reactivity and that cyclization reaction can be ignored. According to this theory, a number-averaged degree of polymerization ($\bar{X}_\mathrm{n}$) is given as follows;

$$\bar{X}_\mathrm{n} = \frac{1+r}{2r(1-p)+(1-r)} \qquad \text{(eq 1)}$$

Here, $r$ is balance of nucleophilic and electrophilic reactive groups ($r < 1$), and $p$ is fractional monomer conversion. Given $r = 1$, eq 1 can be converted as follows:

$$\bar{X}_\mathrm{n} = \frac{1}{1-p} \qquad \text{(eq 2)}$$

This equation indicates that the elemental reaction must proceed quantitatively to generate polymers with high degree of polymerization. When 90% of the reactive groups are consumed ($p = 0.9$), $\bar{X}_\mathrm{n}$ is 10. Even if 99% of reactive groups consumed ($p = 0.99$), the expectable $\bar{X}_\mathrm{n}$ was only $100$. Thus, strictly quantitative conversion of elemental

reaction and an absence of any side reactions are required in polycondensation.

In practice, polycondensation suffer from other limitations. For example, the solubility of monomers and polymers restricts applicable solvents, although organic reactions are often influenced on solvation. Increased viscosity by polymer products can decrease reaction rate and prevent chain-growth. High temperature is possible to cause thermal degradation of monomers and polymers. These issues should be considered for design of polycondensation.

### *1.2 Elemental Reactions in Step-growth Polymerization*

As described above, the demands for elemental reaction in polycondensation limits the applicable candidates. Reaction controls by external manipulation, e.g. vacuuming to remove liberated byproducts, are alternative way to overcome these limitations. In fact, polyesters by transesterification or direct polymerization of dicarboxylic esters/acids and diols are industrially produced under high-vacuum at higher than 300 °C. However, polycondensation in nature does not require such external controls, and polymerization under ambient condition is convenient in practical use. Thus, this thesis focuses on polycondensation without such external controls.[6]

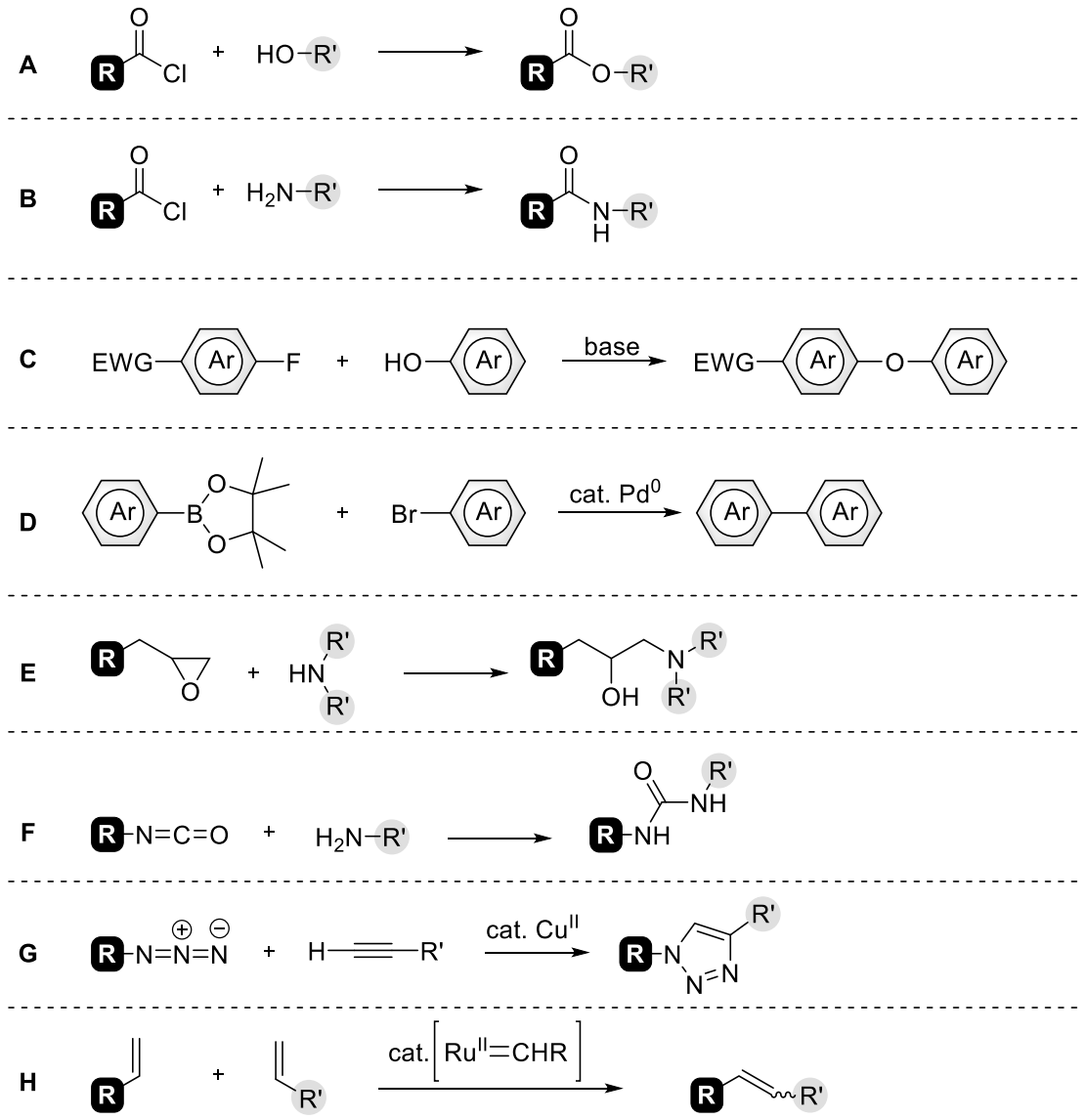


**Scheme 1-1.** Typical organic reactions used in step-growth polymerization. Nucleophilic acyl substitution (**A/B**), aromatic nucleophilic substitution (**C**), aromatic cross-coupling reaction (**D**), ring-opening of epoxides (**E**), nucleophilic addition to isocyanates (**F**), 1,3-dipol cycloaddition (**G**) and olefine metathesis reaction catalyzed by ruthenium carbene complex (**H**).

**Scheme 1-1** shows typical elemental reactions in step-growth polymerization. For quantitative and selective conversion, acyl substitution (**A**, **B**) for polyesters, polyamides and polycarbonates,[7] nucleophilic aromatic substitution (**C**) for aromatic polyethers and polysulfides,[8] and aromatic cross-coupling reactions for conjugated polymers[9] are employed. Among them, cross-coupling reaction often suffers from relatively low degree of polymerization owing to the unperfect conversions and precipitation of the resulting

polymers. Addition reactions of epoxides (**E**) and isocyanates (**F**) are also quantitative and effective to prepare polyamines/polyethers and polyureas/polyurethanes, respectively.[10] Since Sharpless introduce the concept of click chemistry,[11] a molecular strategy by organic reactions in quantitative yields without any side reactions not required purification process and applicable under ambient condition, 1,3-dipol cycloaddition reaction (**G**) such as copper-catalyzed azide-alkyne cycloaddition (CuAAC) reaction have gains researchers' attention in polymer chemistry.[12] Nowadays, many reports are available on polyaddition by click chemistry. Olefin metathesis reactions by Grubbs' catalyst (**H**) is also a new class of elemental reaction in polycondensation.[13]

Although these reactions are applicable in step-growth polymerization, the number of reactions is extremely confined, comparing that in organic synthesis. This barrier is a significant problem to produce new types of condensation polymer.

### *1.3 Monomer Design in Polycondensation*

Flory–Carothers theory is based on the hypothesis that the reactivity of reactive groups does not change over the reaction. In practical, however, the reactivity of functional groups is often influenced by the substituents; for example, terephthaloyl chloride exhibits higher electrophilicity than its monoester. In such case, polymerization does not obey Flory–Carothers theory and optimization of feeding ratio of monomers ($r$) are required to achieve high degree of polymerization.

In order to avoid such errors from the theory, a long spacer separating two reactive groups are often incorporated into monomers (AA+BB type polycondensation; **Scheme 1-2**). For a long time, this design strategy has not been reconsidered as long as some technical problems are found. However, the author claims that the classical strategy encounters significant issues: (A) As spacers occupy a large composition in backbone structure, polymer properties and functions are often dominated by the spacers. (B) The use of large carbon chains is contrary to the modern molecular strategy aiming reduces of carbon atoms. (C) The strategy may prevent the emergence of new polymerization design completely different from the classical polycondensation. In the next section, some

examples challenging to propose new monomer and polymerization designs with removing spacers are introduced.

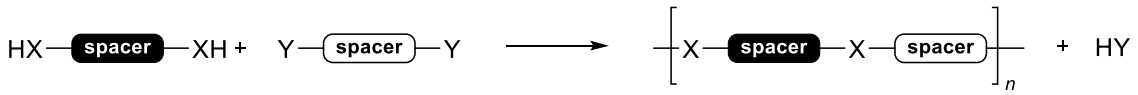


**Scheme 1-2.** AA+BB type polycondensation.

## *1.4 Challenges toward Novel Design of Polycondensation*

*Nonstoichiometric polycondensation*

As described by Flory–Carothers theory, degree of polymerization in polycondensation is generally dependent on the feeding ratio of reactive groups (*r*). On the other hand, some monomer design enables to elude the law, leading to polymerization under non-stoichiometry.[14] The first example has been reported by Takata and Endo for the polycondensation of dichloromethane derivatives **1-1** and bisphenol A (**1-2**); since the intermediate **1-3** exhibited 27-folds higher reactivity against the nucleophile than the **1-1**, high molecular weight was achieved even excess **1-1** was used (**Scheme 1-3**). The nonstoichiometric polymerization was thus attributed to the dichloromethane monomer that did not contain any spacer separating two chlorine atoms. Recently, nonstoichiometric polymerization was also reported for polycondensation by Friedel-Crafts reaction, using the change of electron density of aromatic rings.[15]

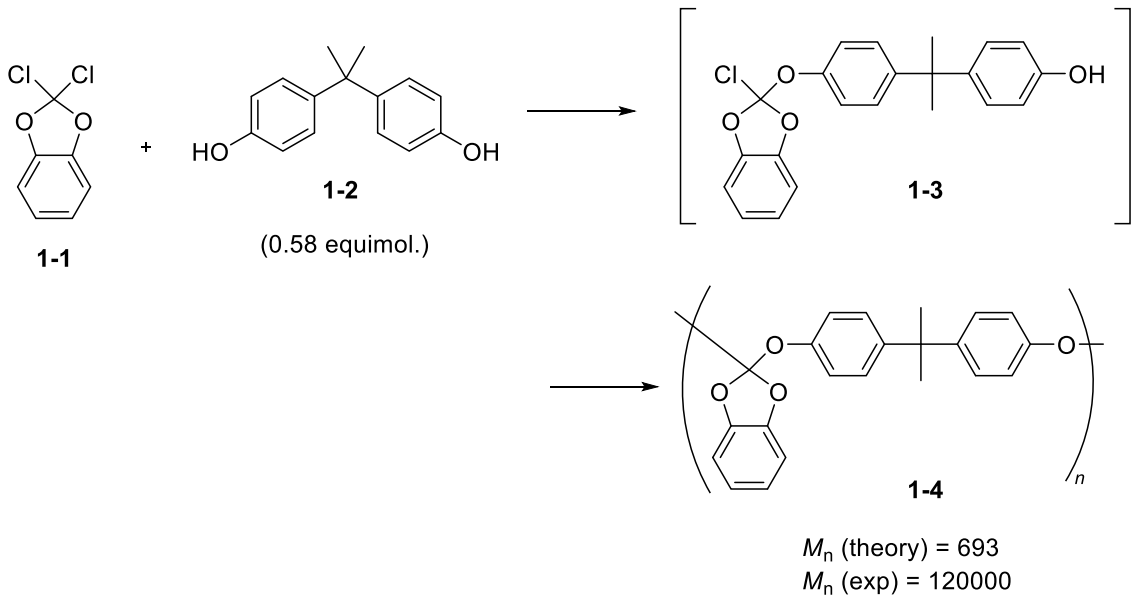


**Scheme 1-3.** Nonstoichiometric polycondensation reported by Takata and Endo.[14b]

*Chain-growth polycondensation*

The Flory-Carothers theory[1] predicts the degree of dispersity in molecular weight ($Đ$, $M_w/M_n$), or polydispersity index (PDI) in an old term, should be 2 at the full conversion of reactive groups. Therefore, a narrow molecular weight distribution is impossible in common polycondensation.

The Flory-Carothers theory is based on a premise that there are no differences in the reactivity of monomers and growing polymer chains. Therefore, if the premise can be broken by designing monomers, polycondensation with completely different behavior from the theory can be achieved. For example, in the polymerization of 4-halothiophenoxide and oxidative polymerization of phenols,[16] the substituent effects on aromatic rings increase the reactivity of growing polymer chains from the monomers, resulting in a polycondensations by chain-growth mechanism. In 2000, Yokozawa *et al.* has reported the first chain-growth polycondensation affording narrow molecular weight distribution by a sophisticated monomer design.[17] The polycondensation of phenyl 4-aminobenzoate proceeded in chain-growth mechanism by similar substituent effects of aromatic rings (**Scheme 1-4**).[17a] In this polymerization, the strong electron-donation of amide anions decreases the reactivity of phenyl ester **1-6** and suppresses the monomer coupling. The initiator **1-7** reacts with a monomer **1-6** to yield an amide intermediate **1-**

**8**, which exhibits higher reactivity than **1-6** due to the less electron-donation of the formed amide bond. That is, the intermediate **1-8** has an activated phenyl ester. The amide anion of the monomer **1-6** can react only with the activated ester at the chain-end, providing chain-growth polymerization.

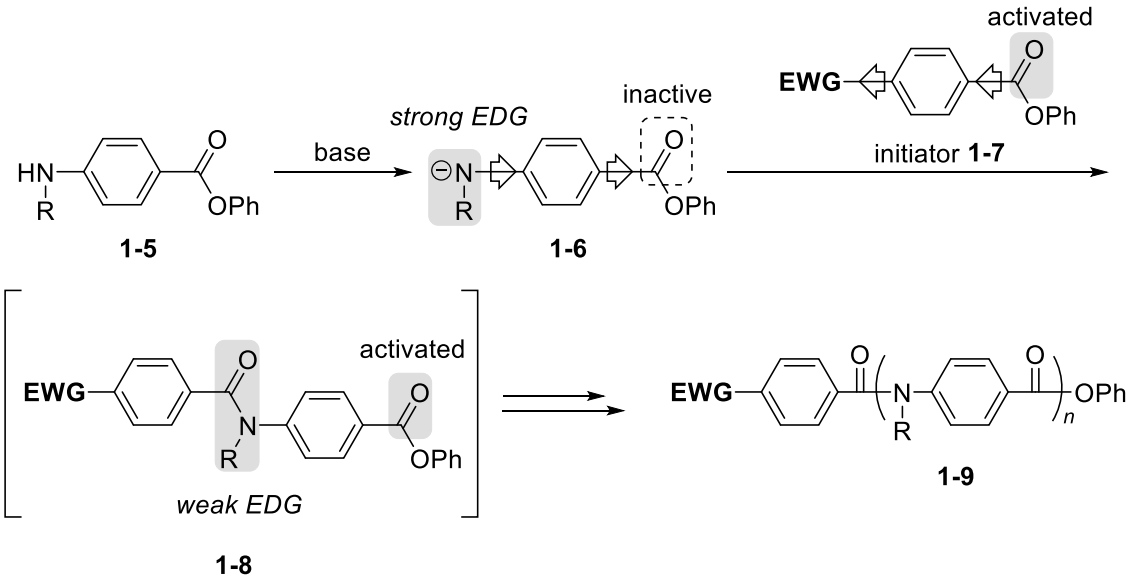


**Scheme 1-4.** Chain-growth polycondensation of phenyl 4-aminobenzoate. EDG: Electron-donating group, EWG: Electron-withdrawing group.[17a]

*Multicomponent polycondensation*

Multicomponent reaction (MCR) is a molecular strategy to combine three- or four-components without isolating any intermediates. Recently, polycondensation by MCRs have gained much attention from the benefit as a straightforward procedure, high atom economy as well as structural diversity of resulting polymers.[18] The most important MCRs in organic chemistry are the isocyanide-based MCRs, namely Passerini three-component and Ugi four-component reactions (**Scheme 1-5A**).[19] First Passerini polyaddition using a dicarboxylic acid and a dialdehyde in combination with various isocyanides was reported in 2011 (**Scheme 1-5B**).[20a] In this polymerization, a polyester bearing amide pendants was obtained. Similarly, Ugi polycondensation affording polyamides was also reported in 2014 (**Scheme 1-5C**).[20b] These polymerizations which different from general design achieved simultaneous construction of main and side chain in one-pot system. Nowadays, MCRs are applied to prepare sequence-controlled polymer,[20c] biocompatible adhesions,[20d] and aggregation-induced emission materials.[20e]

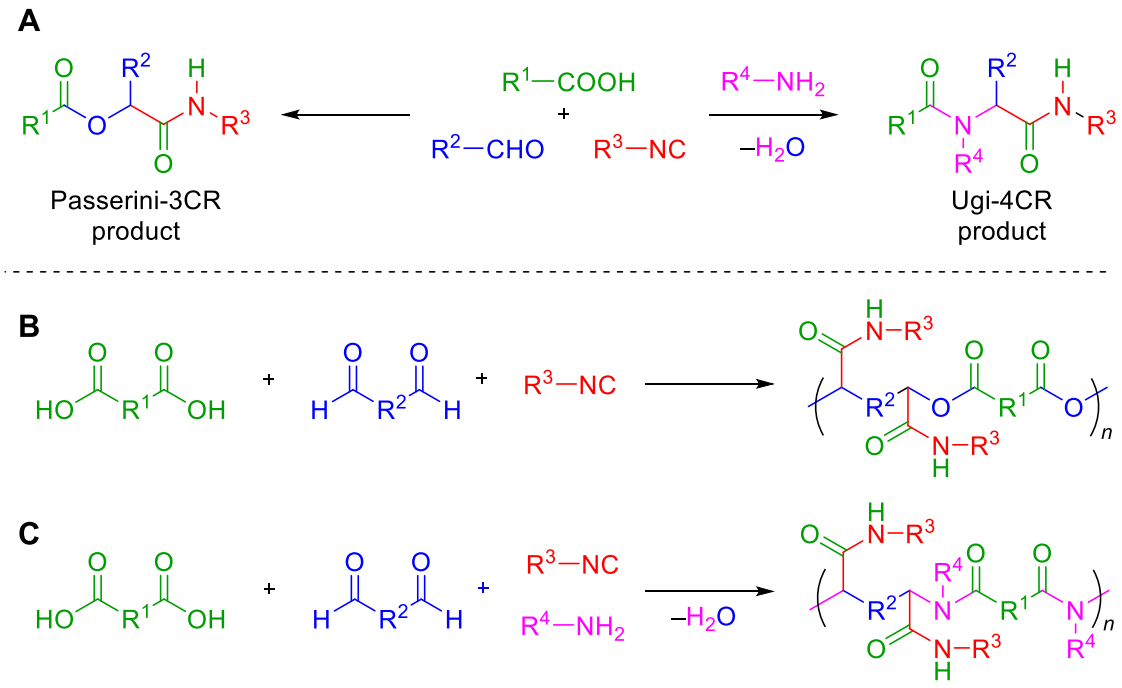


**Scheme 1-5.** Multicomponent reactions and polymerization.

The recent trends in polymer chemistry described as above examples suggest that monomer design is a key to break the limitations provided by the Flory-Carothers theory. In this thesis, therefore, monomer design for utilizing conjugate substitution reaction is studied. In the next section, chemistry on conjugate substitution is presented.

## 2. Nucleophilic Conjugate Substitution Reaction of Allyl Compound

Nucleophilic substitution reactions have an integral role in organic synthesis; substitution with nucleophiles containing heteroatoms such as hydroxide, cyanide, azide and hydrosulfide are typical reaction to incorporate functional groups, whereas those with enolates, Grignard reagents, alkyllithiums and other metalorganic reagents are often employed to extend carbon chains.

Allyl compounds **1-10** are known as efficient substrates for nucleophilic substitution in $S_N1$ (elimination–addition) and $S_N2$ (direct substitution) mechanisms (**Scheme 1-6**). In addition, allylic compounds undergo the third mechanism, $S_N2'$ (addition–elimination) reaction.

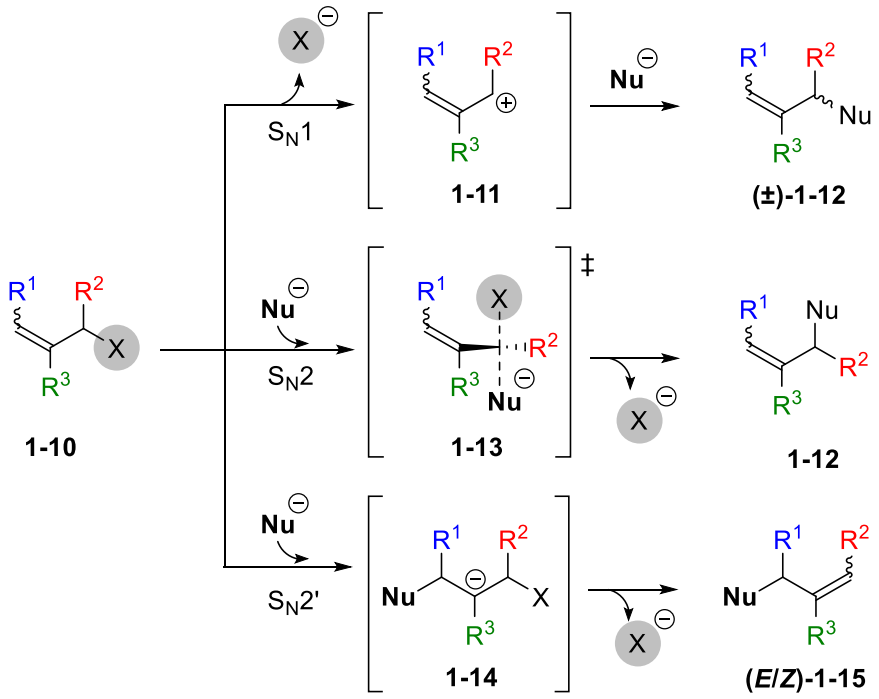


**Scheme 1-6.** Nucleophilic substitution reactions of allyl compounds.

### *2.1 Conjugate Substitution*

Nucleophilic substitution of allyl halides **1-10** occurs through two pathways: $S_N2$ process composed of the attack of a nucleophile to the allylic carbon, and $S_N2'$ process

by the addition of a nucleophile to vinyl group and the subsequent regeneration of double bond, following the elimination of halogen atom (**Scheme 1-6**).[21] Notably, these processes are competitive to afford a pair of isomeric products, **1-12** and **1-15**; the two processes gives a single product if $R^1$ and $R^2$ are same substituents. The substituents, $R^1$ and $R^2$, influences the selectivity of two processes.[22] Substituent $R^1$ prevents a nucleophilic addition to vinyl group due to the steric hindrance, leading to dominative $S_N2$ process to afford product **1-12**. On the other hand, substituent $R^2$ interrupts $S_N2$ attack and enhances $S_N2$' process to yield $S_N2$' product **1-15**. The selectivity of $S_N2$/$S_N2$' processes are also influenced by other factors. $S_N2$' reaction become dominative for large nucleophiles due to the expense of $S_N2$ reaction.[22] In certain cases, the leaving groups X affect the selectivity.[23] Polar solvents favor $S_N2$' mechanism.[24]

## ***2.2 Effects of Electron-withdrawing Group***

Allyl halides **1-16**, bearing electron-withdrawing groups (EWGs), *e.g.* α-(halomethyl)acrylates and α-(halomethyl)acrylonitriles, have electron-poor vinyl groups to enhance the selectivity of the $S_N2$' process (**Scheme 1-7**).[25] Due to the strong electrophilicity of the electron-poor double bond, the $S_N2$' reaction proceeds with the various nucleophile such as carbon nucleophiles,[26] hydride,[27] amines,[28] carboxylates,[28] thiols[28] and phenols[28] under ambient condition. Notably, as the conjugated ester structure is regenerated, the subsequent nucleophilic conjugate addition (Michael addition) is applicable to the products **1-17**.[29] The quantitative and facile performances of conjugate substitution of **1-16** were attractive for polymer synthesis, the reaction was mainly employed in polycondensations described in this thesis.

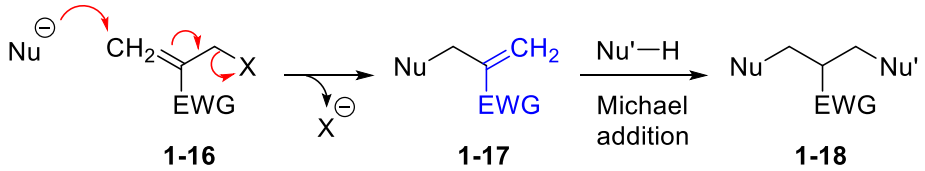


**Scheme 1-7.** conjugate substitution ($S_N2$') reactions of allyl compound bearing EWGs and the subsequent conjugate addition (Michael addition) reaction.

## ***2.3 Diversity in Conjugate Substitution by Other Substituents***

Allyl halide **1-19**, bearing a substituent R at the allyl position shows high selectivity

of $S_N2$' process due to steric hindrance by the substituent R, yielding an *endo*-olefin product **1-20** (Scheme 1-8).[30] On the other hand, a tertiary amine catalyzed the generation of an *exo*-olefin product **1-23** via continuous $S_N2'$ reactions resulting in an ammonium intermediate **1-21**.[31] Thus, two different products can be obtained from **1-19** by choosing a base. Note that an allyl compound bearing a methyl substituent (**1-24**) suffers from a side reaction composed of E2 reaction and the following Diels-Alder reaction with unreacted **1-24** (**Scheme 1-9**).

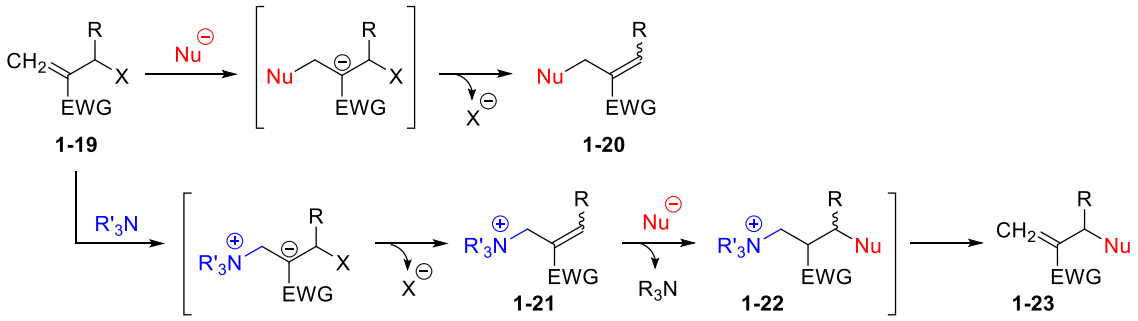


**Scheme 1-8.** Conjugate substitution ($S_N2'$) reactions of allyl halides with an allyl substituent leading to different isomeric products.

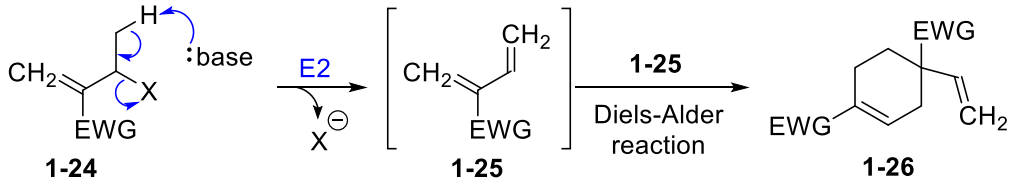


**Scheme 1-9.** Side reaction in the conjugate substitution of allyl halides with methyl substituent at the allylic position.

## *2.4 Diversity in Conjugate Substitution of 1,3-Dihaloganopropene*

1,3-Dihalogenopropenes bearing electron-withdrawing group, **1-28**, can provide three different products by the nucleophilic substitution reaction (Scheme 1-10).[32] The simple $S_N2$ and $S_N1$ reactions afforded **1-29**, while the $S_N2'$ reaction resulting in an *exo*-methylene compound, **1-31**. The halogen atom of **1-31**, which is located at the β-position

in **1-29**, is now in the allylic position formed by the regeneration of double bonds, and the regenerated allyl halide structure can accept further $S_N2$' reaction to afford an *endo*-olefin compound **1-33**. In certain cases, the intermediate **1-31** is accepted $S_N2$ or $S_N1$ reaction to yield an *exo*-olefin compound **1-32**. The diversity of this reaction system was applied polycondensation in Chapter 4.

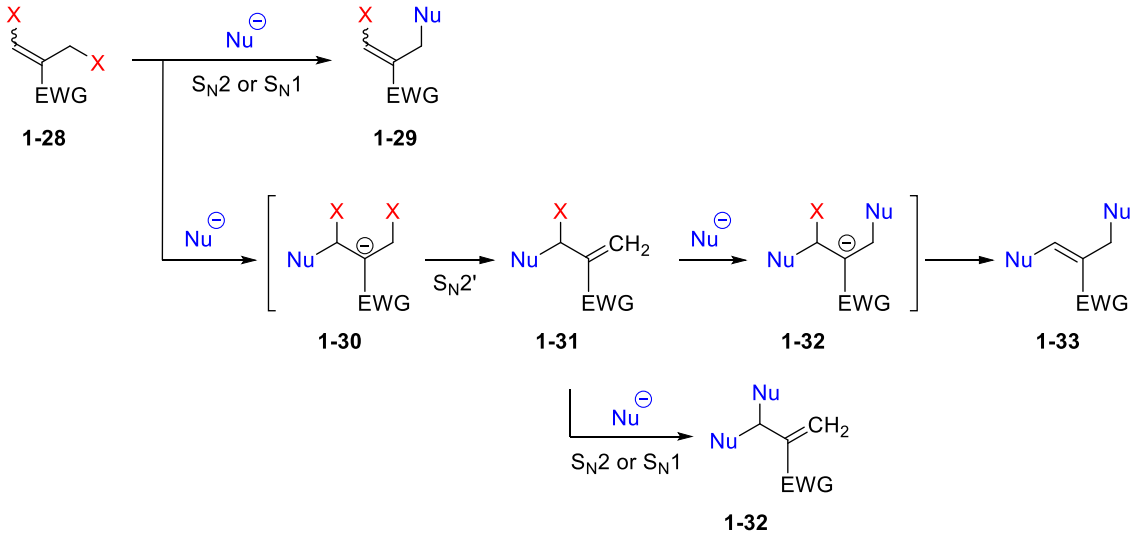


**Scheme 1-10.** Nucleophilic substitution of 1,3-dihalogeneted propenyl compounds with electron withdrawing groups.

## 3. Objective and Outline of This Thesis

As mentioned above, monomer design is a key to develop novel modes of polycondensation different from the Flory–Carothers theory. Particularly, nature have sophisticated molecular strategy that produces a variety of monomer from a single monomer. In this thesis, the author aimed to imitate such natural polymerization.

Although $S_N2$' reaction of allyl halides, particularly α-(halomethyl)acrylates proceeds quantitatively with various nucleophiles under ambient conditions, it has not been applied to polycondensation as an elemental reaction. Importantly, the introduction of substituents to α-(halomethyl)acrylates allows a diversity of $S_N2$' products as presented in **Schemes 1-6 – 1-9**. Therefore, the author envisioned that the $S_N2$' reaction is promised to lead a new class of polycondensation.

In ***Chapter 2***, the polycondensation involving $S_N2'$ and thiol−ene Michael addition reactions of α-(halomethyl)acylates has been investigated (**Scheme 1-11**). In this polymerization, the author proposed two concepts: (1) The first polycondensation based on conjugate substitution reaction of α-(halomethyl)acrylates. (2) The first examples of main-chain construction by tandem reaction composed of conjugate substitution ($S_N2'$ reaction) and the subsequent conjugate addition. In contrast to the typical polycondensation using bifunctional monomers containing spacers, the current polycondensation was operated with a monomer of a single acrylate skeleton. Thus, the polycondensation shows perspective to the reduce of carbon atoms.

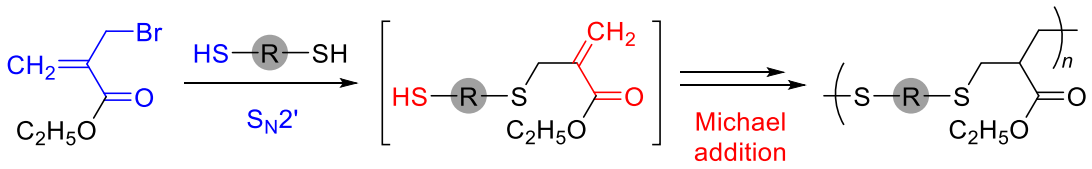


**Scheme 1-11.** Tandem polymerization based on $S_N2'$ and Michael addition reactions described in Chapter 2.

After this report, Miyazaki and Kohsaka have found that the poly(thioether) is degradable by $E_1cB$ reaction, a reverse reaction of Michael addition (**Scheme 1-12**). Since the $E_1cB$ reaction is reversible, the degradation was not quantitative. Nevertheless, the addition of monofunctional thiol resulted in almost complete main chain scission with capping of the acrylate end by Michael addition.

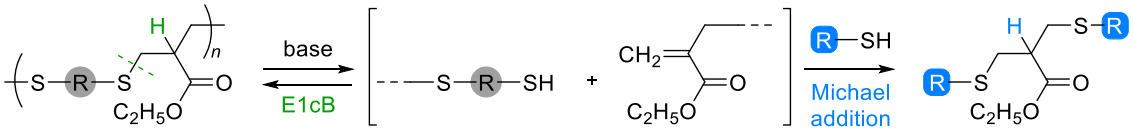


**Scheme 1-12.** Main chain scission of poly(thioether) by $E_1cB$ and Michael addition reactions.

In ***Chapter 3***, the polycondensation described above was improved to afford poly(thioether) that irreversibly decomposed (**Scheme 1-13**). As described in **Scheme 1-7**, α-(substituted methyl)acylates with an allyl substituent affords a series of isomers by

$S_N2$' products. Then, the reaction was controlled to yield *exo*-olefin products by sequential $S_N2$' reactions using an amine catalyst, and the subsequent Michael addition resulted in poly(thioester)s. The poly(thioether)s underwent main chain scission by E1cB reaction, which was irreversible due to the formation of sterically hindered *endo*-olefine structure.

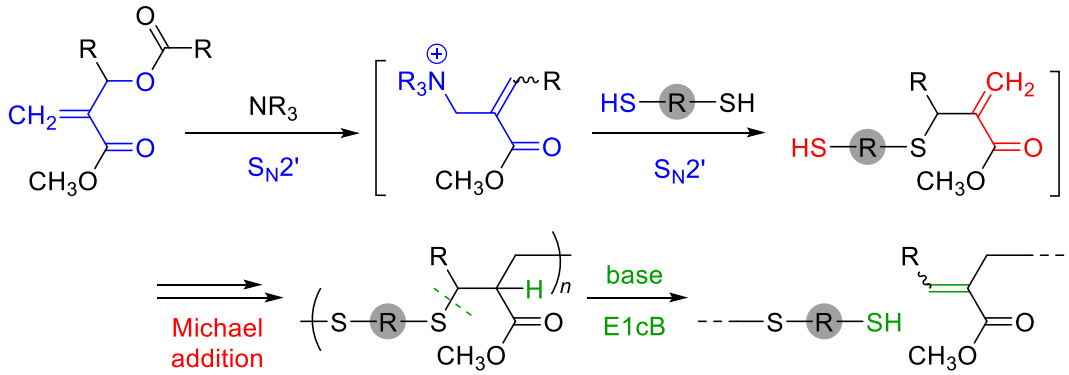


**Scheme 1-13.** Polycondensation affording poly(thioether)s that undergo irreversible main chain scission by E1cB reaction.

In ***Chapter 4,*** another designed polymerization based on sequential $S_N2$' reactions has been developed. The tandem reaction of β-bromo-α-(bromomethyl)acrylate was applied for polycondensation (**Scheme 1-14**). In this polymerization, the isomeric repeating units, *endo*- or *exo*-olefin units, were generated. The backbone structure was controllable by the nucleophilicity of bases. Notably, the controls of backbone structure were allowed tuning of thermal properties of the resulting polymers.

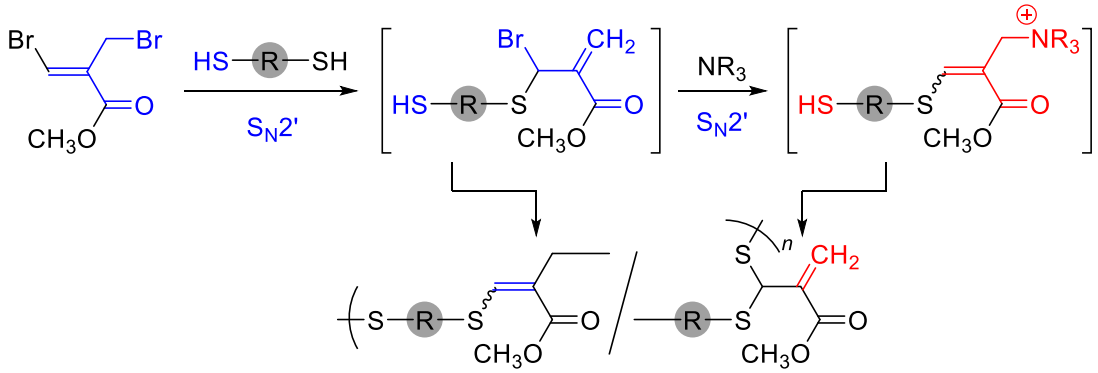


**Scheme 1-14.** Tandem polymerization based on sequential $S_N2$' reactions.

In ***Chapter 5***, the $S_N2$' reaction of α-(substituted methyl)acylates, was applied to immortal (living) ring-opening polymerization (ROP) of lactones based on a novel

mechanism induced outside of the rings. Generally speaking, ROP of lactones occurs by transesterification reaction of alcohol chain-ends and lactones at high temperature under vacuum. Thus, the development of catalysts for transesterification is a key to achieve ROP under ambient condition.[6] In contrast, the authors designed ROP not by transesterification reaction but by $S_N2$' reaction at the outside of the rings (**Scheme 1-15**). In this polymerization, δ-valerolactone moiety was introduced to the allylic position of acrylates. The ROP was achieved by the initiation and propagation of $S_N2$' reaction with the elimination of carboxylate anion, keeping livingness even after isolation of the resulting polymer (immortal polymerization). The ring-opening polymerization proceeded even under ambient condition to afford unsaturated polyester.

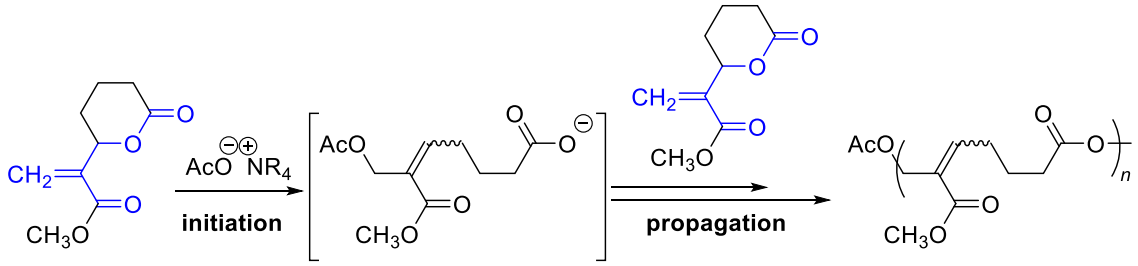


**Scheme 1-15.** Ring-opening polymerization induced by $S_N2$' reaction of side-group.

**References**

(1) (a) W. H. Carothers, *Trans. Faraday. Soc.*, **1936**, 32, 39. (b) P. J. Flory, *J. Am. Chem. Soc.*, **1936**, 58, 1877. (c) P. J. Flory, *Chem. Rev.*, **1946**, 39, 137.

(2) A. Buleon, P. Colonna, V. Planchot, S. Ball, *Int. J. Biol. Macromol.*, **1998**, 23, 85

(3) (a) K. Kittayama, K. Hatada, *Polym. Int.*, **2000**, 49, 11. (b) K. Ute, N. Miyatake, K. Hatada, *Polymer*, **1995**, 36, 1415.

(4) T. Kodaira, *Prog. Polym. Sci.*, **2000**, 25, 627.

(5) (a) G. B. Butler, *J. Polym. Sci. Part A: Polym. Chem.*, **2000**, 38, 3451. (b) X. Tang, M. Hong, L. Falivene, L. Coporaso, E. Y.-X. Chen, *J. Am. Chem. Soc.*, **2016**, 138, 14326. (c) A. E. Neitzel, M. A. Petersen, E. Kokkoli, M. A. Hillmyer, *ACS Macro. Lett.*, **2014**, 3, 1156.

(6) (a) N. Yamazaki, F. Higashi, *J. Polym. Sci. Poolym. Chem. Ed.*, **1974**, 12, 2149. (b) M. Ueda, A. Kameyama, K. Hashimoto, *Macromolecules*, **1988**, 21, 19. (c) A. Takasu, Y. Iio, Y. Oishi, Y. Narukawa, T. Hiyabayashi, *Macromolecules*, **2005**, 38, 1048. (d) H. R. Kricheldorf, M. A. Masri, N. Lomadze, G. Schwarz, *Macromolecules*, **2005**, 38, 9085.

(7) (a) E. L. Wittbecker, P. W. Morga, *J. Polymer Sci.*, **1959**, 40, 289. (b) P. W. Morgan, S. L. Kwolek, *J. Polymer Sci.*, **1959**, 40, 299. (c) R. G. Beaman, P. W. Morgan, C. R. Koller, E. L. Wittbecker, E. E. Magat, *J. Polym. Sci.*, **1959**, 40, 329. (d) M. Katz, *J. Polym. Sci.*, **1959**, 40, 337. (e) V. E. Shashoua, W. M. Eareckson, *J. Polym. Sci.*, **1959**, 40, 343. (f) C. W. Stephens, *J. Polym. Sci.*, **1959**, 40, 359. (g) E. L. Wittbecker, M. Karz, *J. Polym. Sci.*, **1959**, 40, 367. (h) J. R. Schaefgen, F. H. Koontz, R. F. Tietz, *J. Polym. Sci.*, **1959**, 40, 377. (i) S. A. Sundet, W. A. Murphey, S. B. Speck, *J. Polym. Sci.*, **1959**, 40, 389. (j) H. Schnell, *Ind. Eng. Chem.*, **1959**, 51, 157.

(8) (a) T. E. Attwood, P. C. Dawson, J. L. Freeman, L. R. J. Hoy, J. B. Rose, P. A. Staniland, *Polymer*, **1981**, 22, 1096. (b) A. Pandya, J. Yang, H. W. Gibson, *Macromolecules*, **1994**, 27, 1367.

(9) (a) T. Yamamoto, A. Yamamoto, *Chem. Lett.*, **1977**, 6, 353. (b) T. Yamamoto, Y. Hayashi, A. Yamamoto, *Bull. Chem. Soc. Jpn.*, **1978**, 51, 2091. (c) T. Yamamoto, T. , Ito, K. Kubota, *Chem. Lett.*, **1988**, 153. (d) T. Yamamoto, A. Morita, Y.

Miyazaki, T. Maruyama, H. Wakayama, Z. H. Zhou, Y. Nakamura, T. Kanbara, S. Sasaki, K. Kubota, *Macromolecules*, **1992**, 25, 1214.

(10) (a) H.-H. Horhold, J. Klee, K. Bellstedt, *Z. Chem*, **1982**, 22, 166. (b) H.-H. Horhold, R. Grutzner, *Acta Polym.*, **1987**, 38, 247. (c) C. C. Clark, *J. Org. Chem.*, **1961**, 26, 3575. (d) T. W. Cambell, E. A. Tomic, *J. Polym. Sci.*, **1962**, 62, 379. (e) E. A. Tomic, T. W. Campbell, V. S. Foldi, *J. Polym. Sci.*, **1962**, 62, 387.

(11) H. C. Kolb, M. G. Finn, K. B. Sharpless, *Angew. Chem. Int. Ed.*, **2001**, 40, 2004.

(12) (a) R. Huisgen, G. Szeimies, L. Mobius, *Chem. Ber.*, **1967**, 100, 2494. (b) W. H. Binder, R. Sachsenhofer, *Macromol. Rapid Commun.*, **2007**, 28, 15. (c) Y. Koyama, T. Takada, *Kobunshi Ronbunshu,* **2011**, 68, 147.

(13) (a) M. Scholl, S. Ding, C. W. Lee, R. H. Grubbs, *Org. Lett.*, **1999**, 1, 953. (b) A. M. Harned, M. Zhang, P. Vedantham, S. Mukherjee, R. H. Herpel, D. L. Flynn, P. R. Hanson, *Aldrichimica Acta.*, **2005**, 38, 3.

(14) (a) N. Nomura, *Kohbunshi*, **2004**, 53, 587. (b) N. Nihara, S. Komatsu, T. Takata, T. Endo, *Macromolecules*, **1999**, 32, 4776. (c) K. Miyatake, A. R. Hill, A. S. Hay, *Macromolecules*, **2001**, 34, 4288. (d) H. Iimori, Y. Shibasaki, S. Ando, M. Ueda, *Macromol. Symp.*, **2003**, 199, 23. (e) N. Nomura, K. Tsurugi, M. Ando, *Angew. Chem., Int. Ed.*, **2001**, 40, 1932. (f) N. Nomura, K. Tsurugi, T. V. RajanBabu, T. Kondo, *J. Am. Chem. Soc.*, **2004**, 126, 5354.

(15) (a) K. Matsumoto, T. Ogawa, M. Jikei, *Polym. Chem.*, **2017**, 8, 7297. (b) K. Matsumoto, C. Fukui, R. Shoji, M. Jikei, *Polym. Chem.*, **2020**, 11, 4221.

(16) (a) R. W. Lenz, C. E. Handlovits, H. A. Smith, *J. Polym. Sci.*, **1962**, 58, 351. (b) W. Koch, W. Risse, W. Heitz, *Makromol. Chem. Suppl.*, **1985**, 12, 105.

(17) (a) T. Yokozawa, T. Arai, R. Sugi, S. Ishigooka, S. Hiraoka, *J. Am. Chem. Soc.*, **2000**, 122, 8313. (b) K. Iwashita, A. Yokoyama, T. Yokozawa, *J. Polym. Sci., Part A: Polym. Chem.*, **2005**, 43, 4109. (c) T. Yokozawa, Y. Suzuki. S. Hiraoka, *J. Am. Chem. Soc.*, **2001**, 123, 9902. (d) T. Yokozawa. T. Taniguchi, Y. Suzuki, A. Yokoyama, *J. Polym. Sci., Part A: Polym. Chem.*, **2002**, 40, 3460. (e) Y. Shibazaki, T. Araki, R. Nagahata, M. Ueda, *Eur. Polym. J.*, **2005**, 41, 2428.

(18) (a) R. Kakuchi, *Angew. Chem., Int. Ed.*, **2014**, 53, 46. (b) J. G. Rudick, *J. Polym. Sci., Part A: Polym. Chem.*, **2013**, 51, 3985. (c) S. Wang, C. Fu, Y. Wei, L. Tao, *Macromol. Chem. Phys*, **2014**, 215, 486. (d) M Rubinshtein, C. R. James, J. L. Young, Y. J. Ma, Y. Kobayashi, N. C. Gianneschi, J. Yang, *Org. Lett.*, **2010**, 12, 3560.

(19) (a) M. Passerini, *Gazz. Chem. Ital*, **1921**, 51, 126. (b) I. Ugi, C. Steinbrückner, *Angew. Chem.*, **1960**, 72, 267.

(20) (a) O. Kreye, T. Tóth, M. A. R. Meier, *J. Am. Chem. Soc.*, **2011**, 133, 1790. (b) A. Sehlinger, P.-K. Dannecker, O. Kreye, M. A. R. Meier, *Macromolecules*, **2014**, 47, 2774. (c) H. Shen, L. Han, H. Ma, P. Liu, L. Yang, C. Li, Y. Ma, Z. Peng, Y. Li, *Polym. Chem.*, **2020**, 11, 1970. (d) A. B. Ihsan, M. Taniguchi, Y. Koyama, *Macromol. Rapid Commun.*, **2020**, 2000480. (e) H. Wei, G. Wang, Y. Wang, B. Li, J. Huang, S. Kashtanov, K. V. Hecke, O. P. Pereshivko, V. A. Peshkov, *Chem. Asian. J.*, **2017**, 12, 825.

(21) (a) A. G. Catchpole, E. D. Hughes, C. K. Ingold, *J. Chem. Soc.*, **1948**, 8. (b) R. D. Kepner, S. Winstein, W. G. Young, *J. Am. Chem. Soc.*, **1949**, 71, 115. (c) R. H. DeWolfe, W. G. Young, *Chem. Rev.*, **1956**, 56, 753. (d) W. G. Young, I. D. Webb, H. L. Goering, *J. Am. Chem. Soc.*, **1951**, 73, 1076. (e) M. J. S. Dewar, *Bull. Soc. Chim. Fr.*, **1951**, C43. (f) F. G. Bordwell, *Acc. Chem. Res.*, **1970**, 3, 281. (g) R. M. Magid, *Tetrahedron*, **1979**, 36, 1901. (h) L. A. Paquette, C. J. M. Stirling, *Tetrahedron*, **1992**, 48, 7383. (i) F. G. Bordwell, H. C. Anthony, J.-P. Cheng, *J. Am. Chem. Soc.*, **1987**, 109, 1773.

(22) (a) L. Fowden, L. Hughew, C. K. J. Ingold, *J. Chem. Soc.*, **1955**, 3187. (b) R. H. DeWolfe, W. G. Young, *Chem. Rev.*, **1956**, 56, 753. (c) S. T. McDowell, C. J. M. Stirling, *J. Chem. Soc. B*, **1967**, 351. (d) F. G. Bordwell, D. A. Schnayder, *J. Org. Chem.*, **1968**, 33, 3240. (e) F. G. Bordwell, *Acc. Chem. Res.*, **1970**, 3, 281. (f) F. G. Bordwell, A. H. Clemens, J. Cheng, *J. Am, Chem, Soc.*, **1987**, 109, 1773. (g) J.-J. Young, L.-J. Jung, K.-M. Cheng, *Tetrahedron Lett.*, **2000**, 41, 3411. (h) V. Bizete, V. Lefebvre, J. Boudoux, M.-C. Lasne, A. Boulangé, S. Leleu, X. Franck, J. Rouden, *Eur. J. Org. Chem.*, **2011**, 4170.

(23) T. Hirabe, M. Nojima, S. Kusabayashi, *J. Org. Chem.*, **1984**, 49, 4084.

(24) T. Hirashima, Y. Hayashi, K. Mitsui, S. Araki, *Tetrahedron Lett.*, **2004**, 45, 3225.

(25) L. A. Paquette, C. J. M. Stirling, *Tetrahedron*, **1992**, 48, 7383.

(26) (a) S. E. Drewes, N. D. Emslie, *J. Chem. Soc., Perkin Trans. I*, **1982**, 2079. (b) F. Ameer, S. E. Drewes, M. S. Houston-McMillan, P. T. Kaye, *J. Chem. Soc., Perkin Trans. I.*, **1985**, 1143. (c) F. Ameer, S. E. Drewes, N. D. Esmlie, P. T. Kaye, R. L. Mann, *J. Chem. Soc., Perkin Trans. I*, **1983**, 2293. (d) F. Ameer, S. E. Drewes, M. S. Houston-McMillan, P. T. Kaye, *Afr. J. Chem.*, **1986**, 39, 57. (e) H. Amri, M. Ramboud, J. Villieras, *J. Organomer. Chem.*, **1990**, 384, 1. (f) H. Amri, M. Ramboud, J. Villieras, *Tetrahedoron*, **1990**, 46, 3535. (g) P. Beltaief, H. Amri, *Synth, Commun.*, **1994**, 24, 2003.

(27) (a) J. Rabe, H. M. R. Hoffman, *Angew, Chem., Int. Ed. Engl.*, **1983**, 22, 796. (b) H. M. R. Hoffman, J. Rabe, *J. Org, Chem.*, **1985**, 50, 3849. (c) D. Basavaiah, P. K. S. Sarma, *J. Chem. Soc., Chem. Commun.*, **1992**, 955.

(28) (a) P. Auvray, P. Knochel, J. F. Normat, *Tetrahedoron*, **1988**, 44, 6095. (b) R. Buchholz, H. M. R. Hoffman, *Helv. Chim. Acta*, **1991**, 74, 1213. (c) A. B. Charette, B. B. Cote, *Tetrahedron*, **1993**, 34, 6833. (d) W. R. Roush, B. B. Brown, *J. Org, Chem.*, **1993**, 58, 2152. (e) H. Mazdiyasni, D. B. Konopacki, D. A. Dickman, T. M. Zydowsky, *Tetrahedron Lett.*, **1993**, 34, 435. (f) D. Colombani, C. Navarro, M. Degueil-Castaing, B. Maillard, *Synth. Commun,* **1991**, 21, 1481. (g) C. Navarro, M. Degueil-Castaing, D. Colombani, B. Maillard, *Synth. Commun.*, **1993**, 23, 1025. (h) A. Foucaud, F. El Guemmout, *Bull. Soc, Chim. Fr.*, **1989**, 403. (i) D. Basavaiah, A. K. D. Bhavani, S. Pandiaraju, P. K. S. Sarma, *Synlett*, **1995**, 3, 243.

(29) (a) Y. Kohsaka, K. Hagiwara, K, Ito, *Polym. Chem.*, **2017**, 8, 976. (b) S. Masuoka, Y. Hoshiyama, K. Tsuchimoto, M. Suzuki, *Chem. Lett.*, **2017**, 46, 1718.

(30) (a) H. Amri, M. Ramboud, J. Villieras, *Tetrahedoron*, **1990**, 46, 3535. (b) P. Beltaief, H. Amri, *Synth, Commun.*, **1994**, 24, 2003. (c) P. Bauchat, E. Le Rouille, A. Foucaud, *Bull. Chim. Soc. Fr.*, **1991**, 267. (d) D. Basavaiah, A. K. D. Bhavani, P. K. S. Sarma, *J. Chem. Soc., Chem. Commun.,* **1994**, 1091.

(31) (a) A. Lin, H. Mao, X. Zhu, H. Ge, R. Tan, C. Zhu, Y. Cheng, *Adv. Synth. Catal.*,

**2011**, 353, 3301. (b) J. Xu, J. Chen, Q. Yang, L. Ding, X. Liu, D. Xu, B. Zhao, *Adv. Synth. Catal.*, **2014**, 356, 3219. (c) H. Mao, A. Lin, Z. Tang, H. Hu, C. Zhu, Y. Cheng, *Chem. Eur. J.*, **2014**, 20, 2454. (d) H. Mao, A. Lin, Y. Shi, Z. Mao, X. Zhu, W. Li, H. Hu, Y. Cheng, C. Zhu, *Angew. Chem. Int. Ed.*, **2013**, 52, 6288. (e) A. Lin, J. Wang, H. Mao, Y. Shi, Z. Mao, C. Zhu, *Eur. J. Org. Chem.*, **2013**, 6241.

(32) (a) D. Gopal, K. Rajagopalan, *Tetrahedron Lett.*, **1987**, 28, 5327. (b) H. Kanno, K. Osanai, *Tetrahedron Asymmetry*, **1995**, 6, 1503.

*Chapter 2*

# Polycondensation by Tandem Reaction of Sequential Conjugate Substitution and Addition Reactions

## 1. Introduction

Tandem reaction, or domino reaction, defined as intramolecular reactions triggered by first inter/intra-molecular reaction, is known efficient synthetic strategy in organic chemistry.[1] Multi-component reaction (MCR) is a similar concept that can be conducted in a one-pot system without isolating the intermediates.[1] Recently, these reactions open a new research field in chemistry of step-growth polymerization. In addition to the polymerization utilizing Ugi[7a] and Passesrini[7b] reactions, polycondensation based on novel reactions have been developed so far.[2] For example, Tang *et al.* have reported tandem polymerization of alkynes and carbonyl chlorides, in which Sonogashira coupling between the alkyne and carbonyl chloride occurs in the first stage, and subsequent addition of thiols results in a Michael-addition-type thiol–yne reaction.[2h] As illustrated by these example, tandem polymerization is generally conducted using a pair of difunctional monomers for polymerization and one or more monofunctional reagents to functionalize the monomers and/or polymers. In contrast, the author designed another type of tandem polymerization between mono- and bifunctional monomers by the regeneration of reactive points.

Conjugate substitution, composed of nucleophilic attack onto the vinyl group, regeneration of double bond and the subsequent elimination of the halogen atom ($S_N2$' mechanism), is a specific reaction of allyl halide derivatives (**Scheme 2-1a)**. $S_N2$' mechanism is competitive to $S_N2$ mechanism, the direct nucleophilic attack to the allylic position. In a sharp contrast, $S_N2$' mechanism become dominate for allyl halides introducing electron-withdrawing groups that can form conjugate structure with the double bond, such as acyl,[3a] oxycarbonyl,[3b-d] cyano,[3b-e] and sulfonyl[3a] groups, e.g. α-(halo methyl)acrylates (**Scheme 2-1b**),[3f] due to the enhancing electrophilicity of the olefin. This molecular design brings drastic changes on not only the selectivity of reaction mechanisms but also on the reaction conditions and applicable nucleophiles. That is to say, α-(halomethyl)acrylates can undergo quantitative conjugate substitution reaction even with weak nucleophile such as amines, thiols, phenols, and carboxylic acids under ambient conditions.[3] Notably, the $S_N2$' product, α-substituted acrylates are attractive compounds for polymer chemists. In fact, the conjugate substitution reaction is often used

to prepare new α-substituted acrylates that functions as monomers,[4a-e] chain-transfer agents[4d,f] and functional initiators.[4g,h] Importantly in this reaction, the resulting α-substituted acrylate is still active towards the conjugate addition (Michael addition) of nucleophiles. Nevertheless, it reacts quantitatively with thiols in the presence of amine or phosphine catalysts, and this is known as a Michael-addition-type thiol–ene click reaction.[5] Therefore, the author expected that the tandem reaction ($S_N2$' + Michael addition) would afford polysulfide bearing ester side groups (**Scheme 2-2**).

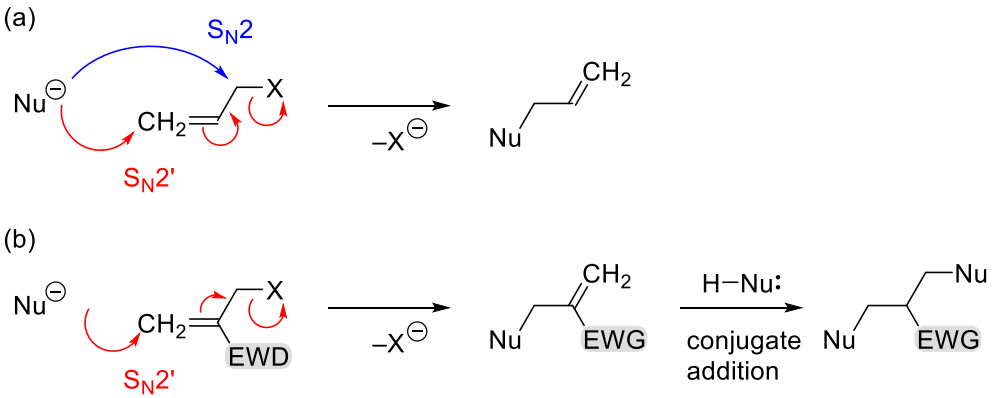


**Scheme 2-1.** (a) Reaction mechanisms of nucleophilic substitution of allyl halides; (b) Selective conjugate substitution of 2-substituted allyl halides and subsequential conjugate addition.

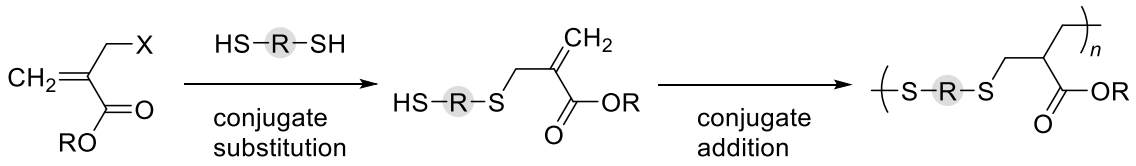


**Scheme 2-2.** Tandem polymerization of α-(halomethyl)acrylates and dhithiols.

# 2. Results and Discussion

## 2.1 Mechanism and Optimization of Polycondensation Reaction

***Model Reaction:*** *Stepwise polymer synthesis with the isolated intermediates*

Polymerization of ethyl α-(bromomethyl)acrylate (**2-1**) and 1,10-decanedithiol (**2-2a**) consists of two steps, conjugate substitution and Michael addition reactions (**Scheme 2-3**). The conjugate substitution reaction requires a base to capture the liberating hydrobromic acid, and the Michael addition reaction requires a catalyst to accelerate addition reaction of thiols. Prior to the one-pot polymerization, a stepwise polymerization was carried out through isolation of the condensation product in order to confirm whether the reactions at each step proceed with high efficiency.

In $CH_3CN$, 3.0 equimolar **2-2a** was reacted with **2-1** in the presence of triethylamine ($Et_3N$) at room temperature to afford model intermediate **2-3a**. In this reaction, a disubstituted product in which the two mercapto groups in **2-2a** reacted with **2-1** was generated, and a monosubstituted product **2-3a** was isolated by column chromatography in a low yield (11%). On the other hand, unreacted **2-1** was not detected, suggesting quantitative and fast conjugate substitution. Although $Et_3N$ performs as a catalyst for the Michael addition, tributylphosphine ($Bu_3P$), a more active catalyst, was added toward the second step.[5f] In addition, the solvent effect on the Michael addition reaction of the thiols is significant, and $CH_3CN$ is known as a solvent with a high reaction acceleration effect.[5f] Thus, the polymerization of **2-3a** was carried out at 50 ºC in $CH_3CN$ using $Bu_3P$ as a catalyst for 17 h to yield the desired polymer **P2-1/2-2a** with number averaged molecular weight ($M_n$) = 10000 and its degree of dispersity ($Đ$) = 1.71 (Entry 0). In the $^1H$ NMR spectrum of the resulting polymer, the signals which assigned vinylidene (6.20 and 5.63 ppm) and mercaptomethyl (2.45 ppm) groups were not observed, suggesting the polymerization as expected (**Figure 2-1a, b**).

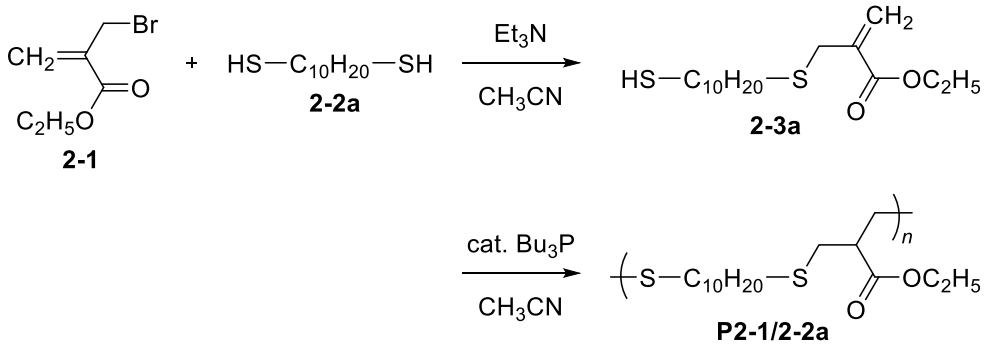


**Scheme 2-3.** The stepwise synthesis of **P2-1/2-2a**.

**Table 2-1.** The effect of bases on polymerizations between **2-1** and **2-2a**.

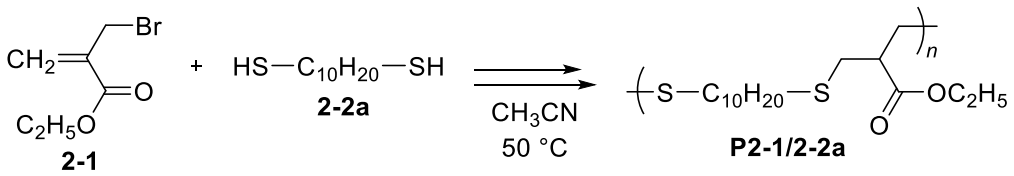


| Entry[a] | Base | Catalyst | Yield / % | $M_n$[b] | $Đ$[b] |
|---|---|---|---|---|---|
| 0[c] | – | $Bu_3P$ | | 10000 | 1.71 |
| 1 | $Et_3N$ | $Bu_3P$ | 96 | 5000 | 1.73 |
| 2 | $Et_3N$ | – | 87 | 5500 | 1.77 |
| 3 | DBU | $Bu_3P$ | 92 | 21000 | 1.72 |
| 4 | DBU | – | 96 | 5500 | 1.67 |
| 5 | $K_2CO_3$ | $Bu_3P$ | 92 | 11000 | 1.89 |

[a] **2-1**: 0.750 mmol, [**2-1**]$_0$/[**2-2a**]$_0$/[base]$_0$/[catalyst]$_0$ = 1 / 1.0 / 1.2 / 0.2, $CH_3CN$: 0.75 mL, 50 °C, 24 h. [b] Determined by SEC (THF, 40 °C, polystyrene standards). [c] Stepwise synthesis.

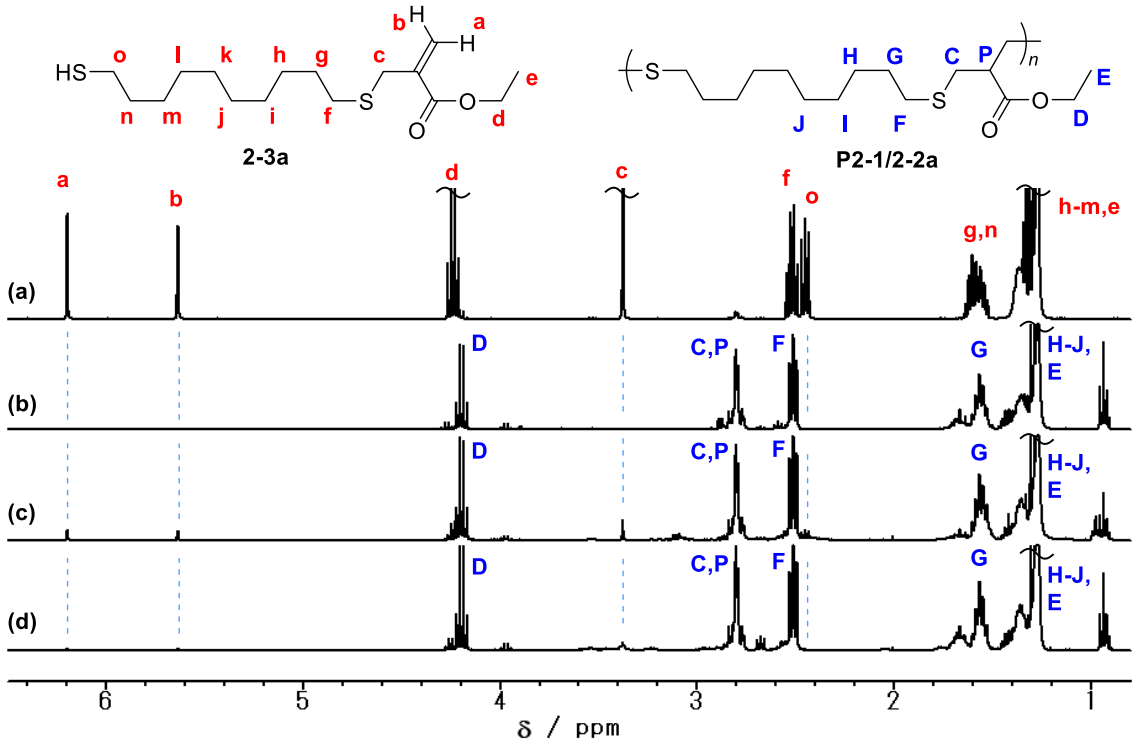


**Figure 2-1.** $^{1}$H NMR spectra of (a) model the intermediate **2-3a** and the product **P2-1/2-2a** in (b) Entry 0, (c) Entry 1 and (d) Entry 6. (400 MHz, $CDCl_3$, 26 °C)

***Polymerization by Tandem Reaction:*** *Effects of Bases and Catalysts*

Similarly to the model polymerization by stepwise synthesis using excess amount of $Et_3N$ and a catalyst of $Bu_3P$, an equimolar mixture of **2-1** and **2-2a** was reacted in $CH_3CN$ at 50 ºC for 24 h to afford the polymer with $M_n$ = 5000 and $Đ$ = 1.73 (**Table 2-1**, Entry 1). The $^{1}$H NMR spectrum clearly showed the signals corresponding to end groups of vinylidene (6.20 and 5.63 ppm) and mercaptomethyl (2.45 ppm, **Figure 2-1c**), and the one-pot polymerization did not proceed sufficiently as compared with polymerization by the stepwise synthesis. The difference between the stepwise synthesis and the one-pot polymerization is the presence of hydrobromide generated in the first step reaction of the substitution. In the stepwise synthesis, the hydrobromide was removed during the isolation and purification of **2-3a**, but in the one-pot polymerization, it was remaining in the reaction system. Focusing on the reaction mechanism of Michael addition as the second reaction (**Scheme 2-4**), the catalyst of $Bu_3P$ adds to the conjugated ester **C** at the initiation step to generate the enolate anion **D**. The enolate anion **D** abstracts the proton

of the thiol, and the active species of the thiolate anion **F** is generated. However, when the hydrobromide or the ammonium salt were present in the reaction system, they should have inhibited the generation of active species **F**. In fact, the Entry 2 without the catalyst of $Bu_3P$ led to a similar result to the Entry 1, and t no significant difference was observed in the resulting molecular weight. Therefore, the catalyst did not work as expected in the case of Entry 1 and the formation of active species **F** might have been inhibited. In order to reduce the acidity of hydrobromide, 1,8-diazabicyclo[5.4.0]undec-7-ene (DBU), which is a stronger base, was applied instead of $Et_3N$ and the polymer with higher $M_n$ was formed (Entry 3, $M_n$ = 21000, $Đ$ = 1.72). The polymerization in the absence of $Bu_3P$ (Entry 4) resulted in similar molecular weight to using $Et_3N$ (Entries 1,2). Therefore, the catalyst definitely performed in Entry 3 and these results confirmed that the catalyst is necessary for efficiently proceeding polymerization. Notably, even in using $K_2CO_3$, which does not afford an acidic salt on neutralization, the polymerization was efficiently proceeded to afford high molecular weight (Entry 5, $M_n$ = 11000, $Đ$ = 1.89).

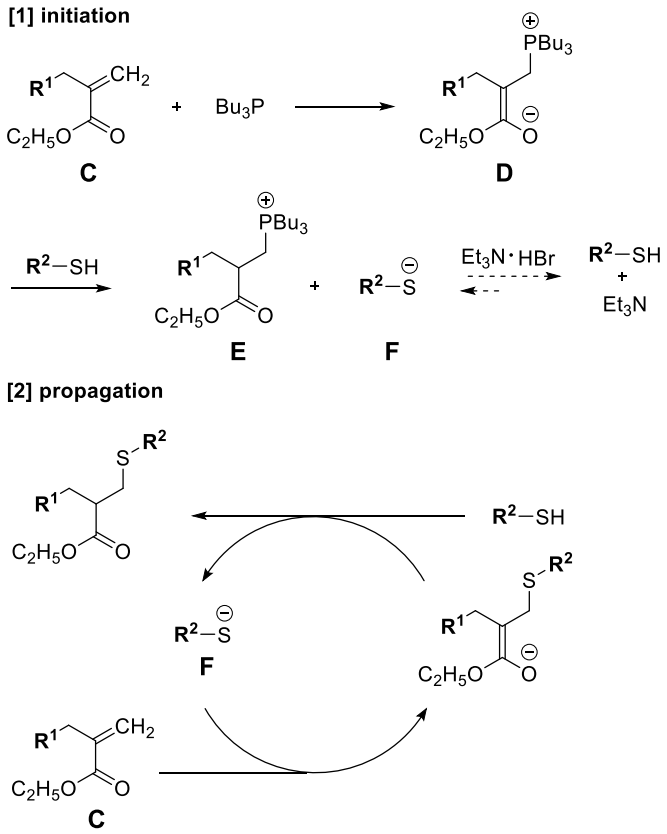


**Scheme 2-4.** Reaction mechanism of Michael-addition of thiol to methacryloyl group catalyzed by $Bu_3P$.

***Polymerization by Tandem Reaction:*** *Effects of Temperature*

In this polymerization, the excess base would make the thiol-Michael addition reversible in an equilibrium via retro-Michael addition, *i.e.* E1cB reaction (**Scheme 2-5**). Temperature is one of factors affecting equilibrium and thus should be significant on the polymerization. In order to investigate the effects of temperature, the similar polymerization carried out under the various temperatures (**Table 2-2**). $M_n$ became exceedingly small (Entry 6, $M_n = 200$, $Đ = 17.1$) in the polymerization with excess amount of DBU under reflux condition. The peak in the size exclusion chromatography (SEC) curve had a tail towards the lower molecular weight region, which suggests that oligomer formation occurred through a cyclization reaction in addition to the polymerization (**Figure 2-2**). In fact, the $^1$H NMR spectrum (**Figure 2-1d**) exhibits much smaller end-group signals than would be expected from the estimated $M_n$. In this polymerization system, the second step of thiol-Michael addition may be in equilibrium states via retro-Michael addition triggered by a base (**Scheme 2-5**). The result of Entry 6 suggested that the formation of cyclic oligomer was thermodynamically favored and became dominant under reflux condition.

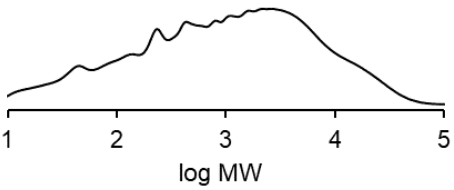


**Figure 2-2.** SEC curve of the product in Entry 6.

**Table 2-2.** The effect of temperature on polymerizations between **2-1** and **2-2a**.

| Entry[a] | Base | Temp / °C | Yield / % | $M_n$[b] | $Đ$[b] |
|---|---|---|---|---|---|
| 6 | DBU | 80[c] | >99 | 200 | 17.1 |
| 7 | $K_2CO_3$ | −20 | 0 | − | − |
| 8 | $K_2CO_3$ | 0 | 0 | − | − |
| 9 | $K_2CO_3$ | 20 | 86 | 23000 | 1.55 |
| 10 | $K_2CO_3$ | 80[c] | 85 | 10100 | 1.96 |

[a] **2-1**: 0.750 mmol, [**2-1**]$_0$/[**2-2a**]$_0$/[base]$_0$/[catalyst]$_0$ = 1 / 1.0 / 1.2 / 0.2, $CH_3CN$: 0.75 mL, 24 h. [b] Determined by SEC (THF, 40 °C, polystyrene standards). [c] Under reflux.

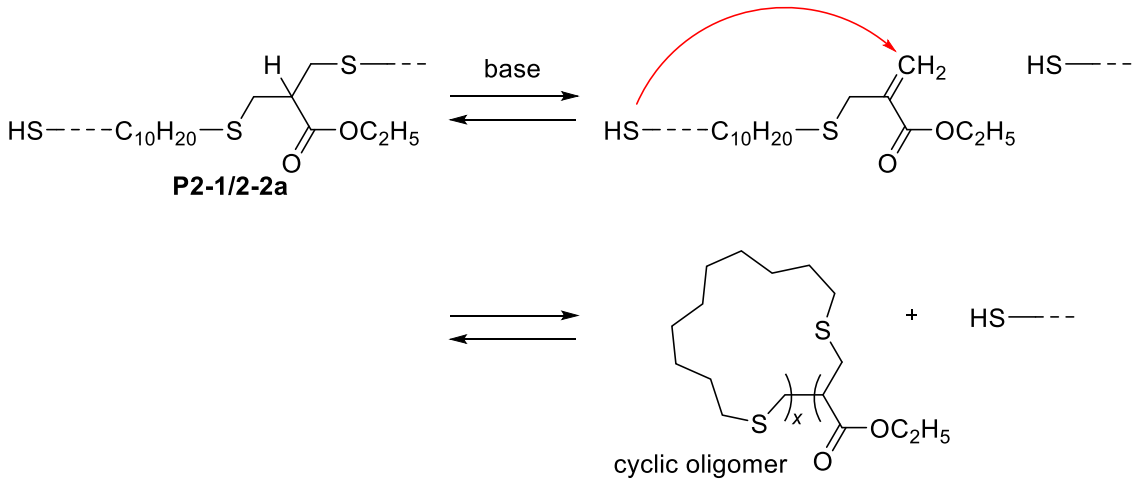


**Scheme 2-5.** Formation of cyclic oligomer via reversible Michael addition.

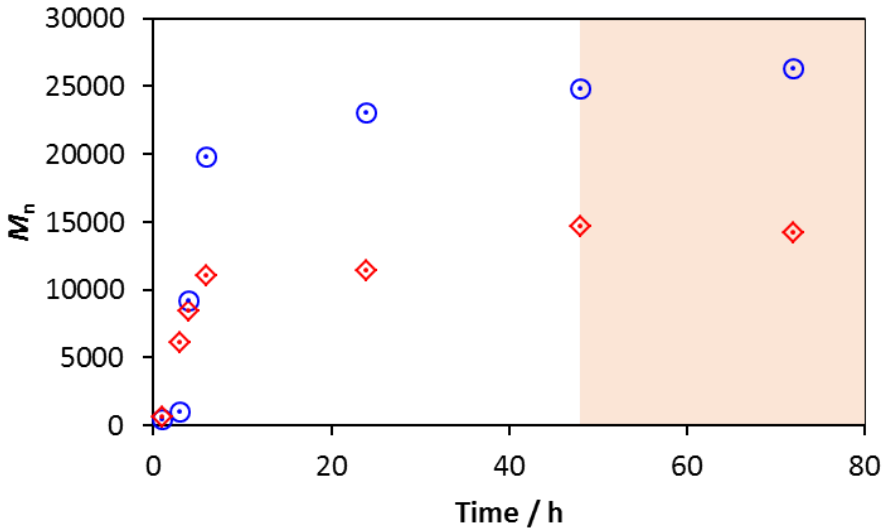


**Figure 2-3.** Time vs. $M_n$ plots in the polymerizations at 20 °C (blue circles) and 50 °C (red diamonds) determined by SEC (THF, 40 °C, PS standards). The orange highlighted area means after increasing temperature to 80 °C.

Furthermore, the effects of temperature on the polymerization with $K_2CO_3$ was investigated; no polymeric products were obtained at lower than 0 °C (Entries 7, 8), probably owing to the poor solubility of $K_2CO_3$. In addition, the largest $M_n$ was achieved at 20 °C (Entry 9, $M_n = 23000$, $Đ = 1.55$), and polymeric product was obtained in reactions carried out even under reflux (Entry 10, $M_n = 10100$, $Đ = 1.96$). It was attributed to the low efficiency of $E_1cB$ reaction (retro-Michael addition) by $K_2CO_3$. To investigate whether the polymerization was reversible in the presence of $K_2CO_3$, the polymerization was carried out at 20 °C for 48 h and then reacted at 80 °C for 24 h to trace the changes of $M_n$ (**Figure 2-3**, blue). $M_n$ increased from the initial stage of the reaction and increased

to 23000 after 48 h. Further reaction at 80 °C for 24 h resulted in the increase of molecular weight up to $M_n$ = 26300. If the main chain cleavage and cyclization reactions via the retro-Michael addition reaction was possible, these reactions, which are entropically favored at high temperatures, should have been promoted to decrease $M_n$. However, as the $M_n$ actually increased, it was reasonable to consider that the retro-Michael addition reaction did not occur. A similar experiment at 50 °C resulted in a polymer ($M_n$ = 14700) after 48 h, and the molecular weight did not decrease after heating at 80 °C for 24 h (**Figure 2-3**, red). Since the reaction at 50 °C afforded a lower $M_n$ than the reaction at 20 °C, the cyclization seems likely to occur for oligomers found in the initial stage of polymerization at high temperatures.

## 2.2 Polycondensation with Various Dithiols

Polymerizations with various thiols were examined (**Table 2-3**). Primary dithiol **2-2b** gave a similar result to **2-2a** (Entry 11). However, polar dithiol with intramolecular hydrogen bond, **2-2c**, and aromatic dithiol **2-2e** resulted in a lower $M_n$ (Entry 12, 14), probably owing to the stability and low reactivity of the corresponding thiolate anion. Secondary dithiol **2-2d** (Entry 13) and $Na_2S$ (Entries 15) also afforded the corresponding oligomers.

**Table 2-3.** Polymerizations of various dithiols **2-1** and **2-2b-e** in $CH_3CN$ at 50 °C.

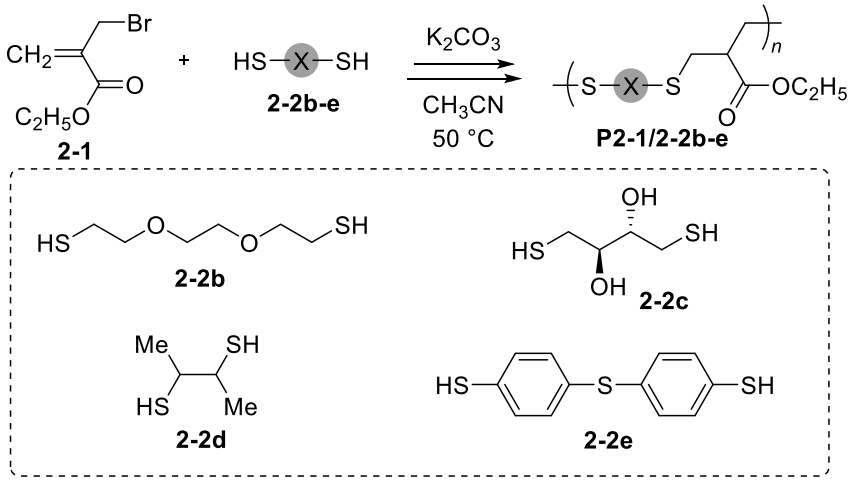


| Entry[a] | Dithiol | Yield/% | $M_n$[b] | $Đ$ [b] |
|---|---|---|---|---|
| 11 | **2-2b** | 79 | 13100 | 1.60 |
| 12 | **2-2c** | 86 | 2000[c] | 1.24 |
| 13 | **2-2d** | 78 | 1000 | 2.13 |
| 14 | **2-2e** | 89 | 2800 | 3.11 |
| 15 | $Na_2S$ | 43 | 1000 | 1.57 |

[a] **2-1**: 0.750 mmol, [**2-1**]$_0$/[**2-2b-e**]$_0$/[base]$_0$/[$Bu_3P$]$_0$ = 1.0 / 1.0 / 1.2 / 0.2, $CH_3CN$: 0.75 mL, 24 h. [b] Determined by SEC (THF, 40 °C, polystyrene standards). [c] Soluble fraction.

## 2.3 Polymerization utilizing Aza-Michael Addition Reaction

### *Model Reaction with n-Propylamine*

That polymerization would proceed even for the nucleophiles such as amines other than thiols. Firstly, a model reaction applied a monoamine compound was examined.

Compared with thiol–ene Michael addition, aza-Michael reaction of primary amines to a methacrylate moiety is inefficient owing to the less electrophilicity of methacrylate than acrylate and lower and harder nucleophilicity of amines than thiols. Therefore, the polycondensation with **2-1** and primary diamines seems more difficult to be achieved. In order to investigate the reaction, *n*-propylamine (**2-4**) was reacted to equimolar **2-1** in $CD_3CN$ in the presence of DBU at room temperature, and the reaction was monitored by $^1H$ NMR spectrometry (**Scheme 2-6**). After 3 h, the intermediate **2-5** was clearly observed (**Figure 2-4a**). Subsequently, a similar reaction was employed using 3.2-hold of **2-4** for 1 h. The $^1H$ NMR spectrum shown in **Figure 2-4b** indicates the disappearance of signals C corresponding to vinylidene groups, suggesting aza-Michael reaction of the intermediate **2-5** to afford a diamine **2-6**. Note that aza-Michael addition of **2-5** would be enhanced by self-activation of intramolecular hydrogen bond via the ammonium intermediate (**Scheme 2-6**).

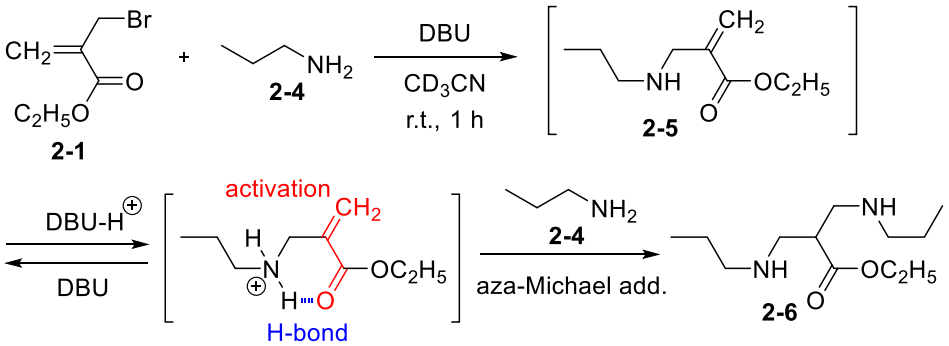


**Scheme 2-6.** The model reaction between **2-1** and **2-4**.

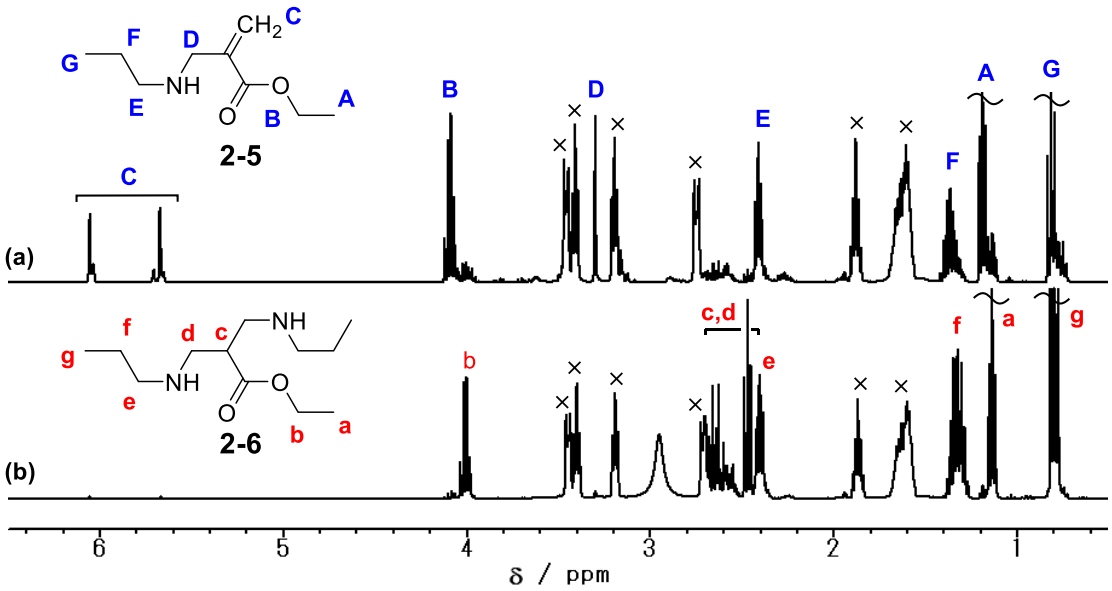


**Figure 2-4.** $^{1}$H NMR spectra of the mixture of (a) equimolar of **2-1** and **2-4**, (b) **2-1** and 3.2 mol equivalent of **2-4**. (400 MHz, $CD_3CN$, 26 °C, ×: DBU)

***Polymerization by Aza-Michael Reaction***

The polymerization of **2-1** and hexamethylenediamine (**2-7a**) was carried out under similar condition to the model reaction. The $^{1}$H NMR signals C corresponding to the vinylidene group of **2-1** were shifted to higher magnetic field area, signal X, after 1 h (**Figure 2-5a, b**), confirming the formation of the intermediate **I2-1/2-7a**. The vinylidene signal X for polymer chain-ends became gradually small and disappeared after 24 h, suggesting the polymerization to **P2-1/2-7a** (**Figure 2-5c, d**). The number-averaged degree of polymerization ($n$) and molecular weight ($M_n$) were estimated as 50 and 11400, respectively, from the integrated intensity ratio of the vinylidene signal X to the *O*-methylene signal b. However, the obtained polymer became insoluble to organic solvents after purification and further analyses by SEC and NMR after purification were impossible.

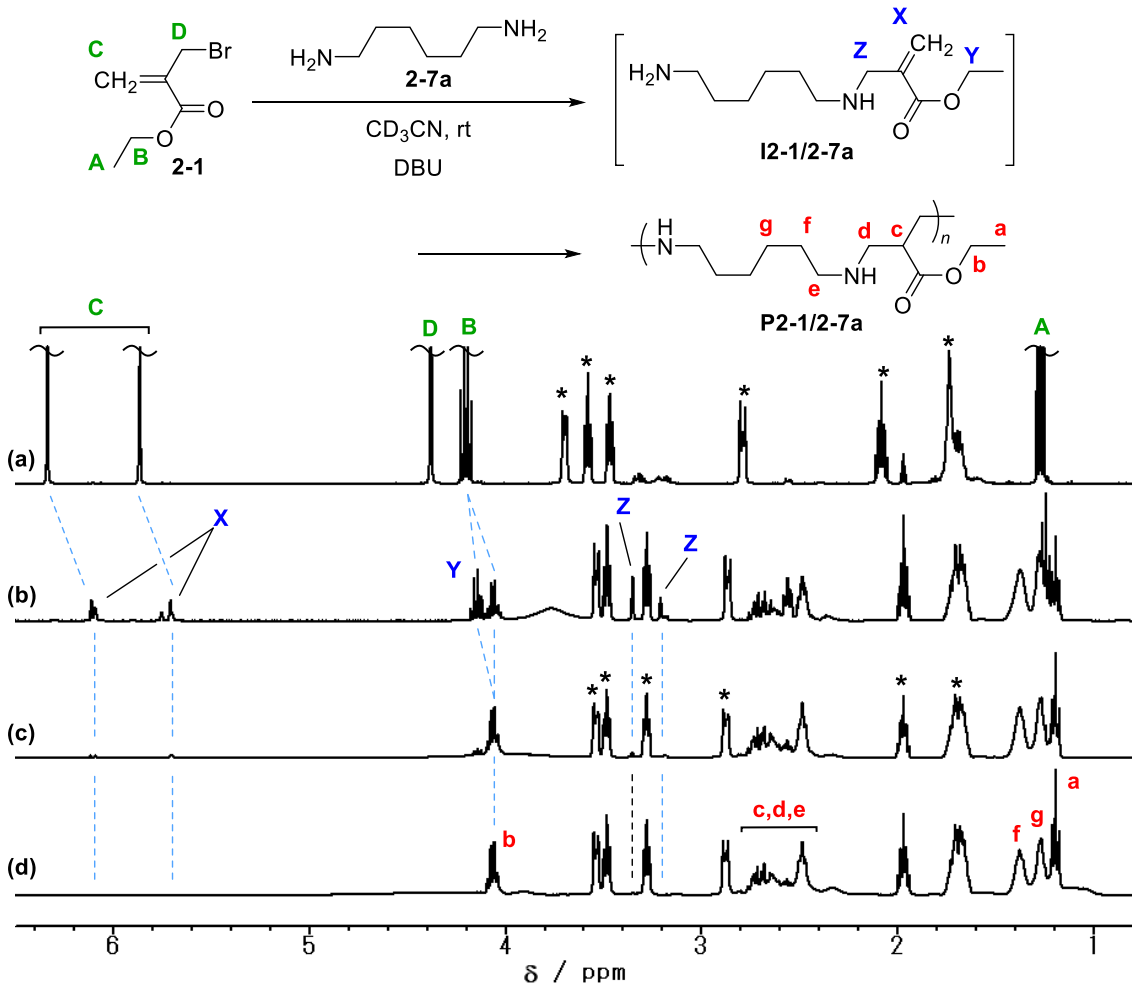


**Figure 2-5.** $^{1}$H NMR spectra of (a) the mixture of **2-1** and DBU, and the polymerization after (b) 1 h, (c) 6 h and (d) 24 h. (400 MHz, $CD_3CN$, 26 °C, *: DBU)

In order to improve the solubility, amidation by benzoylchloride (**2-8**) followed by polymerization was attempted. The polymerization was conducted in $CH_3CN$ for 24 h, and subsequently a solution of **2-8** and DBU in $CH_3CN$ was added. The almost quantitative amidation was achieved (conversion: 94 %) to lead the improvement of solubility. Although the $M_n$ estimated by SEC was low ($M_{n,\,SEC}$ = 2100), the $^{1}$H NMR spectrum suggested higher molecular weight ($M_{n,\,NMR}$ = 9800, **Table 2-4**, Entry 16, **Figure 2-6a**). The largest $M_{n,\,NMR}$ was achieved at 50 °C (Entry 17, $M_{n,\,NMR}$ = 18500) and the resulting $M_{n,\,NMR}$ was decreased under reflux condition (Entry 18, $M_{n,\,NMR}$ = 4400, **Figure 2-6b**). The polymerization in other solvents was affected by the solvent to decrease the resulting $M_{n,SEC}$ (Entries 19-23). Moreover, the polymerization with other

diamines **2-7b-e** similarly resulted the polymeric product except a using the aromatic amine. (Entries 24-27).

**Table 2-2.** Polymerizations between **2-1** and diamines **2-7a-e**.

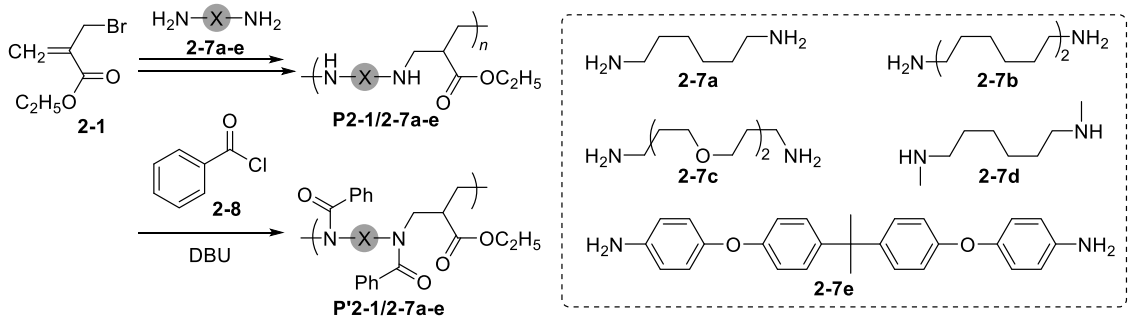


| Entry[a] | **2-7** | Solvent | Temp. [°C] | Yield [%] | $M_{n,\,NMR}$[b] | $M_{n,\,SEC}$[c] | $Đ$[c] | Amidation[d] [%] |
|---|---|---|---|---|---|---|---|---|
| 16 | **2-7a** | $CH_3CN$ | 25 | >99 | 9800 | 2100 | 2.19 | 94 |
| 17[e] | **2-7a** | $CH_3CN$ | 50 | >99 | 18500 | 1700 | 2.18 | >99 |
| 18[f] | **2-7a** | $CH_3CN$ | 80[e] | 77 | 4400 | 1400 | 1.91 | >99 |
| 19 | **2-7a** | THF[g] | 25 | >99 | 1600 | 1700 | 2.47 | 66 |
| 20 | **2-7a** | 1,4-dioxane | 25 | >99 | 1600 | 1000 | 1.98 | 58 |
| 21 | **2-7a** | DMF[h] | 25 | >99 | 2700 | –[i] | –[i] | 60 |
| 22 | **2-7a** | $CHCl_3$ | 25 | >99 | 6800 | 1800 | 2.64 | 81 |
| 23 | **2-7a** | $CH_2Cl_2$ | 25 | >99 | 4400 | 1300 | 2.64 | 79 |
| 24 | **2-7b** | $CH_3CN$ | 25 | >99 | 2200 | 1600 | 1.83 | 91 |
| 25 | **2-7c** | $CH_3CN$ | 25 | 88 | 11000 | 2500 | 2.18 | 86 |
| 26 | **2-7d** | $CH_3CN$ | 25 | >99 | 2200 | 1500 | 1.29 | – |
| 27 | **2-7e** | $CH_3CN$ | 25 | 0[j] | – | – | | – |

[a] **2-1**: 0.750 mmol, [**2-1**]$_0$/[**2-7a-e**]$_0$/[DBU]$_0$ = 1.0 / 1.0 / 1.2, Solvent: 0.75 mL, 24 h. [b,d] Determined by $^1$H NMR spectrometry (400 MHz, DMSO$_{d\text{-}6}$, 26 °C). [c] Determined by SEC (THF, 40 °C, polystyrene standards). [e] Polymerization at 50 °C. [f] Polymerization at 80 °C. [g] Tetrahydrofuran.

[h] *N,N*-dimethylformamine. [i] Insoluble for THF. [j] No polymeric product.

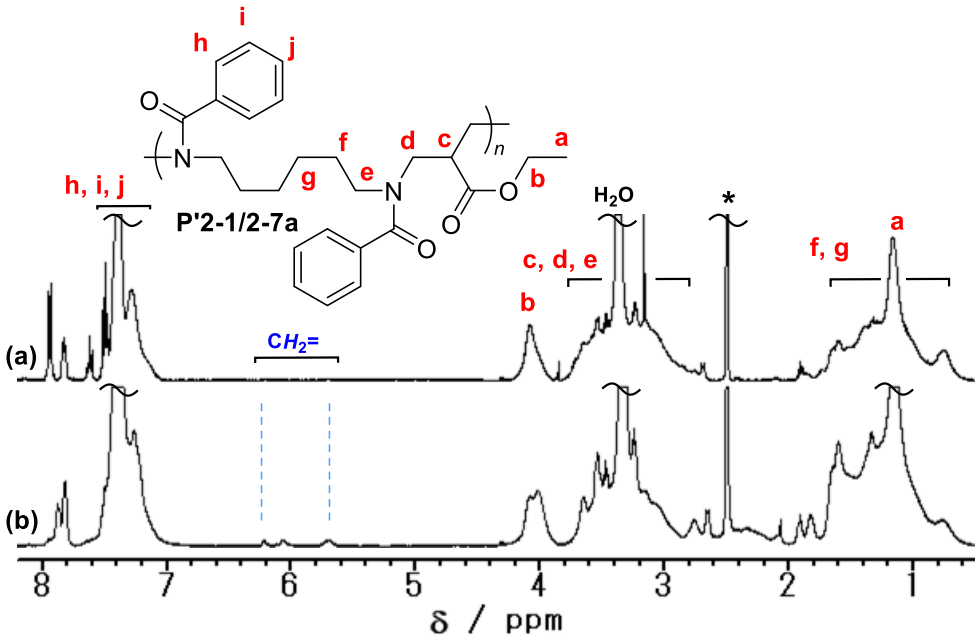


**Figure 2-6.** $^{1}$H NMR spectra of the product in Entries 16 (a) and 18 (b). (400 MHz, $DMSO_{d\text{-}6}$, 26 °C, *: DMSO)

## 3. Conclusion

In this chapter, the author aimed that the novel polycondensation constituted on $S_N2$' and subsequential Michael addition reactions onto α-(halomethyl) acrylates. Since $S_N2$' and thiol–ene Michael addition reactions have robustness under various conditions, the author expected similar robustness to the polycondensation. However, the biproduct of hydrobromic acid in the $S_N2$' reactions prevented the second step, Michael addition, and a base that does not afford an acidic salt, e.g., DBU or $K_2CO_3$ was necessary to achieve a high degree of polymerization. In addition, the contribution of retro-Michael addition ($E1_cB$ reaction) was observed to decrease of degree of polymerization at high temperature. Therefore, the polymerization system was less robust than expected. This is attributed to the combination of two different reactions that have different characters. Therefore, polymerization with similar monomers but based on $S_N2$' reaction only was investigated in Chapter 4. Nevertheless, the optimized condition was ambient environment. This indicates that the polymerization acquires convenience for facile procedure.

The polymerization was achieved with asymmetric pair of monomers, α-(bromomethyl)acrylate and dithiols/diamines. In addition to the reduction of carbon atoms, the polymerization provides a benefit in synthetic strategy of polymers; as described in **Scheme 2-7**. That is to say, the alternating ring-opening polymerization (ROP) of 3-ethoxycarbonyl azetidine (**2-8**) and azepane (**2-9**) are impossible, but the same product can be prepared from **2-1** and **2-7** as described in this chapter.

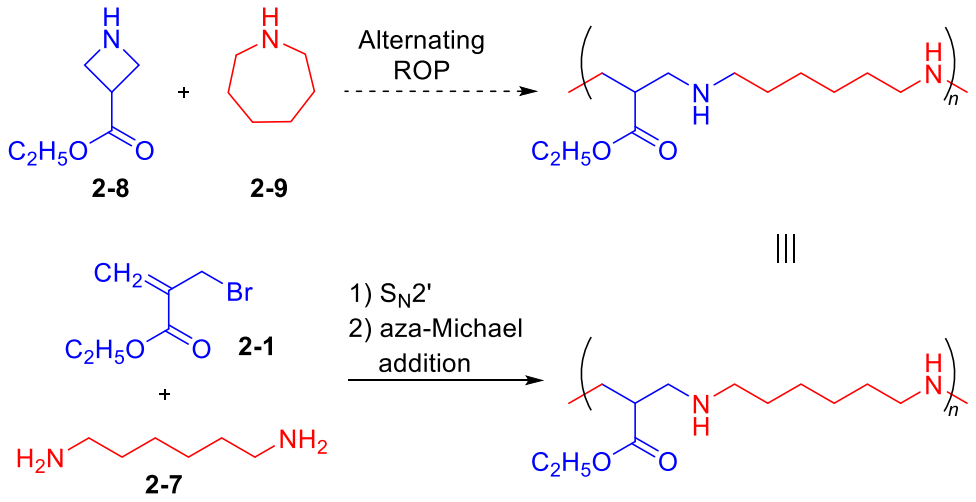


**Scheme 2-7**. Synthetic significance of polymerization by $S_N2$' and aza-Michael reactions.

Generalized strategy of this concept is summarized in **Scheme 2-8**. Consequently, the developed new polycondensation system has a significance as an alternative way to access alternating ROP of heterocycle. The concept to develop new ROPs by $S_N2$' reaction is applied to another monomer design described in Chapter 5.

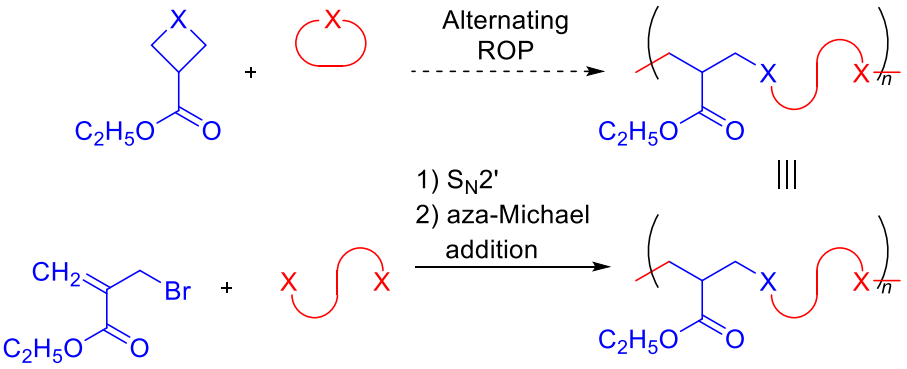


**Scheme 2-8**. Polymerization by $S_N2$' and aza-Michael reactions as an alternative route to alternating ROP.

## 4. Experimental

***Instruments.***

$^{1}H$ and $^{13}C$ NMR spectra were recorded in $CDCl_3$ (Kanto Chemical) on AVANCE 400 (Bruker) and AVANCE NEO (Bruker) spectrometers. Chemical shifts in $^{1}H$ and $^{13}C$ NMR spectra were referred to the signal of tetramethylsilane (TMS) and solvent ($CDCl_3$), respectively. Molecular weight and its distributions were determined at 40 °C by size-exclusion chromatography (SEC) on an EXTREMA chromatograph (JASCO) equipped with two SEC columns [PL-gel, Mixed C (300 mm _7.5 mm), Polymer Laboratories], using tetrahydrofuran (THF, Wako Pure Chemical Industries, for HPLC grade) as an eluent (flow rate = 0.8 mL $min^{-1}$), and calibrated against standard polystyrene (PS) samples (TSK-gel oligomer kit, Tosoh, Mn: $1.03 \times 10^6$, $3.89 \times 10^5$, $1.82 \times 10^5$, $3.68 \times 10^4$, $1.36 \times 10^4$, $5.32 \times 10^3$, $3.03 \times 10^3$, $8.73 \times 10^2$) and detected with UV (UV-4070, JASCO) and RI (RI-4030, JASCO) detectors.

***Materials***

Triethylamine ($Et_3N$), 1,8-diazabicyclo[5.4.0]undec-7-ene (DBU), tributylphosphine ($Bu_3P$), 1,10-decanedithiol, 2,3-butanedithiol, 3,6-dioxa-1,8-octanedithiol, dithioerythritol, 4,4'-thiobisbenzenethiol, hexamethylenediamine, 1,12-diaminododecane, 1,2-bis(3-aminopropoxy)ethane, *N,N'*-dimethyl-1,6-diaminohexane, 2,2-bis[4-(4-aminophenoxy)phenyl]propane were purchased from Tokyo Chemical Industry Co., Ltd. Sodium thiosulfate ($Na_2SO_3$), ethyl acetate, potassium carbonate ($K_2CO_3$) were purchased from Yoneyama Yakuhin Kogyo Co, Ltd. Magnesium sulfate ($MgSO_4$), sodium sulfate ($Na_2SO_4$), chloroform ($CHCl_3$), dichloromethane ($CH_2Cl_2$), tetrachloromethane ($CCl_4$), tetrahydrofuran (THF), acetonitrile ($CH_3CN$) and *N,N*-dimethylformamide (DMF) were purchased from Wako Pure Chemical Industries, Ltd. α-(Bromomethyl)acrylate was a kind gift from Chemicrea Inc. Benzoylchloride was a kind gift from Iharanikkei Chemical Industry Co., Ltd,.

***Synthesis***

**2-3a**: A solution of **2-1** (2.92 g, 15.1 mmol) in $CH_3CN$ (15 mL) was added dropwise to a solution of **2-2a** (9.32 g, 45.1 mmol) and $Et_3N$ (4.2 mL, 30 mmol) in $CH_3CN$ (30 mL).

After 1 h, water (100 mL) was added, and the organic products were extracted with $Et_2O$ (100 mL). The organic layer was washed with $Et_2O$ (100 mL), dried over $MgSO_4$ and concentrated under reduced pressure to afford the crude product (10.5 g). The product was purified by silica gel column chromatography using Wakogel C-400HG (Wako Pure Chemical Industry, 100 g) and hexane. After the removal of unreacted **2-2a**, the eluent was changed to a co-solvent of hexane–EtOAc (v/v = 10/1). The concentrated residue was then purified again by silica gel column chromatography using Wakogel C-400HG (200 g) and co-solvent of hexane–EtOAc (v/v = 25/1) to afford **2-3a** (0.244 g, 5.07%). $^1$H NMR spectrum (400 MHz, $CDCl_3$, 26 °C): δ/ppm 6.20 (1H, d, $J$ = 1.2 Hz, $CH_2$=), 5.65 (1H, dd, $J_1$ = 1.2 Hz, $J_2$ = 0.8 Hz, $CH_2$=), 4.24 (2H, q, $J$ = 7.2 Hz, *O*-$CH_2$), 3.38 (2H, d, $J$ = 0.8 Hz, allyl), 2.52 (2H, q, $J$ = 7.2 Hz, *S*-$CH_2$), 2.46 (2H, q, $J$ = 7.2 Hz, $\underline{CH_2}$SH), 1.64-1.52 (4H, m, S$CH_2\underline{CH_2}$) and 1.35-1.27 (15H, m, $CH_2$, $CH_3$)

**Stepwise synthesis of P2-1/2-2a:** $Bu_3P$ (16.2 mg, 80 μmol) was added to a solution of **2-3a** (0.127 mg, 0.400 mmol) in $CH_3CN$ (0.40 mL). The reaction mixture was heated at 50 °C for 17 h. After cooling to room temperature, $CHCl_3$ (5.0 mL) was added, and the organic layer was washed with 0.13 M HCl aq (4.5 mL). The organic layer was collected, and the aqueous layer was extracted again with $CHCl_3$ (4.0 mL). The combined organic layers were dried over $MgSO_4$ and then concentrated under reduced pressure. The residual solution was dried *in vacuo* to afford the polymer (0.112 g, 79%). $M_n$ = 10000, $Đ$ = 1.71.

**One-pot synthesis of P2-1/2-2a**: Typical procedure is shown. A solution of **2-1** (0.164 g, 0.759 mmol) in $CH_3CN$ (0.25 mL) was added dropwise to a solution of **2-2a** (0.156 g, 0.808 mmol) and $Et_3N$ (0.13 mL, 0.96 mmol) in $CH_3CN$ (0.25 mL). After 30 min, $Bu_3P$ (31 mg, 0.15 mmol) in $CH_3CN$ (0.25 mL) was added. The reaction mixture was heated at 50 °C for 24 h. After cooling to room temperature, $CHCl_3$ (7.0 mL) was added, and the organic layer was washed with 0.2 M HCl aq. (8.5 mL). The organic layer was collected, and the aqueous layer was extracted again with $CHCl_3$ (5.0 mL). The combined organic layers were washed with brine (10 mL), dried over $MgSO_4$ and then concentrated under reduced pressure. The residual solution (*ca*. 0.5 mL) was poured into hexane (20 mL). The precipitate was collected by centrifugation and dried *in vacuo* to afford the polymer

(0.217 g, 86%). $M_n$ = 5000, $Đ$ = 1.73.

**Model reaction of 2-1 and 2-4**: **2-4** (0.12 mL, 1.5 mmol) was added dropwise to a solution of **2-1** (0.290 g, 1.50 mmol) and DBU (0.27 mL, 1.80 mmol) in $CD_3CN$ (1.50 mL). After 1 h, an appropriate amount of the reaction mixture was collected and $^1H$ NMR spectrum was measured.

**One-pot synthesis of P' 2-1/2-7a**: Typical procedure is shown. A solution of **2-1** (0.145 g, 0.750 mmol) in $CH_3CN$ (0.30 mL) was added dropwise to a solution of **2-7a** (0.156 g, 0.808 mmol) and DBU (0.13 mL, 0.87 mmol) in $CH_3CN$ (0.45 mL) under room temperature. After 24 h, DBU (0.13 mL, 0.87 mmol) and a solution of **2-8** (0.210 g, 1.50 mmol) in $CH_3CN$ (0.30 mL) was added dropwise to the reaction mixture under room temperature. After 2 h, the reaction mixture and precipitate were poured into water (30 mL). The precipitate was collected by centrifugation and dried *in vacuo* to afford **P' 2-1/2-7a** (0.396 g, >99%). $M_{n,NMR}$ = 9800, $M_{n,\,SEC}$ = 2100, $Đ$ = 2.29, Amidation ratio = 94%.

**References**

(1) (a) K. C. Nicolaou, T. Montagnon, S. A. Snyder, *Chem. Commun.*, **2003**, 551. (b) P. J. Parsons, C. S. Penkett, A. J. Shell, *Chem. Rev*, **1996**, 96, 195.

(2) (a) R. Hu, W. Li, B. Z. Tang, *Macromol. Chem. Phys.*, **2016**, 217 , 213. (b) H. Deng, T. Han, E. Zhao, R. T. K. Kwok, J. W. Y. Lam, B. Z. Tang, *Macromolecules*, **2016**, 49, 5475. (c) Y. Liu, J. W. Lam, X. Zheng, Q. Peng, R. T. K. Kwok, H. H. Y. Sung, I. D. Williams, B. Z. Tang, *Macromolecules*, **2016**, 49, 5187. (d) W. Li, X. Wu, Z. Zhao, A. Qin, R. Hu, B. Z. Tang, *Macromolecules*, **2015**, 48, 7747. (e) Z.-Q. Chen, T. Chen, J.-X. Liu, G.-F. Zhang, C. Li, W.-L. Gong, Z.-J. Xiong, N.-H. Xie, B. Z. Tang, M.-Q. Zhu, *Macromolecules*, **2015**, 48, 7823. (f) Y. Liu, Z. Zhao, J. W. Y. Lam, Y. Zhao, Y. Chen, Y. Liu, B. Z. Tang, *Macromolecules*, **2015**, 48, 4241. (g) H. Deng, E. Zhao, H. Li, J. W. Y. Lam, B. Z. Tang, *Macromolecules*, **2015**, 48, 3180. (h) C. Zheng, H. Deng, Z. Zhao, A. Qin, R. Hu, B. Z. Tang, *Macromolecules*, **2015**, 48, 1941. (i) H. Kim, T.-L. Choi, *ACS Macro Lett.*, **2014**, 3, 791. (j) A. Sehlinger, P.-K. Dannecker, O. Kreye, M. A. R. Meier, *Macromolecules*, **2014**, 47, 2774. (k) O. Kreye, T. Tóth, M. A. R. Meier, *J. Am. Chem. Soc.*, **2011**, 133, 1790.

(3) (a) N. H. Gromwell, D. S. Soriano, E. Doomes, *J. Org. Chem.*, **1980**, 45, 4983. (b) S.Nowaczyk , C. Alayrac, P. Metzner, M.-T. Averbuch-Pouchot, *J. Org. Chem.*, **2002**, 67, 6852. (c) C. Madelaine, V. Valerio, N. Maulide, *Angew. Chem. Int. Ed.*, **2010**, 49, 1583. (d) S. Patil, L. Chen, J. M. Tanko, *Eur. J. Org. Chem.*, **2014**, 2014, 502. (e) D. Scharnagel, A. Müller, F. Prause, M. Eck, J. Goller, W. Milius, M. Breuning, *Chem. Eur. J.*, **2015**, 21, 12488. (f) The detailed reactivity of **2-1** is reviewed on web: J. Villiéras and M. Villiéras, Ethyl 2-(Bromomethyl)acrylate, in *e-EROS Encyclopedia of Reagents for Organic Synthesis,* John Wiley & Sons, DOI: 10.1002/047084289X.re048.pub2.

(4) (a) 7 S. Habaue, H. Yamada, Y. Okamoto, *Macromolecules*, **1996**, 29, 3326. (b) S. Habaue, H. Yamada, T. Uno, Y. Okamoto, *J. Polym. Sci. Part A: Polym. Chem.*, **1997**, 35, 721. (c) S. Habaue, M. Morita, Y. Okamoto, *Macromolecules*, **2002**, 35, 2432. (d) R. A. Evans, G. Moad, E. Rizzardo, S. H. Thang, *Macromolecules*, **1994**, 27, 7935. (e) Y. Kohsaka, Y. Matsumoto, T. Kitayama, *Polym. Chem.*, **2015**, 6, 5026. (f)

B. Yamada, O. Konosu, K. Tanaka, F. Oku, *Polymer*, **2000**, 41, 5625. (g) A. Onen, Y. Yagci, *Macromol. Chem. Phys.*, **2001**, 202, 1950. (h) F. Yilmaz, A. Sudo, T. Endo, *J. Polym. Sci. Part A: Polym. Chem.*, **2010**, 48, 4178.

(5) (a) Y. Kohsaka, S. Ishihara, T. Kitayama, *Macromol. Chem. Phys.*, **2015**, 216, 1534. (b) Y. Kohsaka, K. Yamamoto and T. Kitayama, *Polym. Chem.*, **2015**, 6, 3601. (c) Y. Kohsaka, T. Kurata, K. Yamamoto, S. Ishihara, T. Kitayama, *Polym. Chem.*, **2015**, 6, 1078. (d) Y. Kohsaka, T. Kurata, T. Kitayama, *Polym. Chem.*, **2015**, 4, 5043. (e) A. Lowe, *Polym. Chem.*, **2010**, 1, 17. (f) A. Lowe, *Polym. Chem.*, **2014**, 5, 4820. (g) H. Durmaz, M. Butun, G. Hizal and U. Tunca, *J. Polym. Sci., Part A: Polym. Chem.*, **2012**, 50, 3116. (h) B. B. Uysal, U. S. Gunay, G. Hizal and U. Tunca, *J. Polym. Sci., Part A: Polym. Chem.*, **2014**, 52, 1581. (i) U. Tunca, *J. Polym. Sci., Part A: Polym. Chem.*, **2014**, 52, 3147.

(6) (a) R. M. Coates, J. W. Williams, *J. Org. Chem.*, **1974**, 39, 3054. (b) H. B. Henbest, R.A. L. Wilson, *J. Chem. Soc.*, **1957**, 1958. (c) K. Takeda, K. Hamamoto, K. Sasaki, N. Maezono, A. Murabayashi, *Steroids*, **1963**, 2, 27. (d) P. A. Brady, J. Carnduff, F. Monaghan, *Tetrahedron Lett.*, **1977**, 3295. (e) U.K. Pandit, F. R. MasCabre, *J. Chem. Soc., Chem. Commun.* **1971**, 552.

(7) (a) I. Ugi, C. Steinbrückner, *Angew. Chem.*, **1960**, 72, 267. (b) M. Passerini, *Gazz. Chem. Ital*, **1921**, 51, 126.

## *(Appendix)*

## *Decomposition of poly(thioether)s by thiol exchange reaction*

After this research, Miyazaki and Kohsaka have found that the poly(thioether), **P2-1/2-2a**, underwent reversible main chain scission by a treatment with $Et_3N$ by retro-Michael addition ($E_1cB$) reaction. This reaction was in equilibrium and incomplete degradation was observed. Nevertheless, the addition of excess benzyl mercaptan (**2-3**) into the reaction system allowed to end-capping of acrylate moieties by Michael addition (**Scheme 2-9**). For example, **P2-1/2-2a** ($M_n$ = 10700, $Đ$ = 1.89), 5.0 mol equivalents of **2-3** per the repeating unit and DBU (20 mol%) was added to cosolvent of chloroform–DMF and reacted for 24 h to lead the decrease of molecular weight ($M_n$ = 2100, $Đ$ = 1.83). A similar experiment with $Et_3N$ instead of DBU resulted in less decrease of molecular weight ($M_n$ = 6200, $Đ$ = 1.70), probably due to less efficiency of $E_1cB$ reaction by lower basicity.

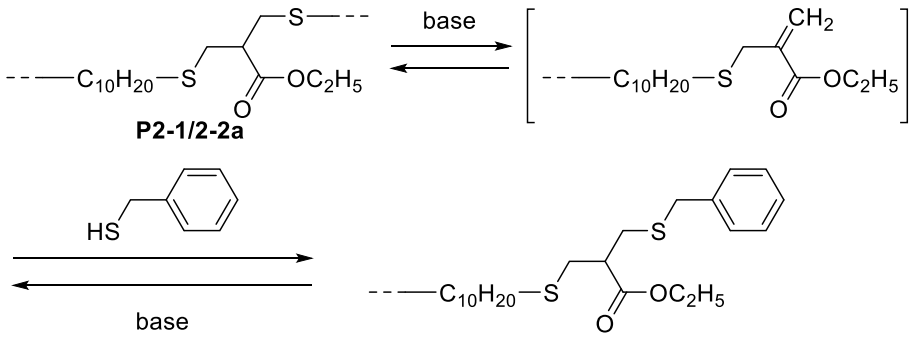


**Scheme 2-9.** Main chain scission of **P2-1/2-2a** via thiol exchange reaction.

*Chapter 3*

# Polycondensation by Tandem Reaction for Degradable Polymers by E1cB Reaction

## 1. Introduction

Environmental pollution by plastic wastes, particularly marine pollution by microplastics, have become a significant issue all over the world. In order to solve this problem, developments of degradable polymers are desirable. In the past decades, biodegradable polymers have gained researchers' attention, such as poly(L-lactic acid) (PLLA),[1] poly(ε-caprolactone) (PCL),[1] poly(butylene succinate) (PBS)[2] and polyamide-4.[3] However, the difficulty in control of biodegradation and limitation in molecular design have remained as significant problems, and other strategy to induce efficient polymer degradation is desirable. For example, Shabat *et al.* have been proposed the concept of self-immolative polymers (SIPs), defined as macromolecules that cause depolymerization or complete degradation to small molecules triggered by external stimuli. In this decades, the many reports to develop SIPs have been reported.[5]

Main chain scissions are other strategy to achieve efficient decompose; a cleavage of one covalent bond leads to significant decrease of molecular weight, enhancing chain motion to increase the degradation rate. However, the scission of carbon chains remains as a technical issue. Recently, Kazama and Kohsaka have reported the main chain scission of vinyl polymers by acid hydrolysis.[6] Although the reaction mechanism has not been detected clearly, retro-Aldol reaction is proposed as a key reaction. Miyazaki and Kohsaka have reported conjugate substitution of α-(substituted methyl)acrylates, *i.e.* $S_N2'$ reaction described in Chapter 1, is also effective to lead main chain scission.[7] On the other hand, Hoyle *et al.* have reported the main chain scission utilizing E1cB reaction.[8] In Chapter 2, the author also has reported the main chain scission by E1cB reaction, but the existence of reversible reaction (Michael addition) demanded end-capping of decomposed fragments by monothiols. In this Chapter, therefore, irreversible main chain scission by E1cB reaction was attempted. The polymerization design was similar to that in Chapter 2, but the α-(substituted methyl)acrylate skeletons in the backbone have a substituent at the allylic position so that the decomposed fragment by E1cB reaction should afford an *endo*-olefin, inactive chain end to reverse reaction (Michael addition, **Scheme 3-1**). In this chapter, design and preparation of such polymers are reported.

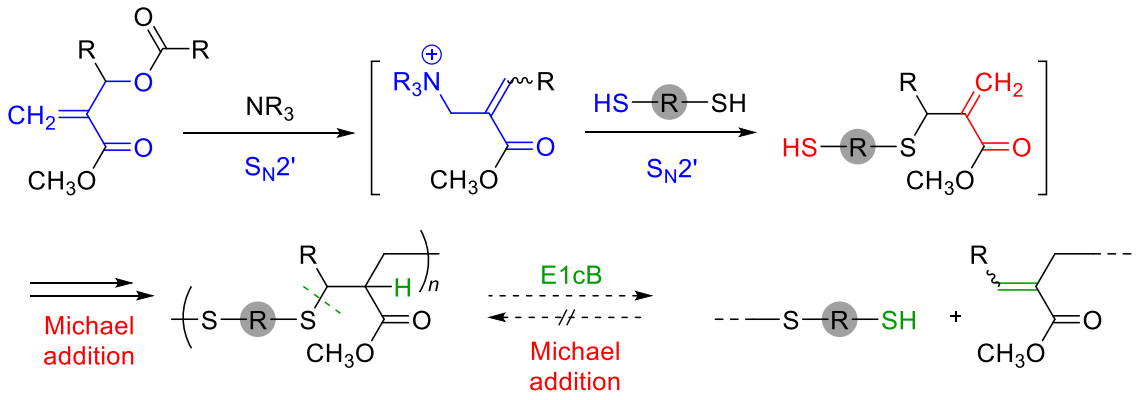


**Scheme 3-1**. Design of degradable polymers by main chain scission via irreversible $E_1cB$ reaction.

# 2. Results and Discussion

## 2.1 Monomer Synthesis

***Synthesis of Methyl 2-(1-benzoyloxyethyl)acrylate (3-2)***

Methyl 2-(1-benzoyloxyethyl)acrylate (**3-2**) was prepared through two steps according to the literatures (**Scheme 3-2**).[9] Morita-Baylis-Hillman reaction between methyl acrylate and acetaldehyde was carried out to yield methyl 2-(1-hydroxyethyl)acrylate (**3-1**). Then, benzoyl chloride was reacted with **3-1** to yield **3-2**. The isolation of **3-2** was confirmed by $^1$H NMR spectrum (**Figure 3-1**).

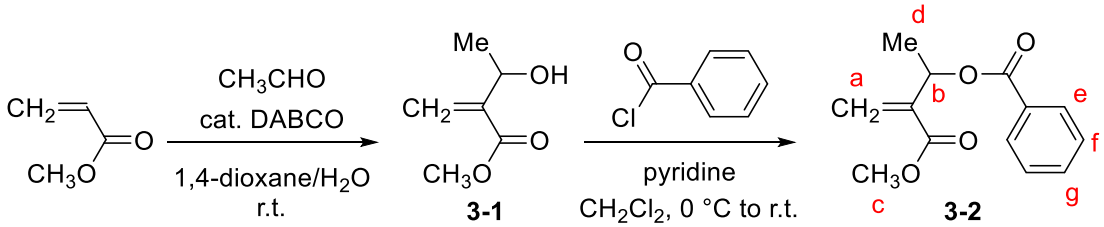


**Scheme 3-2.** Synthesis of Methyl 2-(1-benzoyloxyethyl)acrylate (**3-2**).

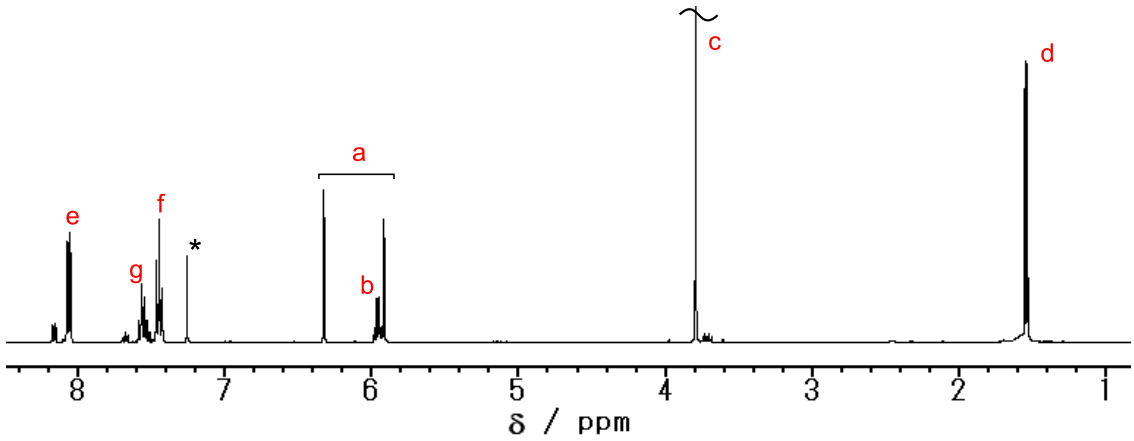


**Figure 3-1.** $^1$H NMR spectrum of purified **3-2** (400 MHz, $CDCl_3$, 25 °C). *: $CHCl_3$

***Synthesis of Methyl 2-[benzoyloxy(phenylmethyl)]acrylate (3-4)***

Methyl 2-(benzoyloxy(phenylmethyl)acrylate (**3-4**) was synthesized through two steps (**Scheme 3-3**). Morita-Baylis-Hillman reactions of methyl acrylate and benzaldehyde were conducted to yield methyl 2-[hydroxy(phenylmethyl)]acrylate (**3-3**). Then, acylation by benzoyl chloride afforded **3-4**, characterized by $^1$H NMR spectrum (**Figure 3-2**).

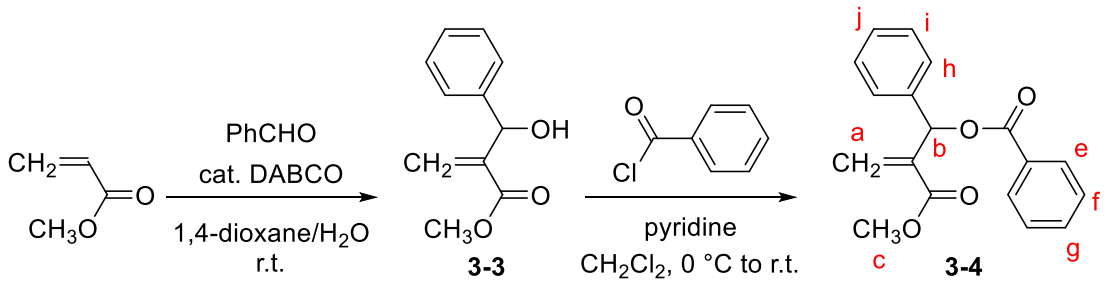


**Scheme 3-3.** Synthesis of methyl 2-(benzoyloxy(phenylmethyl)acrylate (**3-4**).

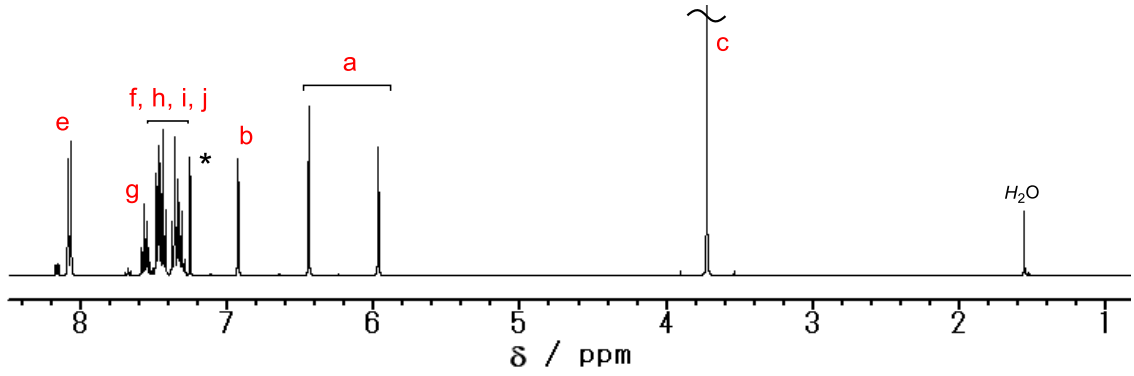


**Figure 3-2.** $^{1}$H NMR spectrum of purified **3-4** (400 MHz, $CDCl_3$, 25 °C). *: $CHCl_3$

## 2.2 Model Experiments of $S_N2$' Reaction

***Model Experiments with 3-2 and Benzyl mercaptan***

As described in **Scheme 3-1**, the aimed polymerization proceeds via two steps: $S_N2$' reaction and the subsequent Michael addition. However, the first step, $S_N2$' reaction, was expected to accompany some side reactions (**Scheme 3-4**). In order to avoid the side reactions, model experiments with benzyl mercaptan (BnSH) were conducted.

BnSH was reacted to **3-2** in the presence of various bases at room temperature in $CDCl_3$ to analyze the product compositions of *exo*-olefin **3-5** and *endo*-olefin **3-6** by $^{1}$H NMR spectrometry (**Scheme 3-4a**). In the absence of base, the $S_N2$' reaction did not proceed (**Table 3-1**, Entry 0). The reaction of **3-2** and 1,4-diazabicyclo[2.2.2]octane (DABCO, 1.2 equiv.) was expected to afford an ammonium salt, but the intermediate was not observed in the $^{1}$H NMR spectrum (Entry 1, **Figure 3-3**); instead, the signals corresponding to diene **3-7**, generated by E2 reaction of **3-2**, and cyclohexene derivatives **3-8**, generated by Diels-Alder reaction of **3-7** and **3-2**, were observed (**Scheme 3-4b**).

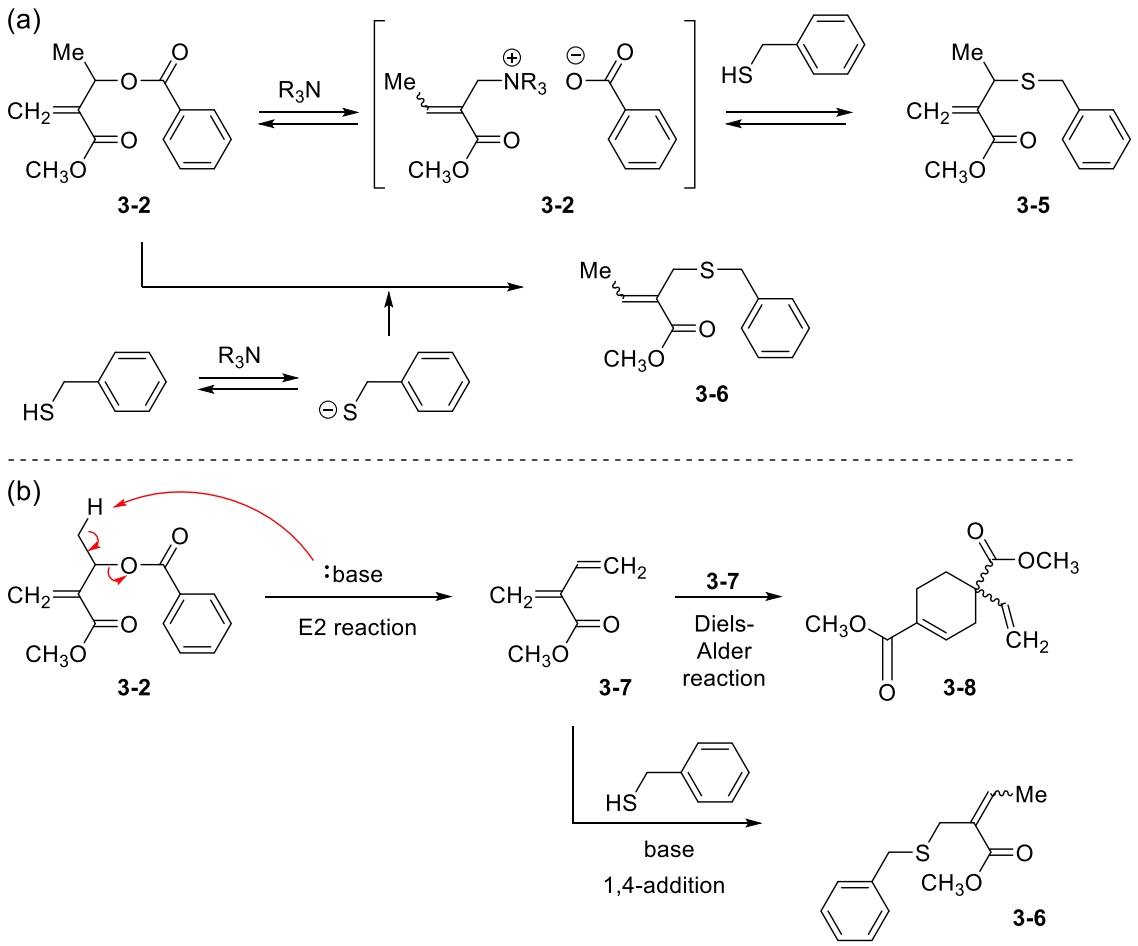


**Scheme 3-4.** (a) $S_N2$' reaction with BnSH and **3-2**, (b) possible side reactions.

**Table 3-1.** $S_N2$' reaction onto **3-2** in the presence of various bases.

| Entry[a] | Base (equimol.) | Time [h] | Conversion[b] [%] | Composition[b] / % | | | |
|---|---|---|---|---|---|---|---|
| | | | | **3-5** | **3-6** | **3-7** | **3-8** |
| 0 | – | 1 | 0 | – | – | – | – |
| 1[c] | DABCO[d] (1.2) | 1 | 86 | – | – | 85 | 15 |
| 2 | DABCO[d] (1.2) | 1 | >99 | 95 | 1 | 1 | 2 |
| 3 | DABCO[d] (0.3) | 15 | 81 | 94 | 1 | 3 | 2 |
| 4 | *i*Pr$_2$NEt (0.3) | 24 | >1 | trace | trace | – | trace |
| 5 | *i*Pr$_2$NEt (1.2) | 24 | >1 | – | trace | – | trace |
| 6 | Et$_3$N (0.3) | 24 | >1 | trace | trace | – | trace |
| 7 | Et$_3$N (1.2) | 24 | 26 | 38 | 58 | – | 4 |
| 8 | DBU[e] (0.3) | 36 | 27 | 1 | 95 | – | 4 |
| 9 | DBU[e] (1.2) | 3 | >99 | 2 | 96 | 1 | 1 |

[a] **1**: 0.0598 mmol, [**3-2**]/[BnSH] = 1/1.0, $CDCl_3$: 0.7 mL, room temperature.
[b] Determined by $^1$H NMR spectra. [c] Without BnSH. [d] 1,4-Diazabicyclo[2.2.2]octane.
[e] 1,8-Diazabicyclo[5.4.0]undec-7-ene.

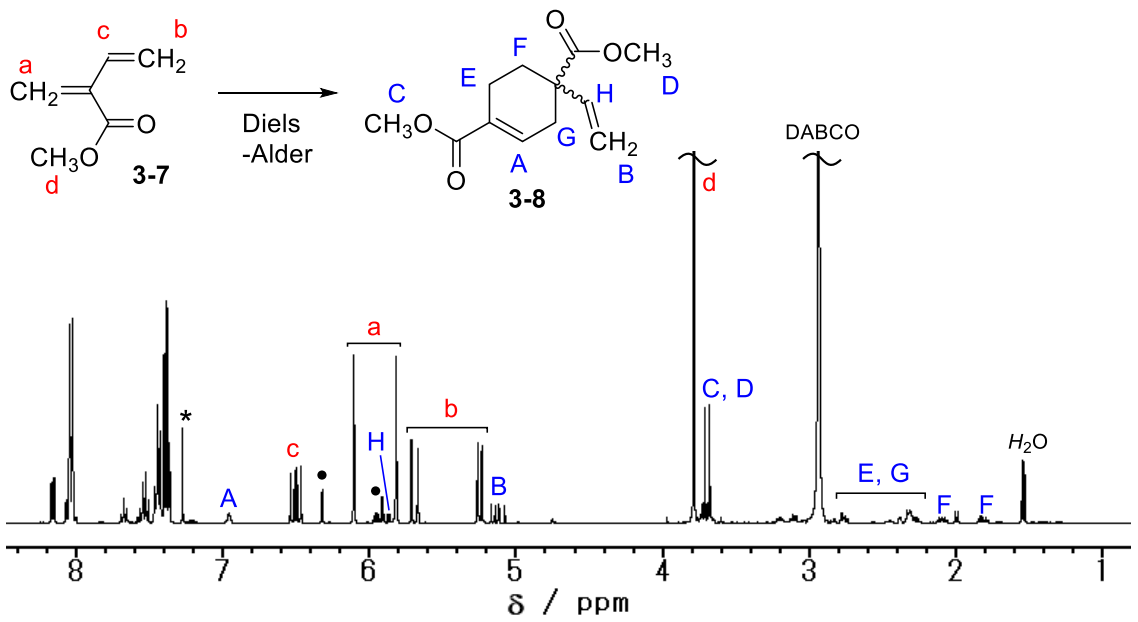


**Figure 3-3.** $^{1}$H NMR spectrum in Entry 2. (400 MHz, $CDCl_3$, 25 °C). *: $CHCl_3$

In the following entries, therefore, a solution of **3-2** and BnSH was prepared in advance, and subsequently a base was added in order to avoid the E2 and Diels-Alder side reactions. The reaction in the presence of 1.2 equimolar of DABCO for 1 h afforded the *exo*-olefin product **3-5** with high selectivity without any side reaction (Entry 2). In addition, similar results were obtained with the catalytic amount of DABCO (30 mol%, Entry 3), although longer reaction time (15 h) was needed for high conversion. The $^{1}$H NMR spectral change at each reaction time shown in **Figure 3-4** indicates the slow reaction rate. If the BnSH or its thiolate anion underwent $S_N2$' reaction directly to **3-2**, **3-6** should be generated as a product (**Scheme 3-4**). However, the reaction proceeded selectively to afford **3-5**, suggesting that the sequential $S_N2$' reaction via the ammonium intermediate. In fact, the reactions in the presence of *i*$Pr_2$NEt, a base with poor nucleophilicity, did not proceed even when excess *i*$Pr_2$NEt was used (Entries 4 and 5). This also suggests that the formation of ammonium intermediate by $S_N2$' reaction was necessary to induce $S_N2$' reaction with BnSH.

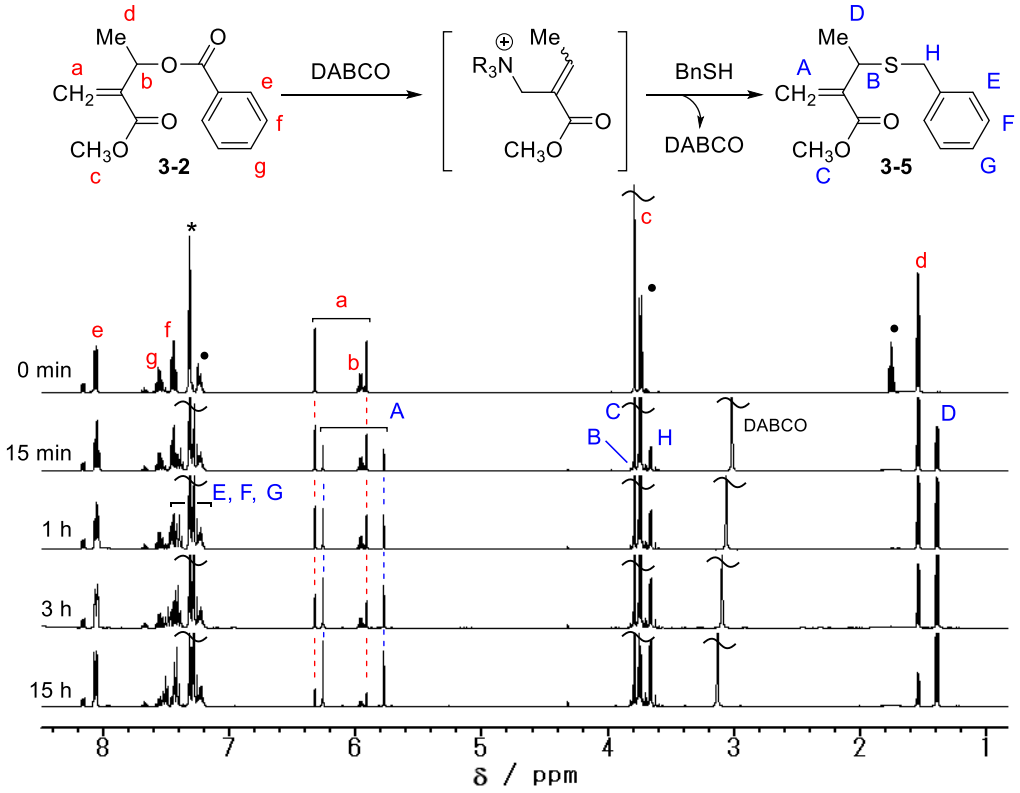


**Figure 3-4.** $^{1}$H NMR spectral changes in Entry 3 at each time (400 MHz, $CDCl_3$, 25 °C, *: $CHCl_3$,●; BnSH)

A catalytic amount of $Et_3N$ resulted in a low conversion (Entry 6), while excess $Et_3N$ slightly promoted the reaction (Entry 7). In this case, the products were a mixture of **3-5** **3-6**, and **3-8**. The formation of **3-5** can be explained by the ammonium intermediate (**Scheme 3-4a**). On the other hand, the above results of *i*$Pr_2$NEt suggested that the direct addition of thiolate anion to **3-2** was difficult. Since **3-8** was afforded in Entry 7, **3-7**, an intermediate with high reactivity should have been formed in the reaction. Then, BnSH or its thiolate anion would reacted to **3-7** to yield **3-6** (**Scheme 3-4b**).

1,8-Diazabicyclo[5.4.0]undec-7-ene (DBU), a stronger base, afforded **3-6** in a high selectivity (Entry 8), although the reaction was slow. The excess feeding of DBU led to high conversion (Entry 9). Since DBU was less nucleophilic but stronger base than DABCO, it simply worked as a base to deprotonate BnSH to promote direct $S_N2$' reaction. Overall, the products were strongly dependent on the bases.

***Model Experiments with 3-4 and Benzyl mercaptan***

In the reaction of **3-2**, the E2 and subsequential Diels-Alder reactions were observed as a side-reaction. These side reactions were triggered by the removal of a proton on the methyl substituent. Therefore, the allyl substituent was changed not to have a C–H bond at the connecting point; **3-4**, of which allyl substituent was a phenyl group, was chosen to avoid the side reactions (**Scheme 3-5**). DABCO (1.2 equiv.) was effective to afford the *exo*-olefin product **3-9** in a high selectivity (**Table 3-2**, Entry 11), excluding the side-reactions. *i*$Pr_2$NEt and DBU gave the *endo*-olefin product **3-10** in high selectivity (Entry 12, 14), and $Et_3N$ resulted in a mixture of **3-9** and **3-10** (Entry 13). These results were agreed with the expectation from the results in the reaction of **3-2**, but the E2 side reaction was almost completely suppressed due to the absence of protons on the allyl substituent.

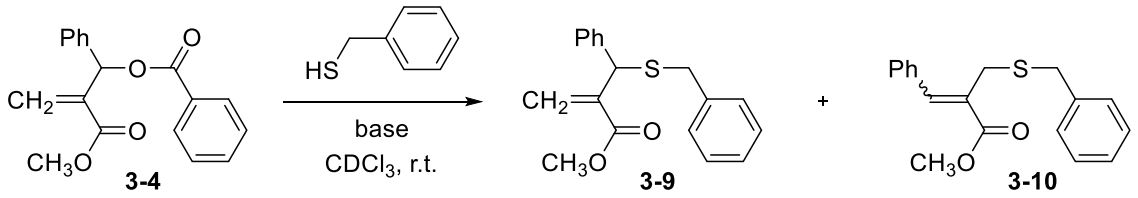


**Scheme 3-5.** The $S_N2$' reaction with BnSH and **3-4**.

**Table 3-2.** $S_N2$' reaction onto **3-4** in the presence of various bases.

| Entry[a] | Base | Time / h | Conversion[b] / % | Product ratio[b] / % | |
|---|---|---|---|---|---|
| | | | | **3-9** | **3-10** |
| 10 | – | 1 | 0 | – | – |
| 11 | DABCO | 1 | 97 | >99 | trace |
| 12 | *i*$Pr_2$NEt | 24 | 18 | trace | >99 |
| 13 | $Et_3N$ | 24 | 35 | 31 | 61 |
| 14 | DBU | 1 | 97 | 3 | 97 |

[a] **3-4**: 0.0598 mmol, [**3-4**]/[BnSH]/[Base] = 1/1.0/1.2, $CDCl_3$: 0.7 mL, room temperature. [b] Determined by $^1$H NMR spectrometry. [c] Without BnSH. [d] 1,4-Diazabicyclo[2.2.2]octane. [e] 1,8-Diazabicyclo[5.4.0]undec-7-ene.

## 2.3 Tandem Polymerization

The results of the model experiments suggested that the reaction of **3-4** and dithiols would proceed by affording an *exo*-olefin product in the presence of DABCO; the subsequent addition of $Bu_3P$ as a catalyst to promote Michael addition resulted in

**Table 3-3.** Tandem polymerization of **3-4** via isomeric controls.

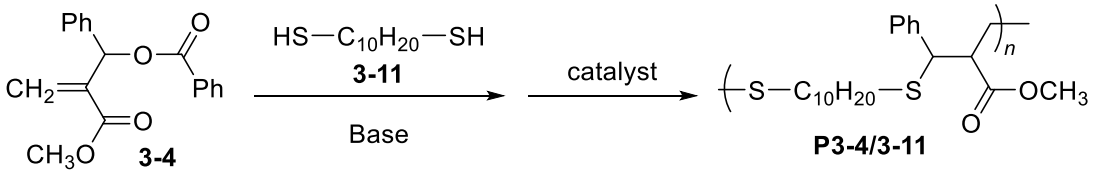


| Entry[a] | Base | Catalyst | Solvent | Temp. / °C | Yield / % | $M_n$[b] | $Đ$[b] |
|---|---|---|---|---|---|---|---|
| 1 | DABCO | $Bu_3P$ | $CHCl_3$ | 25 | 10 | 1000 | 2.25 |
| 2 | DABCO | $Bu_3P$ | $CH_3CN$ | 25 | 27 | 1600 | 2.09 |
| 3 | DABCO | $Bu_3P$ | $CH_3CN$ | 50 | 66 | 1100 | 2.02 |
| 4[d] | DABCO | $Et_3N$ | $CH_3CN$ | 25 | 51 | 1900 | 1.78 |
| 5[d] | DABCO | $iPr_2NEt$ | $CH_3CN$ | 25 | 49 | 1800 | 2.31 |
| 6[d] | DABCO | DBU[c] | $CH_3CN$ | 25 | 83 | 5400 | 2.16 |
| 7 | DBU | $Bu_3P$ | $CHCl_3$ | 25 | >99 | 5600 | 2.10 |
| 8 | DBU | $Bu_3P$ | $CH_3CN$ | 25 | >99 | 4900 | 2.32 |
| 9 | DBU | $Bu_3P$ | $CH_3CN$ | 50 | >99 | 4800 | 2.08 |

[a] **3-4**: 0.750 mmol, [**3-4**]$_0$/[dithiol]$_0$/[DABCO]$_0$/[catalyst]$_0$ = 1 / 1.0 / 1.2 / 0.2, solvent: 0.75 mL, room temperature, 24 h. [b] Determined by SEC (THF, 40 °C, polystyrene standards). [c] 1,8-Diazabicylo[5.4.0]-undec-7-ene. [d] [**3-4**]$_0$/[dithiol]$_0$/[DABCO]$_0$/ [catalyst]$_0$ = 1 / 1.0 / 1.2 / 1.2

poly(thioether)s. Thus, the polymerization of **3-4** and dithiol **3-11** was conducted in the presence of DABCO (1.2 equiv.) in $CHCl_3$ at room temperature, *.i.e.* a similar condition to the model experiments. However, the resulted $M_n$ was not so high (**Table 3-3**, Entry 1, $M_n$ = 1000, $Đ$ = 2.25). Similar results were obtained even from the polymerizations in $CH_3CN$ at 25 °C (Entry 2, $M_n$ = 1600, $Đ$ = 2.09) and 50 °C (Entry 3, $M_n$ = 1100, $Đ$ = 2.02). In order to identify the reason why the polymerization did not proceed well, the polymerization was conducted in $CD_3CN$ and the reaction was traced by $^1$H NMR spectrometry (**Figure 3-5**). The $^1$H NMR spectrum of the reaction mixture after 1 h from the addition of DABCO showed the signals a-c corresponding to the *exo*-olefin intermediate (**Figure 3-5b**). In this stage, thus, the reaction proceeded as expected. After the addition of $Bu_3P$, a set of the *exo*-methylene signals a of the intermediate completely disappeared, indicating the Michael addition (**Figure 3-5c**). However, signal X assigned to the *endo*-olefin proton was clearly observed around 7.7 ppm. This indicated that an unexpected reaction proceeded in the second step on Michael addition and that the formation of a stable *endo*- olefin structure inhibited the further propagation. A proposed

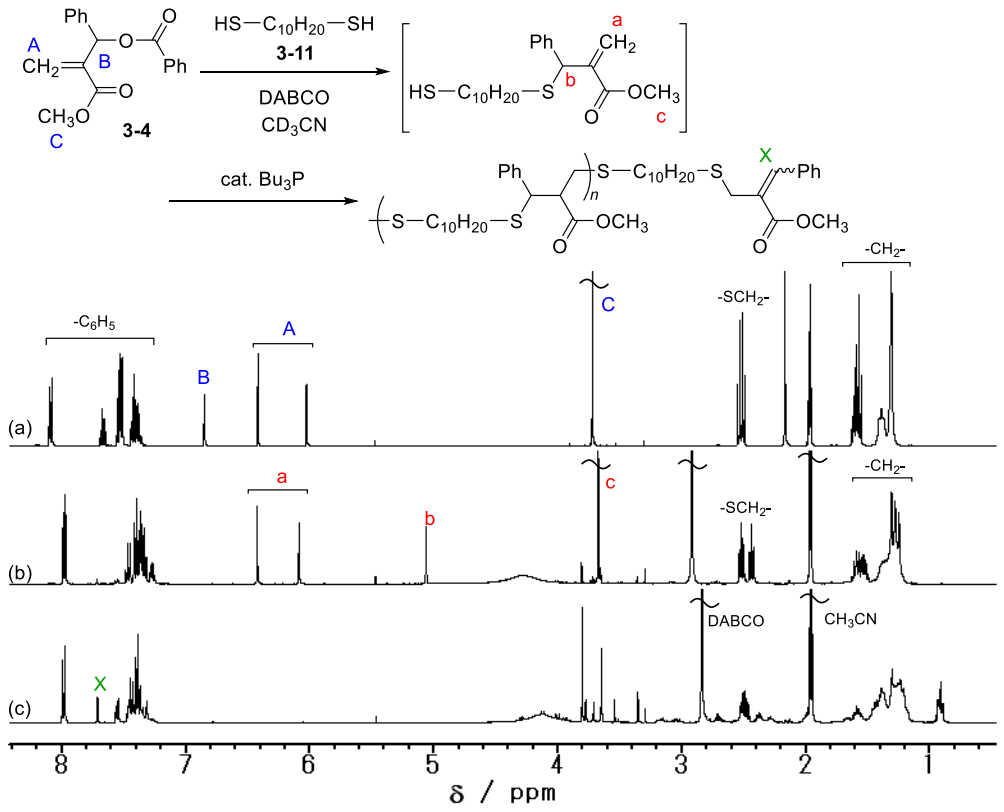


**Figure 3-5.** $^{1}$H NMR spectra of the reaction mixture (a) before adding DABCO, (b) 1 h after adding DABCO and (c) 16 h after adding $Bu_3P$. (400 MHz, $CD_3CN$, 25 °C).

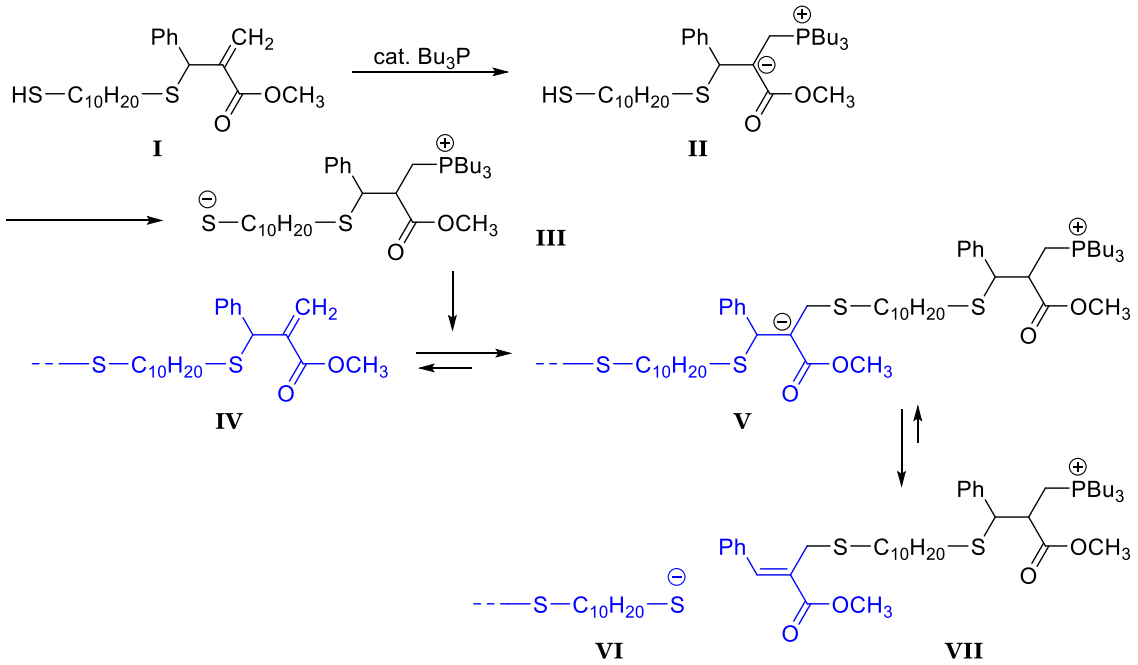


**Scheme 3-6.** Proposed termination reaction.

mechanism of the termination reaction is described in **Scheme 3-6**. The Michael addition catalyzed by $Bu_3P$ proceeds through the addition of thiolate anion **III** to form enolate intermediate **IV**, and the following elimination affords poorly active terminal-end **VII**.

Therefore, the catalyst of the Michael addition was investigated. The polymerization with catalysts of $Et_3N$ and $iPr_2NEt$ yielded similar results to the polymerization with $Bu_3P$ (Entries 4 and 5). On the other hand, a catalyst of DBU promoted the Michael addition (Entry 6). The $^1H$ NMR spectrum of the product is shown **Figure 3-6**. Although the signals x-z corresponding to the *endo*-olefin structure was still observed, relatively high molecular weight was achieved ($M_n$ = 5400, $Đ$ = 2.16). Remarkably, even when polymerization was conducted with DBU as the base in the absence of DABCO, which was a key to promote the formation of *exo*-methylene intermediate, similar polymeric products were obtained (**Scheme 3-7**, Entries 7–9). This implies that DBU can catalyze the Michael addition of the thiol end to the *endo*-olefin intermediate.

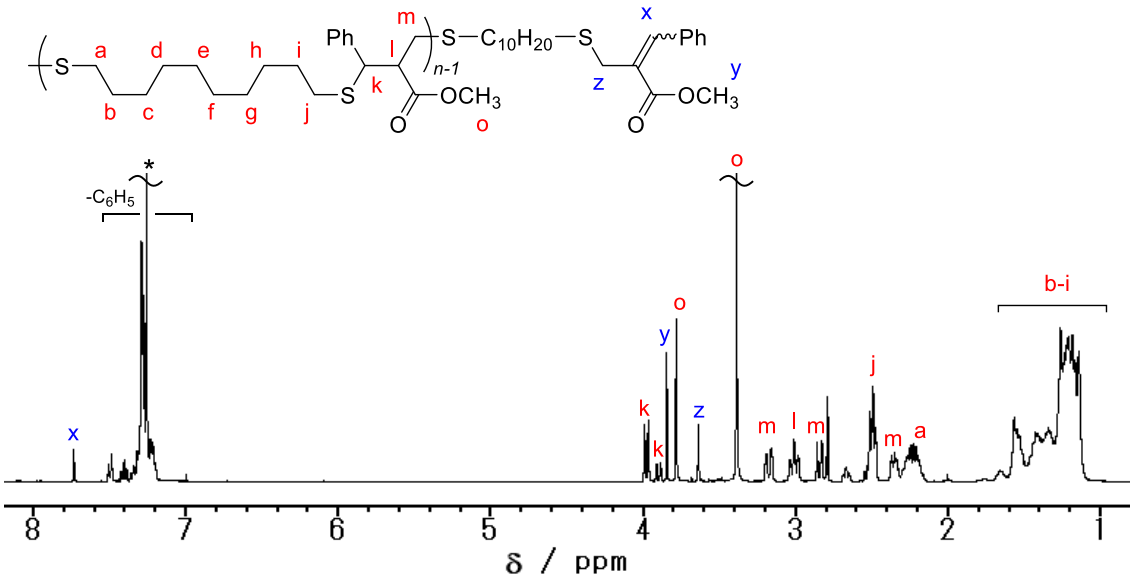


**Figure 3-6.** $^1H$ NMR spectrum of the product in Entry 6.
(400 MHz, $CDCl_3$, 25 °C) *:$CHCl_3$

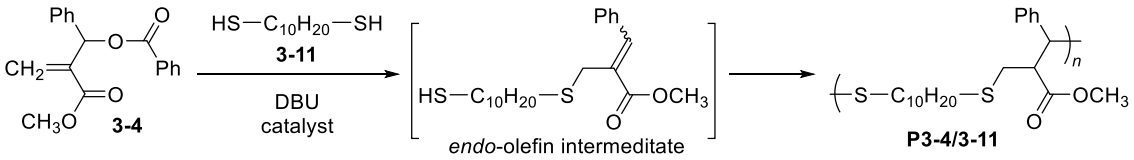


**Scheme 3-7.** Polymerization without DABCO catalyzed isomeric controls.

## 2.4 Main Chain Scission by E1cB Reaction

In Chapter 2, the main chain scission by E1cB reaction was reported, but the existence of reversible reaction (Michael addition) demanded the end-capping of decomposed fragments by monothiols. On the other hand, the resulted polymers in this chapter were introduced a phenyl group at the β-position so that the decomposed fragment by E1cB reaction should afford an *endo*-olefin, inactive chain end to reverse reaction (**Scheme 3-8**). Therefore, it is expected that the main chain scission by E1cB on **P3-4/3-11** can conducted without end-capping.

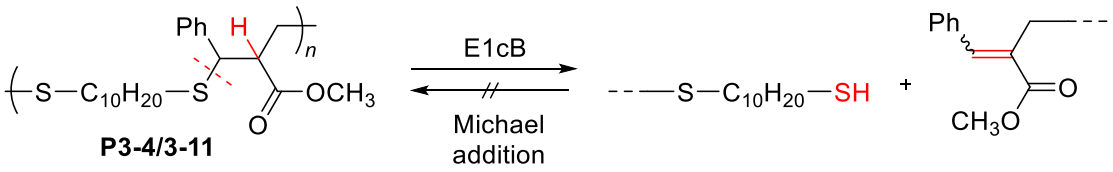


**Scheme 3-8.** Main chain scission by E1cB reaction.

The polymer obtained in Entry 7 was treated with excess DBU (1.2 equimolar to the repeating unit) in various solvents for 17 h. Although the polymer was not completely dissolved in $CH_3CN$ and DMSO, the main chain scission in these solvents resulted in decreases of molecular weights (**Figure 3-7a-c**). However, the SEC curves showed that the high molecular weight components remained, suggesting incomplete degradation. In these cases, it was expected that the E1cB reaction did not proceed efficiently because the polymer did not dissolve for $CH_3CN$ and DMSO. On the other hand, the reaction in DMF

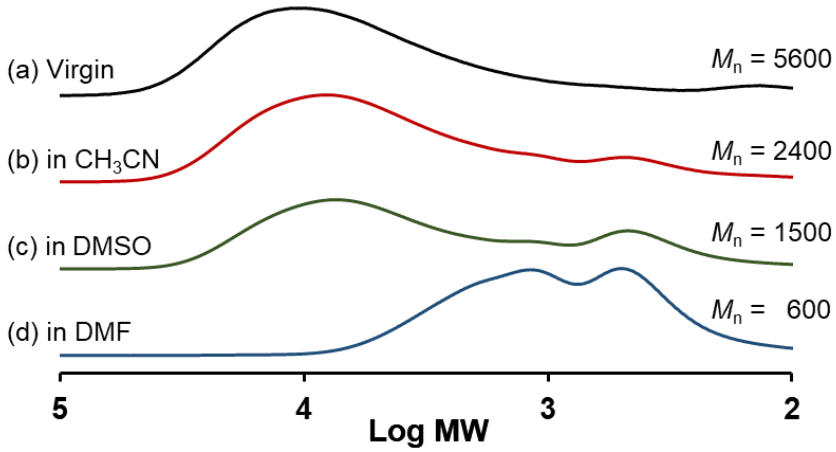


**Figure 3-7.** SEC curves of (a) virgin polymer and after E1cB reaction in (b) $CH_3CN$, (c) DMSO and (d) DMF. (THF, 40 °C, polystyrene standards)

proceeded in homogeneous system to lead efficient degradation to small molecules (**Figure 3-7d**). **Figure 3-8** shows the $^{1}$H NMR spectra before and after the reaction. The signals k-m assigned to the main chain structure scarcely observed after the reaction, and the signals x-z assigned to the chain-end structure were clearly observed. Those changes suggest the main chain scission by E1cB reaction.

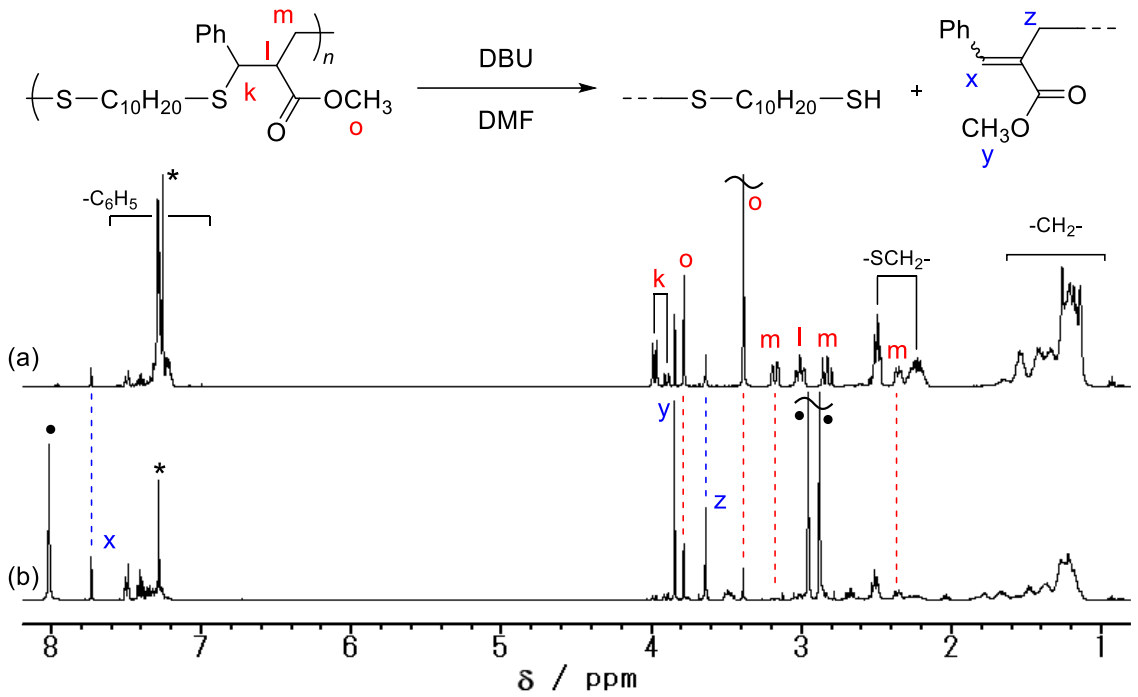


**Figure 3-8.** $^{1}$H NMR spectra (a) before and (c) after E1cB reaction. (400MHz, $CDCl_3$, 25°C) *: $CHCl_3$, ●: DMF

## 3. Conclusion

In this chapter, the author described the design of the poly(thioether)s irreversibly degradable by E1cB reaction. The design was similar to that in Chapter 2, but a substituent was introduced to the allylic position of the α-(substituted methyl)acrylates; this minor change was effective to increase the stability of decomposed products so that the E1cB degradation became irreversible. The incorporation of a methyl substituent resulted in some side reactions, E2 and the subsequent Diels-Alder reactions, while substitution with a phenyl group was effective monomer design to lead the reaction to $S_N2'$ mechanism selectively. The model reaction with thiols revealed that DBU dominatingly afforded an *endo*-olefin product less active to Michael addition, while DABCO afforded more active *exo*-olefin product via sequential $S_N2'$ reaction. Thus, the polymerization with dithiols were investigated by using DABCO, but it did not result in high molecular weights due to the formation of inactive chain-end. Surprisingly, DBU, which was expected as unsuitable base as it yields a less active *endo*-olefin intermediate, resulted in the highest molecular weight. The resulting polymers were easily decomposed to small molecules via irreversible E1cB reaction by treating with DBU in DMF. These results indicate that the substituent at the allylic position of α-(substituted methyl)acrylates contributes to the improvement of the degradability of the resulted polymer.

## 4. Experimental

***Instruments.***

$^{1}H$ and $^{13}C$ NMR spectra were recorded in $CDCl_3$ (Kanto Chemical) on AVANCE 400 (Bruker) and AVANCE NEO (Bruker) spectrometers. Chemical shifts in $^{1}H$ and $^{13}C$ NMR spectra were referred to the signal of tetramethylsilane (TMS) and solvent ($CDCl_3$), respectively. Molecular weight and its distributions were determined at 40 °C by size-exclusion chromatography (SEC) on an EXTREMA chromatograph (JASCO) equipped with two SEC columns [PL-gel, Mixed C (300 mm _7.5 mm), Polymer Laboratories], using tetrahydrofuran (THF, Wako Pure Chemical Industries, for HPLC grade) as an eluent (flow rate = 0.8 mL $min^{-1}$), and calibrated against standard polystyrene (PS) samples (TSK-gel oligomer kit, Tosoh, $M_n$: $1.03 \times 10^6$, $3.89 \times 10^5$, $1.82 \times 10^5$, $3.68 \times 10^4$, $1.36 \times 10^4$, $5.32 \times 10^3$, $3.03 \times 10^3$, $8.73 \times 10^2$) and detected with UV (UV-4070, JASCO) and RI (RI-4030, JASCO) detectors.

***Materials***

Methyl acrylate, acetaldehyde, 1,4-diazabicyclo[2.2.2]octane (DABCO), 1,10-decanedithiol, benzyl mercaptan were purchased from Tokyo Chemical Industry Co., Ltd. Sodium sulfate ($Na_2SO_4$), pyridine, hexane, ethyl acetate (EtOAc), chloroform ($CHCl_3$), dichloromethane ($CH_2Cl_2$), tetrahydrofuran (THF), acetonitrile ($CH_3CN$), toluene, *N,N*-dimethylformamide (DMF), dimethyl sulfoxide (DMSO), 1,4-dioxane, methanol (MeOH), hydrochromic acid (HCl aq.), 1,8-diazabicyclo[5.4.0.]undec-7-ene, $Et_3N$, and *i*PrNEt were purchased from Fujifilm Wako Pure Chemical Industries, Ltd. Benzoyl chloride was kind gift from Iharanikkei Chemical Industry Co., Ltds.

***Synthesis***

**Methyl 2-(1-hydroxyethyl)acrylate (3-1):**[9] Methyl acrylate (25.8 g, 300 mmol) and 1,8-diazabicyclo[2.2.2]octane (11.2 g, 100 mmol) were added to the solution of acetaldehyde (4.41 g, 100 mmol) in co-solvent of 1,4-dioxane and $H_2O$ (v/v = 1/1) at room temperature. After 24 h, the mixture was extracted with $Cl_2CH_2$ (100 mL × 2). The organic layer was washed with brine (100 mL) and dried over with $Na_2SO_4$. The organic layer was concentrated to yield a crude **3-1** (6.06 g, yield: 46.2%). The obtained **3-1** was used in the

next reaction without further purification. $^1$H NMR spectrum (400 MHz, $CDCl_3$, 25 °C): δ/ppm 6.22 (1H, s, $CH_2$=), 5.83 (1H, s, $CH_2$=), 4.63 (1H, quin, $J$ = 6.50 Hz, $\underline{CH}CH_3$), 3.80 (3H, s, $OCH_3$), 1.39 (3H, d, $J$ = 6.50 Hz, $CH\underline{CH_3}$)

**Methyl 2-(1-benzoyloxyethyl)acrylate (3-2):**[9] Pyridine (4.35 g, 55.0 mmol) was added to the solution of **3-1** (6.51 g, 50.0 mmol) in $CH_2Cl_2$ (80 mL) at 0 °C. After stirred the mixture for 10 min, the solution of benzoyl chloride (9.14 g, 65.0 mmol) in $CH_2Cl_2$ (20 mL) was added dropwise to the mixture at 0 °C. After stirred for 1 h, the mixture was stirred at room temperature for 24 h. Then, $H_2O$ (100 mL) was added to the reaction mixture at 0 °C, and the organic layer was collected. The aqueous layer was extracted with $CH_2Cl_2$ (50 mL × 2). The organic layers were combined and washed with $H_2O$ (100 mL) and brine (150 mL). The combined organic layer was dried over with $Na_2SO_4$ and concentrated to yield crude **3-2**. The yielded 3-2 was purified by the vacuum distillation using a Kugel Rohr (10 Torr/170 °C, 7.62g, 65.1%). $^1$H NMR spectrum (400 MHz, $CDCl_3$, 25 °C): δ/ppm 8.07 (2H, m, CH), 7.59-7.53 (1H, m, CH), 7.45(2H, m, CH), 6.33 (1H, s, $CH_2$=), 5.96 (1H, q, $J$ = 6.53 Hz, $\underline{CH}CH_3$), 5.29 (1H, s, $CH_2$=), 3.80 (3H, s, $OCH_3$), 1.55 (3H, d, $J$ = 6.53 Hz, $CH\underline{CH_3}$)

**Methyl 2-(hydroxy(phenylmethyl))acrylate (3-3):** Methyl acrylate (25.83 g, 300 mmol) and 1,8-diazabicyclo[2.2.2]octane (6.50 g, 58 mmol) were added to the solution of benzaldehyde (31.8 g, 300 mmol) in co-solvent of 1,4-dioxane and $H_2O$ (v/v = 1/1, 10 mL) at room temperature. After 24 h, $H_2O$ (150 mL) was added to the reaction mixture, and the mixture was extracted with $Cl_2CH_2$ (150 mL × 2). The organic layer was washed with brine (100 mL) and dried over with $Na_2SO_4$. The organic layer was concentrated and washed with hexane to yield a crude **3-3** (17.8 g, yield: 30.9%). The obtained **3-3** was used in the next reaction without further purification. $^1$H NMR spectrum (400 MHz, $CDCl_3$, 25 °C): δ/ppm 7.40-7.33 (4H, m), 7.31-7.26 (1H, m), 6.34 (1H, s, $CH_2$=), 5.83 (1H, t, $J$ = 1.22 Hz, $CH_2$=), 5.57 (1H, $J$ = 5.73 Hz, $\underline{CH}OH$), 3.73 (3H, s, $OCH_3$), 2.99 (1H, d, $J$ = 5.73 Hz, $CH\underline{OH}$)

**Methyl 2-(benzoyloxy(phenylmethyl))acrylate (3-4):** Pyridine (5.14 g, 65.0 mmol) was added to the solution of **3-3** (9.61 g, 50 mmol) in $CH_2Cl_2$ (40 mL) at 0 °C. After stirred the mixture for 10 min, the solution of benzoyl chloride (9.14 g, 65.0 mmol) in $CH_2Cl_2$

(40 mL) was added dropwise to the mixture at 0 °C. After stirred for 1 h, the mixture was stirred at room temperature for 24 h. Then, $H_2O$ (150 mL) was added to the reaction mixture at 0 °C, and the organic layer was collected. The aqueous layer was extracted with $CH_2Cl_2$ (20 mL × 2). The organic layers were combined and washed with 0.1 M HCl aq. (150 mL × 2 ) and brine (150 mL). The combined organic layer was dried over with $Na_2SO_4$ and concentrated to yield crude **3-4**. The yielded **3-4** was purified by silica gel column chromatography (hexane/EtOAc = 5/1, v/v) using Wakogel C-400HG (280 g) and recrystallization in hexane (4.44g, yield: 30.0%). $^1$H NMR spectrum (400 MHz, $CDCl_3$, 25 °C): δ/ppm 8.09-8.07 (2H, m, CH), 7.55-7.59 (1H, m, CH), 7.49-7.42 (4H, m, CH), 7.38-7.29 (3H, m, CH), 6.93 (1H, s, CCH), 6.45 (1H, s, $CH_2$=), 5.97 (1H, s, $CH_2$=), 3.73 (3H, s, $OCH_3$),

**Model experiment:** Typical procedure is shown. The solution of benzyl mercaptan (8.1 mg, 0.0718 mmol) in $CDCl_3$ (0.5 mL) was added to the solution of **3-2** (14.0 mg, 0.0598 mmol) in $CDCl_3$ (0.2 mL). Then, DABCO (0.22 mg, 0.0196 mmol) was added to the mixture at room temperature. The reaction mixture was analyzed by $^1$H NMR spectroscopy.

**P3-4/3-11:** Typical procedure is shown. The solution of 1,10-decanedithiol (**3-11**, 0.155 g, 0.750 mmol) in $CH_3CN$ (0.55 mL) and the solution of 1,8-diazabicyclo[2.2.2]octane (0.101 g, 0.900 mmol) in $CH_3CN$ (0.20 mL) was added to **3-4** (0.222 g, 0.750 mmol). After 1 h, $Bu_3P$ (0.0304 g, 0.150 mmol) was added to the reaction mixture. After 24 h, the reaction mixture was reprecipitated to MeOH (30.0 mL). The precipitate was collected by centrifugation and dried in vacuo to afford the polymer (7.8 mg, 27.4%).

**Degradation of P3-4/3-11:** Typical procedure is shown. The solution of 1,8-diazabicyclo[5.4.0]undec-7-ene (6.3 mg, 0.0414 mmol) in DMF (1.0 mL) was added to **P3-4/3-11** (12.6 mg, 0.0331 mmol/repeating unit). After 17 h, small portion of reaction mixtures was sampled to monitor by $^1$H NMR spectrometry and SEC.

**References**

(1) (a) J. C. Middleton, A. J. Tipton, *Biomaterials*, **2000**, *21*, 2335. (b) Y. Ikeda, H. Tsuji, *Macromol. Rapid Commun.* **2000**, *21*, 117.

(2) Y. Tokiwa, B. P. Calabia, C. U. Ugwu, S. Aiba, *Int. J. Mol. Sci.* **2009**, *10*, 3722.

(3) N. Yamano, A. Nakayama, N. Kawasaki, N. Yamamoto, S. Aiba, *J. Polym. Env.* **2008**, *16*, 141.

(4) A. Sagi, R. Weinstain, N. Karton, D. Shabat, *J. Am. Chem. Soc.* **2008**, *130*, 5434

(5) G. I. Peterson, M. B. Larsen, A. J. Boydston, *Macromolecules*, **2012**, *45*, 7317.

(6) A. Kazama, Y. Kohsaka, *Polym. Chem.* **2019**, *10*, 2764.

(7) Y. Kohsaka, T. Miyazaki, K. Hagiwara, *Polym. Chem.* **2018**, *9*, 1610.

(8) G. W. Fahnhorst, T. R. Hoye, *ACS Macro Lett.* **2018**, *7*, 143.

(9) G. Poklukar, M. Stephan, B. Mohar, *Adv. Synth. Catal.*, 2018, 360, 2566

*Chapter 4*

# Polycondensation by a Tandem Reaction Leading to Divergence in Backbone Structure

## 1. Introduction

Nature has an efficient molecular strategy that one monomer produces many polymers with different properties and functions. For example, amylose and pullan exhibit completely different water solubility, although both are derived from α-glucose. A similar molecular strategy has been achieved in certain chain polymerization, e.g., stereospecific polymerization of vinyl monomers,[1] cyclopolymerization/asymmetric polymerization of divinyl monomers,[2] and polymerization of bifunctional cyclic monomers in multiple modes.[3] For example, atactic and syndiotactic poly(methyl methacrylate)s (PMMAs) have glass transition temperatures ($T_g$s) of approximately 120 °C, while that of isotactic PMMA is 50 °C.[1] In contrast, as described in Chapter 1, the relationship between monomer(s) and the resulting polymer are one-by-one in a typical step-growth polymerization, which affords a definite polymer. Thus, in this chapter, the author designed a polycondensation affording a diverse structure from one monomer pair by using their tandem reaction.

Methyl β-bromo-α-(bromomethyl)acrylate (**4-1**), derived from methyl acrylate via 3 steps,[4a] has been reported to accept a sequential conjugate substitution ($S_N2'$) reaction with phenol (**Scheme 4-1a**). The first reaction results in intermediate **4-2**. At this stage, an α-(bromomethyl)acryloyl group is regenerated following the second reaction to yield a di-substituted product **4-3a**. It should be noted that acetal **4-3b** was also generated via the $S_N1$ or $S_N2$ reactions of **4-2** (**Scheme 4-1a**).[4b] Therefore, **4-1** can be regarded as an electrophile that undergoes two different reaction modes. Hence, the polycondensation of **4-1** with bisphenols affords two different repeating units. However, the total yield of **4-3a** and **4-3b** were low (70%), which was detrimental for step-growth polymerization. In our previous studies, thiols were determined to be effective nucleophiles in the $S_N2'$ reaction. Therefore, polycondensation with dithiol was attempt (**Scheme 4-1b**). Most importantly, the polymer structure could be controllable via ammonium intermediate which accept further $S_N2'$ reaction. In this chapter, the author describes a polycondensation by a tandem reaction leading to divergence in backbone structure.

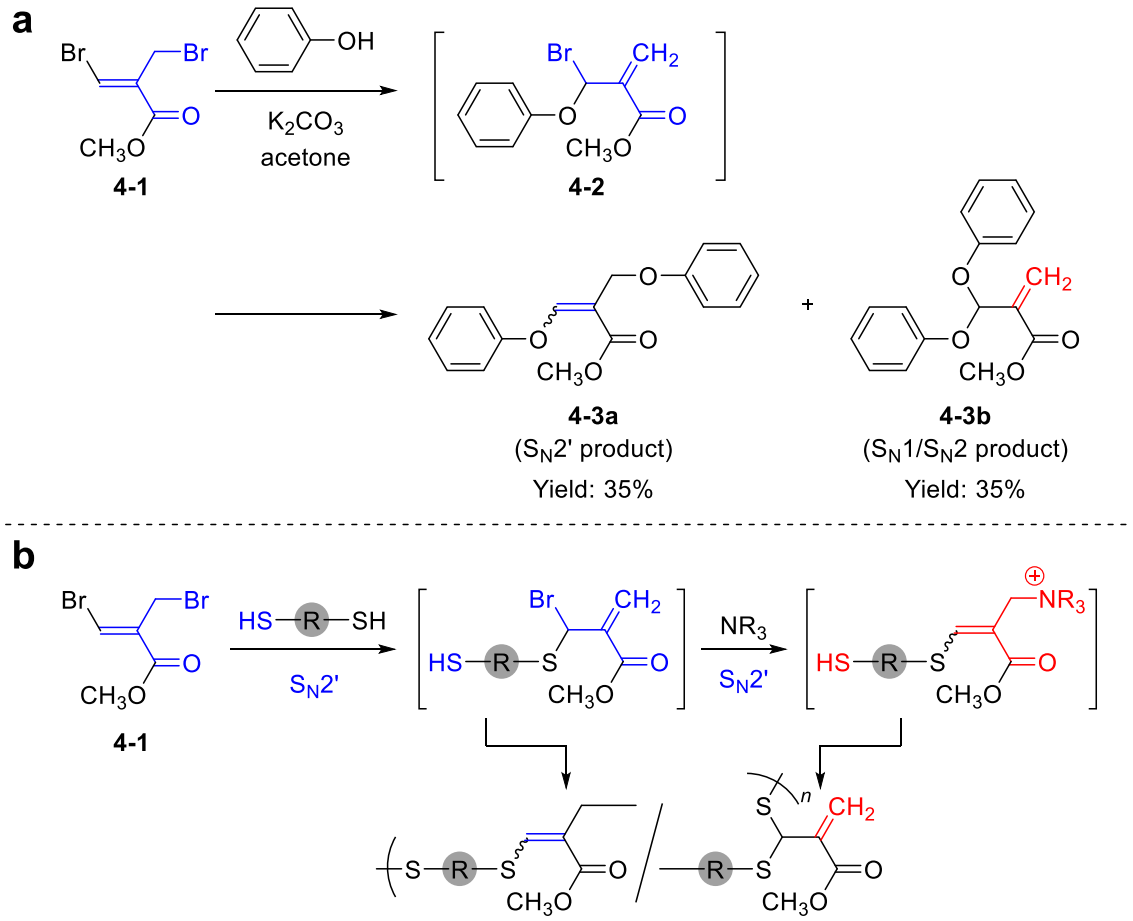


**Scheme 4-1**. (a) Tandem reaction of **4-1**, (b) Polycondensation of **4-1** and **4-4**.

# 2 Results and Discussion

## 2.1 Synthesis of Methyl β-bromo-α-(bromomethyl)acrylate

The synthesis of methyl β-bromo-α-(bromomethyl)acrylate (**4-1**) was attempted according to the literature.[4a,b] Bromide was reacted to methyl acrylate (**4-5**) to yield methyl 2,3-dibromopropionate (**4-6**). Subsequently, E1cB reaction of **4-6** by 1,8-diazabicyclo[5.4.0]undec-7-ene (DBU) was conducted to yield methyl β-bromo-methacrylate (**4-7**) in an *E*-geometry (**Scheme 4-2**). The bromination of allylic position by *N*-bromosuccinimide (NBS) was conducted to afford **4-1** with a single isomer in an *E*-geometry, supported by $^1$H NMR spectrum (**Figure 4-1**).

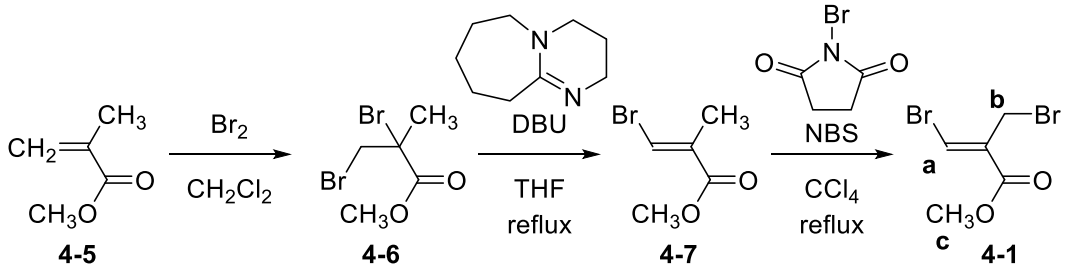


**Scheme 4-2.** Synthesis of methyl β-bromo-α-(bromomethyl)acrylate (**4-1**).

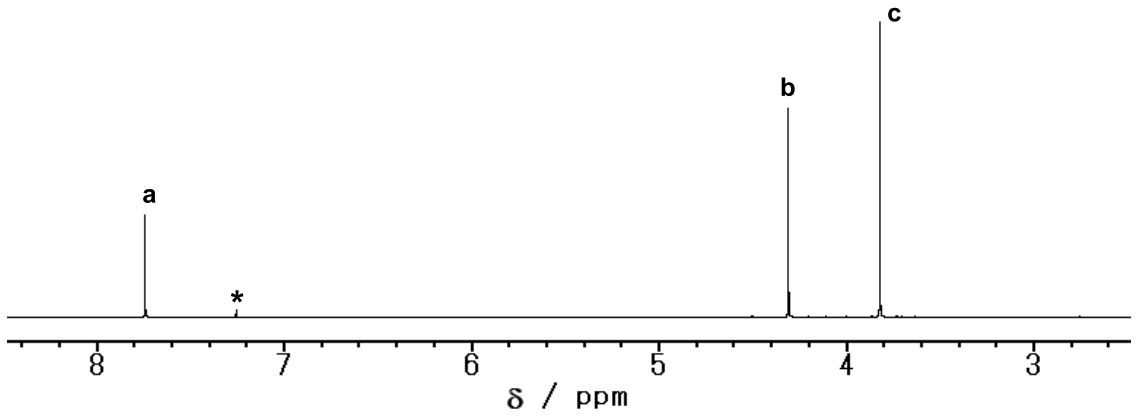


**Figure 4-1.** $^1$H NMR spectrum of **4-1** after purification (400 MHz, $CDCl_3$, 26 °C).

## 2.2 Polymerization via Sequential $S_N2$' Reactions in the Presence of $K_2CO_3$

*Model Experiments with a Monothiol*

To investigate the sequential $S_N2$' reactions of **4-1**, the model experiment using monothiol, benzyl mercaptan (**4-8**), was conducted. **4-8** (2.0 equimol.) was reacted with **4-1** in DMF at 25 °C in the presence of excess $K_2CO_3$ as a base to capture the liberated

hydrobromic acid (**Scheme 4-3**). In the $^1$H NMR spectrum of the product, the $S_N2'$ product, **4-9**, was identified, whereas no $S_N1/S_N2$ products, **4-10**, were observed. Thus, it was confirmed that **4-1** selectively accepted sequential $S_N2'$ reaction as expected (**Figure 4-2**). Speaking about the composition of geometric isomers, (*Z*)-isomer was formed dominantly (*E*/*Z* = 25/75).

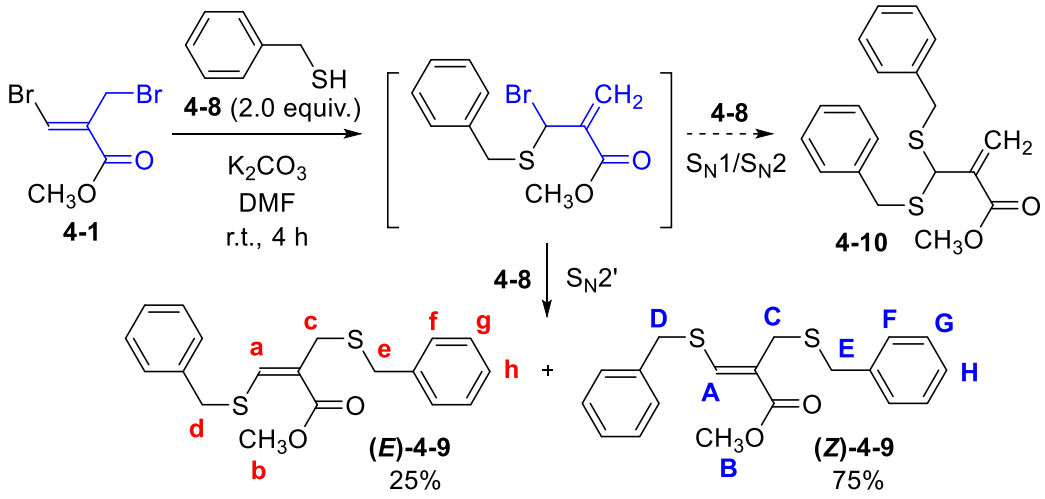


**Scheme 4-3.** Model reaction with **4-1** and **4-8**.

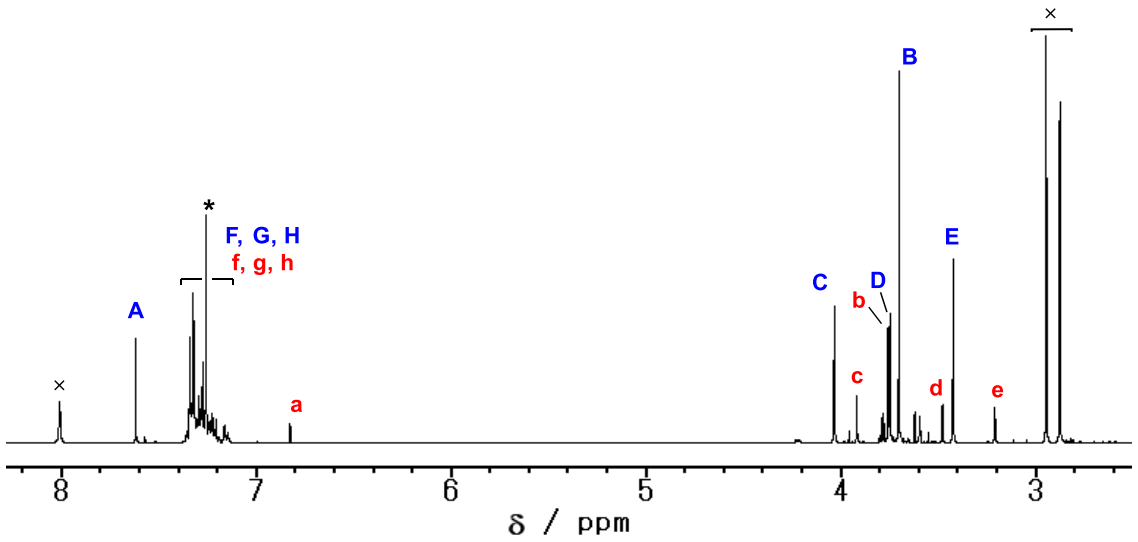


**Figure 4-2.** $^1$H NMR spectrum of the product **4-9** (400 MHz, $CDCl_3$, 26 °C)

*Polymerization with Dithiol via Sequential $S_N2'$ Reactions*

The discovery of the selective $S_N2'$ reaction of **4-1** with a thiol encouraged the author to investigate the polymerization of **4-1** and dithiols. The polymerization of **4-1**

**Table 4-1.** Polymerization of **4-1** and **4-4** in the presence of $K_2CO_3$.

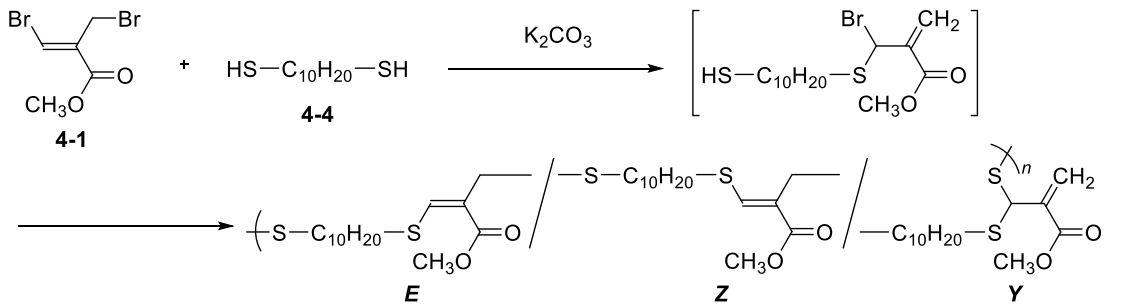


| Entry[a] | Solvent | Temp. / °C | Yield / % | $M_n$[b] | $Đ$[b] | Composition[c] / % | | |
|---|---|---|---|---|---|---|---|---|
| | | | | | | ***E*** | ***Z*** | ***Y*** |
| 1 | DMF | 25 | >99 | 12800 | 3.37 | 24 | 76 | 0 |
| 2 | DMF | 80 | >99 | 8000 | 3.45 | 19 | 81 | 0 |
| 3 | $CH_3CN$ | 25 | >99 | 4000 | 2.25 | 51 | 47 | 2 |
| 4 | $CH_3CN$ | 80 | 82 | 36000 | 5.59 | 24 | 76 | 0 |

[a] **4-1**: 0.750 mmol, [**4-1**]$_0$/[**4-4**]$_0$/[$K_2CO_3$]$_0$ = 1/1.0/2.1, solvent: 0.75 mL, 24 h. [b] Determined by SEC (polystyrene standard, THF, 40 °C). [c] Calculated by $^1$H NMR spectrum.

and 1,10-decanedithiol (**4-4**) was thus conducted in DMF at 25 °C in the presence of excess $K_2CO_3$ for 24 h to afford the polymer with $M_n$ = 12800, $Đ$ = 3.37 (**Table 4-1**, Entry 1). The polymerization at 80 °C gave almost similar results (Entry 2, $M_n$ = 8000, $Đ$ = 3.45). As similar to the model reaction described in **Scheme 4-3**, the polymerization has a potential to give three kinds of isomeric units, *endo*-olefin ***Z***, ***E***, and *exo*-olefin **Y**. **Figure 4-3a**/**b** shows $^1$H NMR spectra of the products in Entries 1 and 2, respectively. The signals corresponding to the *endo*-olefin units were observed; signal c (7.0 ppm) for the olefinic proton exhibits NOESY correlation with signal d (3.4 ppm) for allylic proton (**Figure 4-4**), suggesting isomeric units of ***E***. Thus, signal e (7.6 ppm) for the olefinic proton was assignable to ***Z***. From the intensity ratios between signals **c** and **e**, the composition was determined; the unit ***Z*** was dominant in similar manner as the model experiment (Entry 1: ***E***/***Z*** = 24/76, Entry 2: ***E***/***Z*** = 19/81).

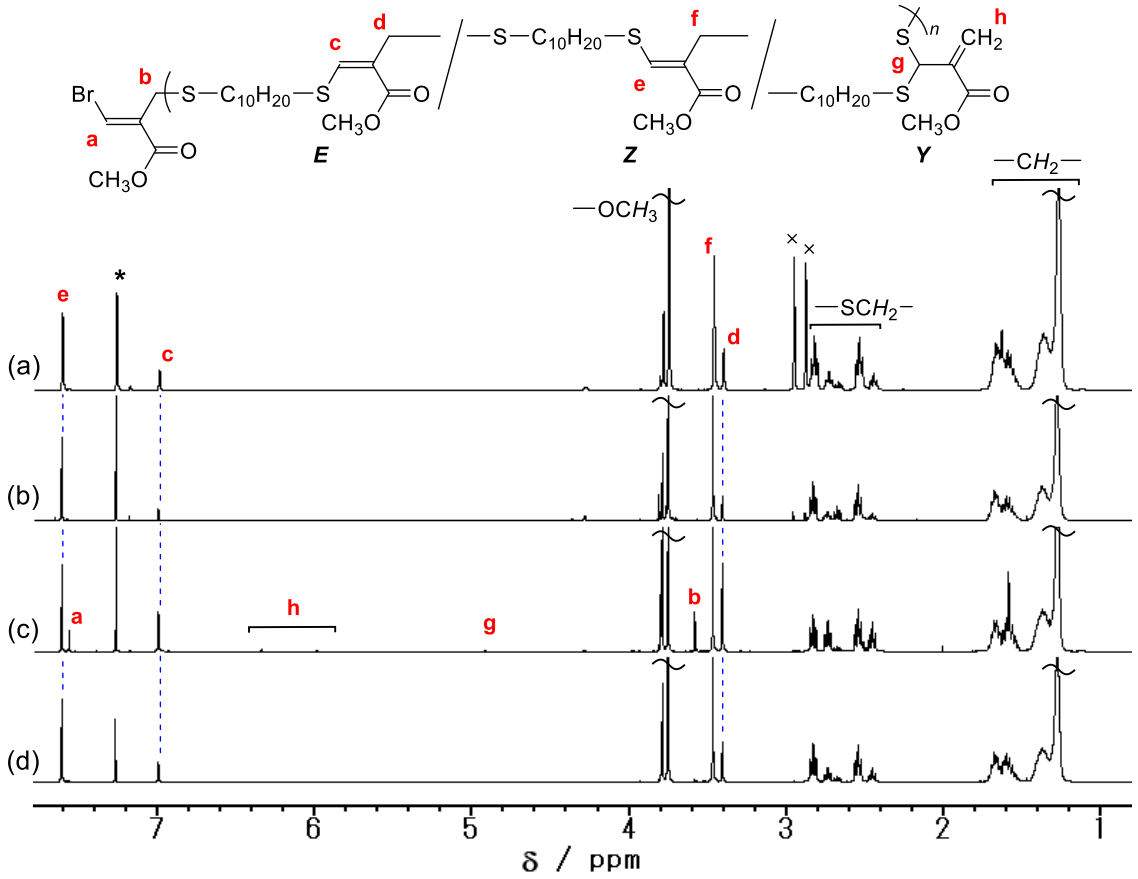


**Figure 4-3.** $^{1}$H NMR spectra of the product in (a) Entry 1, (b) Entry 2, (c) Entry 3 and (d) Entry 4. (400 MHz, $CDCl_3$, 26 °C, *: $CHCl_3$, ×: DMF)

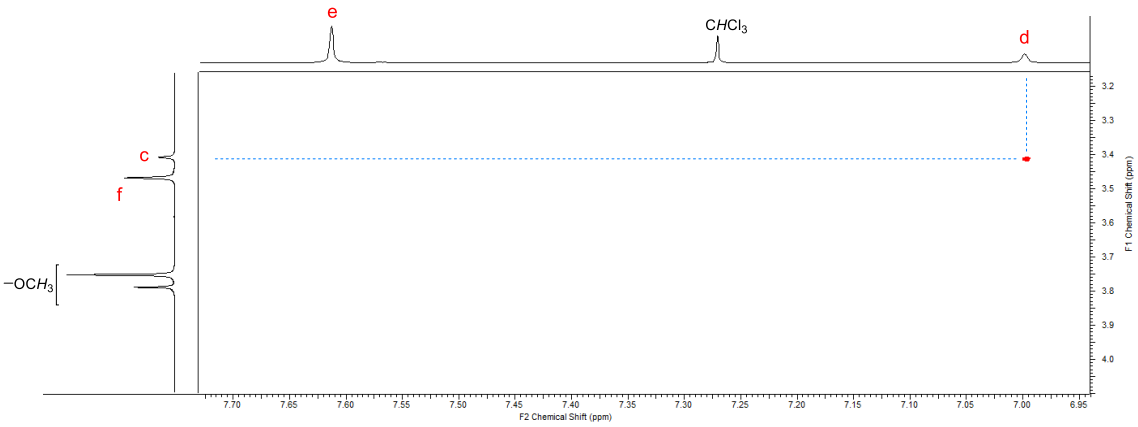


**Figure 4-4.** NOESY spectrum of the product in Entry 4 (400 MHz, $CDCl_3$, 25 °C).

On the other hand, the polymerization in $CH_3CN$ at 25 °C resulted in a different behavior (Entry 3). In the $^{1}$H NMR spectrum (**Figure 4-3c**), the vinyl signal h (6.0 and 6.4 ppm) and allyl signal g (4.9 ppm) of *exo*-olefin unit ***Y*** were observed. From the intensity rations between signals c, e and h, the composition was determined (***E***/***Z***/***Y*** =

51/47/2). In addition, signal a and b, which were quite small in **Figure 4-3a/b**, were observed near 7.5 and 3.6 ppm, respectively. The signals were assigned to an inactive chain-end group generated by a side reaction of $S_N1$ and $S_N2$ mechanism of **4-1**(**Scheme 4-4a**). Because the formed chain-end did not have any leaving group, the chain growth no longer proceeded. In fact, $M_n$ was lower ($M_n$ = 4000, $Đ$ = 2.25) than other entries, and the SEC curve showed a shoulder over lower molecular weight region (**Figure 4-5c**). The side reaction was suppressed at 80 °C, as signals a and b were not observed in the $^1$H NMR spectrum (**Figure 4-3d**). Then, high $M_n$ was achieved (Entry 4, $M_n$ = 36000, $Đ$ = 5.59), but the SEC curve was multimodal (**Figure 4-5d**); several peaks at higher molecular weight region were observed, indicating the formation of a branched structure by the Michael addition of a mercapto chain-end to the acyl skeletons in unit ***Y*** (Scheme 4-4b). Nevertheless, the repeating unit ***Z*** occupied 76% of backbone.

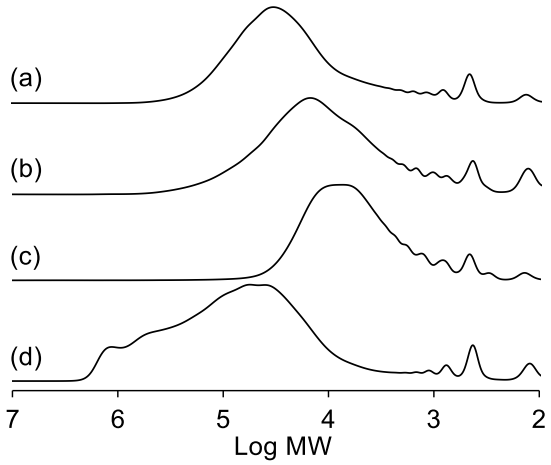


**Figure 4-5.** SEC curves of the product in (a) Entry 1, (b) Entry 2, (c) Entry 3 and (d) Entry 4.

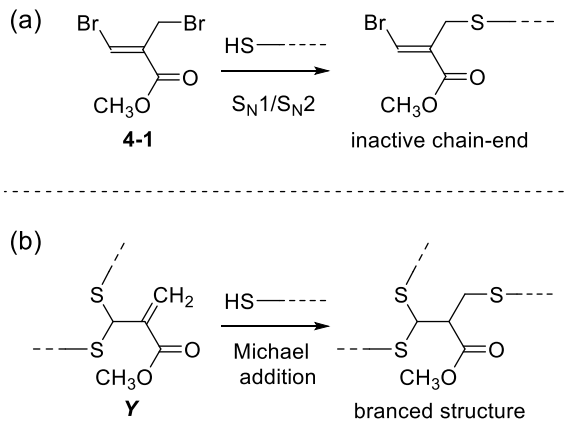


**Scheme 4-4.** Side reactions (a) affording inactive chain-end group and (b) forming a branched structure.

*Molecular Mechanics Calculations to Understand the Selectivity of E and Z*

The selectivity of ***E*** and ***Z*** is determined during the elimination step of a bromide anion from the four conformers of intermediate **4-6** (**Scheme 4-5**); unit ***E*** is generated from **4-6a** and **4-6d** with two sulfur atoms on the opposite sides, whereas **4-6b** and **4-6c** lead to unit ***Z***. **4-6a**/**4-6b** and **4-6c**/**4-6d** are the pairs of interconvertible conformers by resonance effect. Notably, the bromine atom and the negative charge need to be anti-

periplanar toward the elimination. Then, molecular mechanics (MM) calculation was performed under MMFF force field to investigate the relative energy of the conformers in each stable conformation. The detailed results are shown in **Tables 4-4**/**4-5** in the experimental section. The most stable conformations similar to the transition states satisfying this restriction are described in **Scheme 4-5**. **4-6a**, yielding unit ***E***, was relatively unstable (+15 kJ/mol) than others. **4-6b** and **4-6c** were the most stable among them, resulting in unit ***Z***. **4-6d** was also stable but the dihedral angle of negative charge–carbon/carbon–bromine was much smaller than 180°, implying the elimination is difficult. Therefore, the elimination reaction favor to form unit **Z**. It should be noted that all conformers described in **Scheme 4-5** are stabilized by the chelating effects of potassium cation on two sulfur atoms and carbonyl oxygen atom. This indicates that the template effects by potassium cation is important to the selective formation of ***Z***. In fact, the polymerizations in DMF at 25 °C and 80 °C resulted in high content of unit ***Z*** (Entry 1, 2). Marcus *et al.* reported that DMF have higher solvation capability of $K^+$ than acetonitrile.[5] Thus, the template effects at the high $K^+$ concentration in DMF emphasized the selective formation of unit ***Z***.

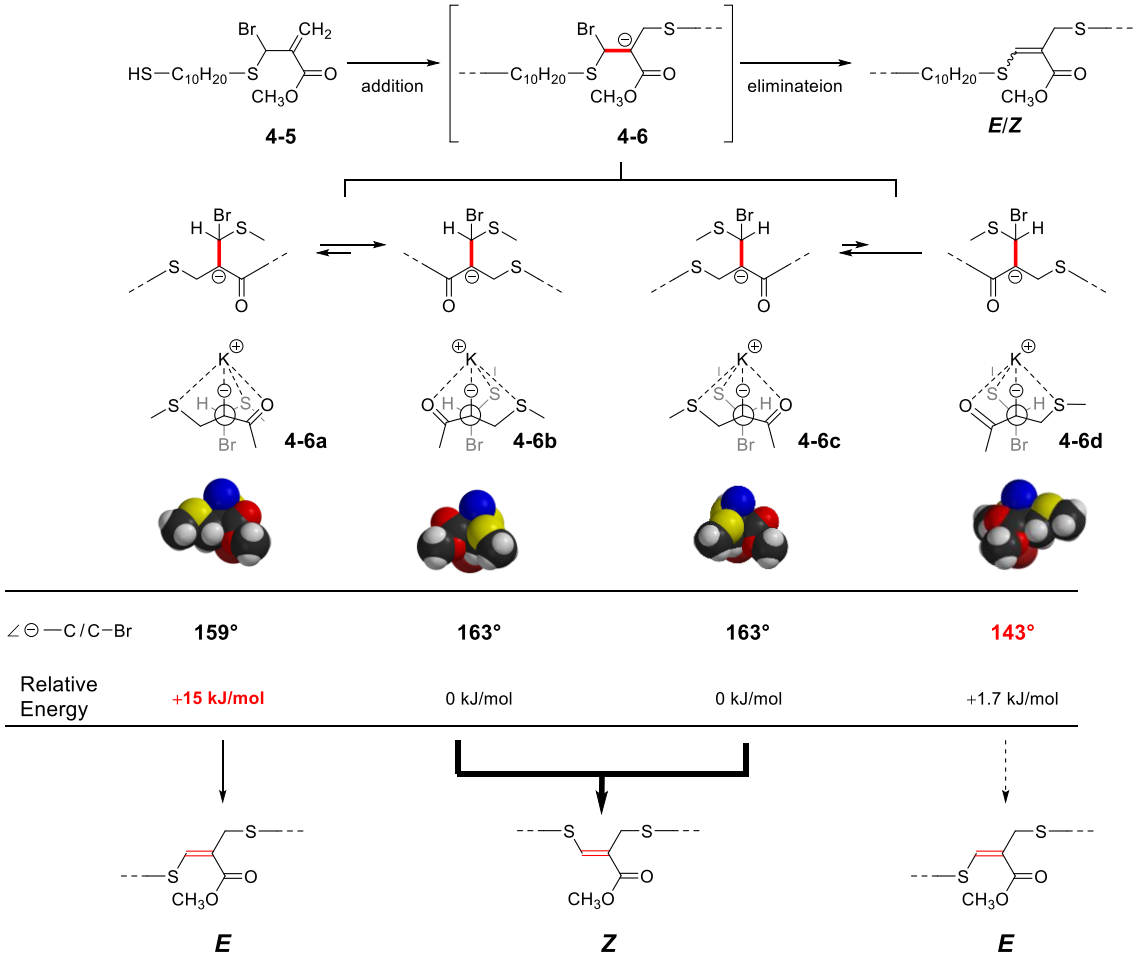


**Scheme 4-5.** Template effects of $K_2CO_3$ leading to unit ***Z***.

## 2.3 Polymerization Leading to Divergence in Backbone Structure

*Structural controls by choosing reaction conditions*

Similar polymerization was conducted with other alkali carbonate salts at 25 °C in DMF (**Table 4-2**). The microstructures of resulting polymers in each experiment are summarized in **Figure 4-6a**. The use of $Li_2CO_3$ led to low molecular weight (Entry 5, $M_n$ = 800, $Đ$ = 1.83) owing to the poor solubility of $Li_2CO_3$; other alkali salts yielded polymers with a high ***Z*** content, which suggested the template effect (Entries 1,6,7). Moreover, the solvent volume changed from 0.25 mL to 2.25 mL for 0.750 mmol of **4-1** (Entries 8–11). The larger volume of solvent also effective to increase the ***Z*** content (**Figure. 4-6b**).

**Table 4-2.** Polymerization of **4-1** and **4-4** with structural controls.

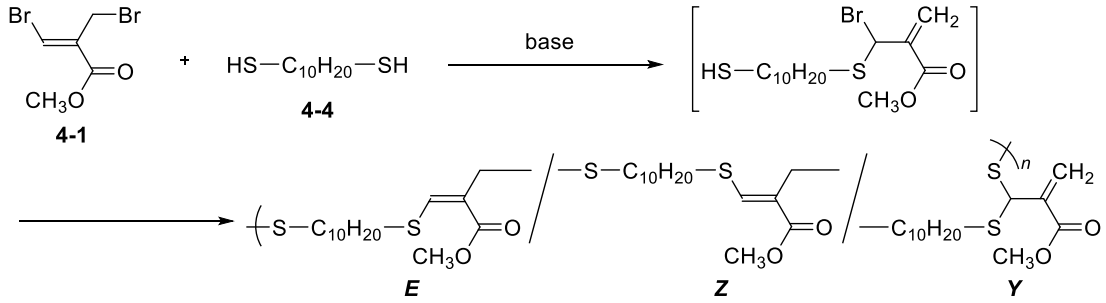


| Entry[a] | Base | Solvent (mL) | Yield / % | $M_n$[b] | $Đ$[b] | Composition[c] / % | | |
|---|---|---|---|---|---|---|---|---|
| | | | | | | ***E*** | ***Z*** | ***Y*** |
| 1 | $K_2CO_3$ | DMF (0.75) | >99 | 12800 | 3.37 | 24 | 76 | 0 |
| 5 | $Li_2CO_3$ | DMF (0.75) | >99 | 800 | 1.83 | 49 | 46 | 1 |
| 6 | $Na_2CO_3$ | DMF (0.75) | >99 | 3200 | 2.15 | 30 | 69 | 1 |
| 7 | $Cs_2CO_3$ | DMF (0.75) | 96 | 9600 | 2.40 | 25 | 75 | 0 |
| 8 | $K_2CO_3$ | DMF (0.25) | >99 | 4800 | 1.89 | 32 | 67 | 1 |
| 9 | $K_2CO_3$ | DMF (0.375) | >99 | 5700 | 1.96 | 30 | 70 | 0 |
| 10 | $K_2CO_3$ | DMF (1.50) | >99 | 11400 | 2.66 | 21 | 79 | 0 |
| 11 | $K_2CO_3$ | DMF (2.25) | >99 | 7200 | 3.57 | 19 | 81 | 0 |
| 12 | $Et_3N$ | $CHCl_3$ (0.75) | 93 | 4200 | 3.56 | 21 | 15 | 64 |
| 13 | *i*$Pr_2NEt$ | $CHCl_3$ (0.75) | >99 | 3200 | 2.15 | 42 | 54 | 4 |
| 14 | DABCO | $CHCl_3$ (0.75) | 90 | 9200 | 1.71 | 3 | 5 | 92 |

[a] **4-1**: 0.750 mmol, $[\mathbf{4\text{-}1}]_0/[\mathbf{4\text{-}4}]_0/[\text{base}]_0$ = 1/1.0/2.1, 24 h. [b] Determined by SEC (polystyrene standard, THF, 40 °C). [c] Calculated by $^1$H NMR spectrum.

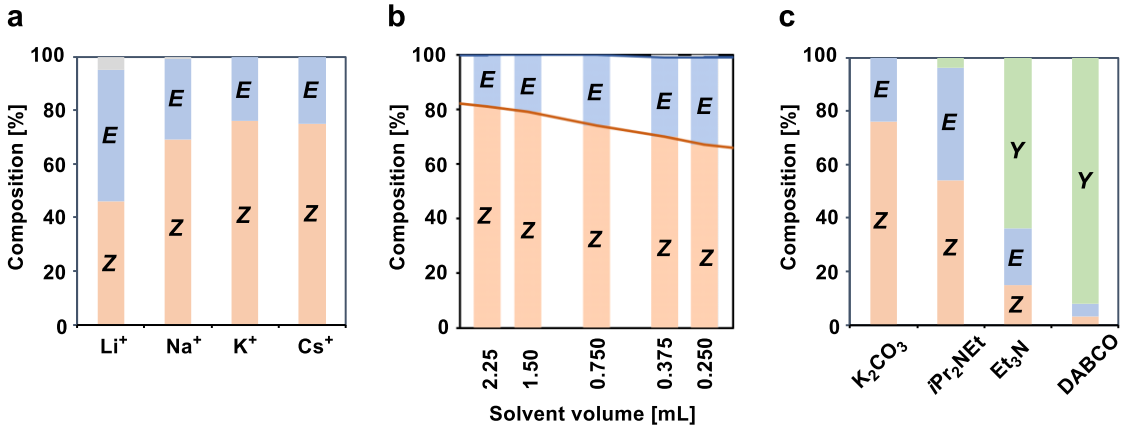


**Figure 4-6.** Effects of reaction conditions on polymer microstructure. (**a**: the products of Entry 1 and 5-7, **b**: the products of Entry 1 and 8-11, **c**: the products of 1 and 12-14).

$Et_3N$ was used instead of alkali salt to the polymerization in $CHCl_3$ (Entry 12). The $^1H$ NMR spectrum of the resulting polymer (**Figure 4-7a**) shows not only the signals corresponding to *endo*-olefin groups (**c**: 7.0 ppm, **e**: 7.6 ppm) but also the signals corresponding to *exo*-olefin groups (**h**: 6.0 ppm, 6.4 ppm). Each integral ratio suggests the obtained polymer composition with 36% of *endo*-olefin units, ***E*** and ***Z***, and 64% of the *exo*-olefin unit ***Y***. Unit ***Y*** can be generated by the $S_N1/S_N2$ reaction of intermediates **4-10** (**Scheme 4-6**, route 3); however, another path through the nucleophilic reaction of $Et_3N$ is also possible (route 4). The amine causes an $S_N2$' reaction with **4-10** and affords ammonium intermediate **4-11**, which accepts another $S_N2$' reaction to generate unit ***Y***. In fact, *i*$Pr_2$NEt, a base with poor nucleophilicity, decreased the content of unit ***Y*** to 4% (Entry 13, **Figure 4-7b**). In an opposite manner, 1,4-diazabicyclo[2.2.2]octane (DABCO), a base with strong nucleophilicity, resulted in the highest content of unit ***Y*** (92%, Entry 14 and **Figure 4-7c**). Therefore, the choice of amine is critical to control microstructure (**Figure 4-6c**).

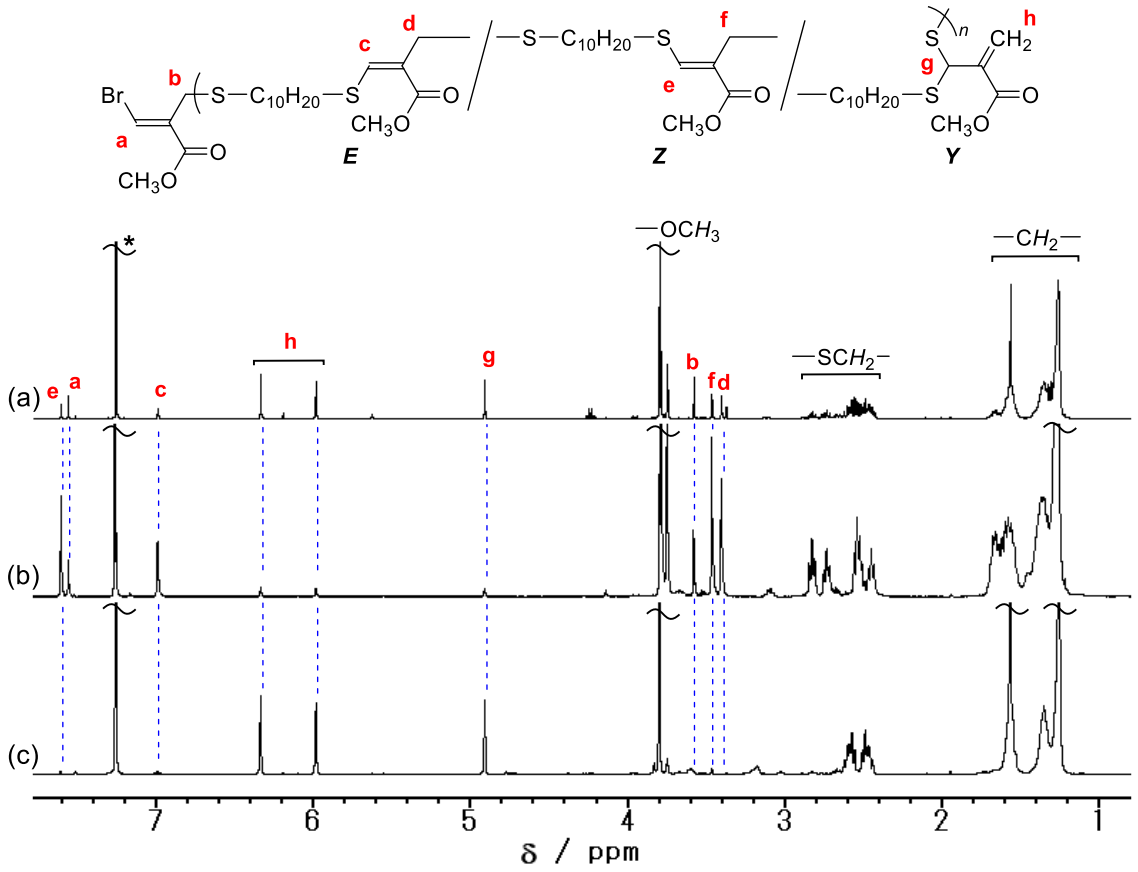


**Figure 4-7.** $^{1}$H NMR spectra of the product in (a) Entry 12, (b) Entry 13 and (14) Entry 15 (400 MHz, $CDCl_3$, 26 °C, *: $CHCl_3$).

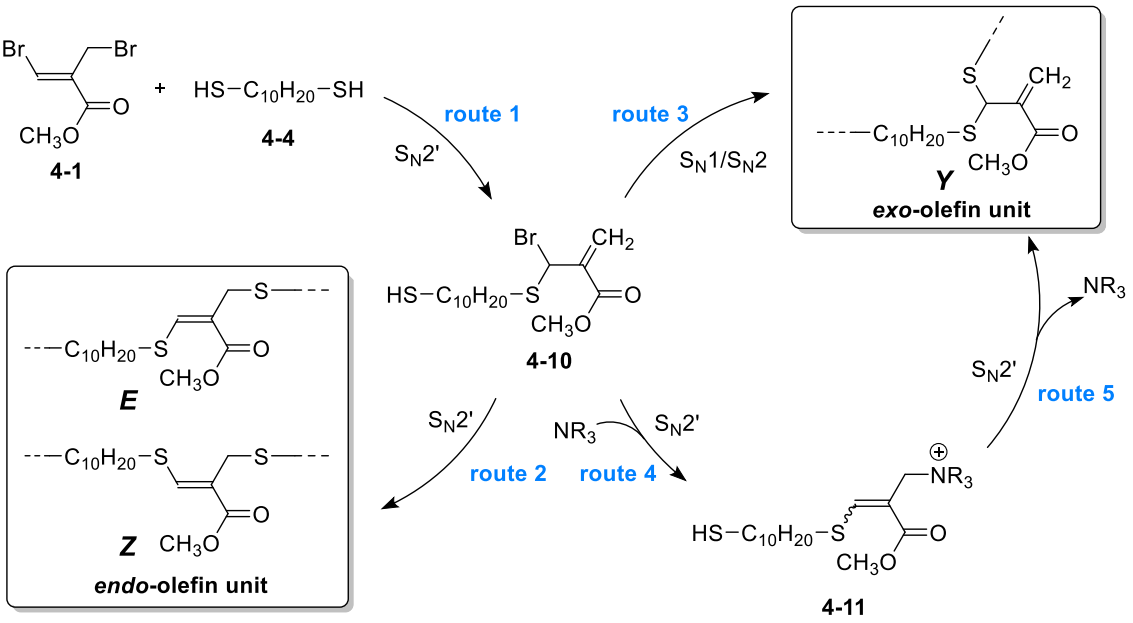


**Scheme 4-6.** Proposed reaction mechanism.

*Thermal Properties*

**Figure 4-8a** shows the relationship between ***Y***-contents and 5% weight-loss temperatures ($T_{d5}$s). Apparently, higher ***Y***-contents resulted in lower $T_{d5}$s. Generally speaking, *exo*-olefin is unstable than *endo*-olefin. In addition, the dithioacetal unit in unit ***Y*** is relatively unstable than sulfides. These natures can explain the correlation of ***Y***-contents and thermal stability. **Figure 4-8b** shows the plots of ***Y***-contents and glass transition temperatures ($T_g$s). Polymers with a high *endo*-olefin content (>98%) obtained in Entry 1 and 3 showed similar glass transition temperatures ($T_g$s) of ca. −75°C, which indicated that the isomeric structures of *endo*-olefin units were not significant. The polymers mainly composed of the *exo*-olefin units (Entry 14, 92%) had higher $T_g$ at −55 °C. Then, the 'copolymer', consisting of 36% of *endo*- olefin units and 64% *exo*-olefin units (Entry 5), exhibited medium $T_g$ of −66 °C (Figure. 4-7b). Therefore, the thermal properties of polymers can be tuned by controlling microstructure.

**Table 4-3.** Thermal properties of the resulting polymers.

| Entry | Composition / % | | | $T_{d5}$ [°C] | $T_g$ [°C] |
|---|---|---|---|---|---|
| | ***E*** | ***Z*** | ***Y*** | | |
| 1 | 24 | 76 | 0 | 278 | –76 |
| 3 | 41 | 47 | 2 | 264 | –75 |
| 12 | 21 | 15 | 64 | 232 | –66 |
| 14 | 3 | 5 | 92 | 214 | –55 |

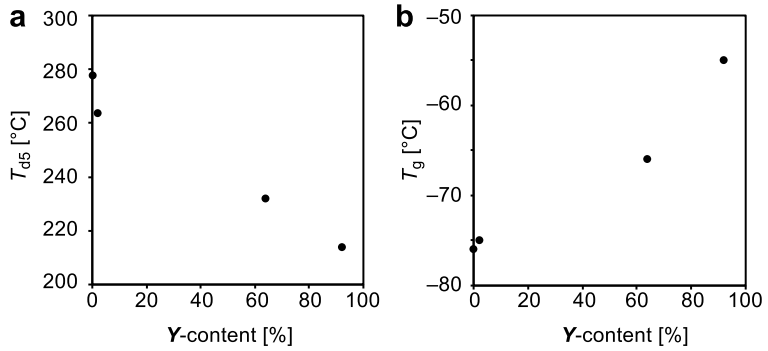


**Figure 4-8.** The plots of ***Y*** contents vs. $T_{d5}$ (**a**) and $T_g$ (**b**).

## 3. Conclusion

In this chapter, the author described a polycondensation strategy, which affords a diverse structure from one monomer pair via the tandem reaction. Although the polycondensation in this chapter was initially designed to improve the tandem polymerization in chapter 2, this design led to the new concept in polymer chemistry, the microstructure controls in step-growth polymerization. The microstructures of polymers were controlled by choosing appropriate bases; low nucleophilic bases (*e.g.* alkali carbonates or *i*Pr$_2$NEt) resulted in highly *endo*-olefin units, while bases with strong nucleophilicity (*e.g.* DABCO) yielded *exo*-olefin units with an almost complete selectivity. The isomeric structure in *endo*-olefin units was influenced by the alkali metal cation through the template effect. The content of *exo*-olefin units was important to increase $T_g$. Polymer synthetic chemistry tries to imitate precise structure of natural polymers such as stereoregularity in polypeptides, uniform degree of polymerization of enzymes, and controlled monomer sequences in DNA. However, the diversity of polymer microstructures in polycondensation from the limited species of monomers, which can be found in polysaccharide, has not received considerable attention. This study is the pioneering example, which focuses on this feature in artificial polycondensation systems, Although the current results are not perfect to achieve the precise controls of polymer microstructure, the author believe that this approach introduces a new molecular strategy in polymer synthetic chemistry to achieve a diversity of polymer structures in step-growth polymerization from a single pair of monomers.

# 4. Experimental

### *Instruments*

$^{1}H$ and $^{13}C$ NMR spectra were recorded in $CDCl_3$ (Kanto Chemical) on AVANCE 400 (Bruker) and AVANCE NEO (Bruker) spectrometers. Chemical shifts in $^{1}H$ and $^{13}C$ NMR spectra were referred to the signal of tetramethylsilane (TMS) and solvent ($CDCl_3$), respectively. Molecular weight and its distributions were determined at 40 °C by size-exclusion chromatography (SEC) on an EXTREMA chromatograph (JASCO) equipped with two SEC columns [PL-gel, Mixed C (300 mm _7.5 mm), Polymer Laboratories], using tetrahydrofuran (THF, Wako Pure Chemical Industries, for HPLC grade) as an eluent (flow rate = 0.8 mL $min^{-1}$), and calibrated against standard polystyrene (PS) samples (TSK-gel oligomer kit, Tosoh, $M_n$: $1.03 \times 10^6$, $3.89 \times 10^5$, $1.82 \times 10^5$, $3.68 \times 10^4$, $1.36 \times 10^4$, $5.32 \times 10^3$, $3.03 \times 10^3$, $8.73 \times 10^2$) and detected with UV (UV-4070, JASCO) and RI (RI-4030, JASCO) detectors. Differential scanning calorimetry (DSC) were measured with a Shimadzu DSC-60 differential scanning calorimeter (scan rate = 10 °C/min) under a $N_2$ atmosphere (flow rate = 50 mL/min). IR spectra were recorded on a Cary 630 FTIR spectrometer equipped with an attenuated total reflection attachment (single reflection). Thermogravimetric–differential thermal analyses (TG–DTA) were carried out from room temperature to 500 °C at a heating rate of 10 °C with Rigaku Thermo plus II TG8120 under an $N_2$ atmosphere.

### *Materials*

Methyl methacrylate, *N*-bromosuccinmide (NBS), triethylamine ($Et_3N$), 1,8-diazabicyclo[5.4.0]undec-7-ene (DBU), 1,4-diazabicyclo[2.2.2]octane (DABCO), deuterochloroform ($CDCl_3$) and 1,10-decanedithiol were purchased from Tokyo Chemical Industry Co., Ltd. Sodium thiosulfate ($Na_2SO_3$) was purchased from Yoneyama Yakuhin Kogyo Co, Ltd. Bromide ($Br_2$), *N,N*-diisopropylethylamine ($iPr_2NEt$), sodium sulfate ($Na_2SO_4$), chloroform ($CHCl_3$), dichloromethane ($CH_2Cl_2$), tetrachloromethane ($CCl_4$), tetrahydrofuran (THF), acetonitrile ($CH_3CN$), , *N,N*-dimethylformamide (DMF), lithium carbonate ($Li_2CO_3$) , potassium carbonate ($K_2CO_3$) and cesium carbonate

($Cs_2CO_3$) were purchased from Wako Pure Chemical Industries, Ltd.

***Molecular Mechanics Calculation***

Molecular mechanics (MM) simulation was performed by Spartan 16' ver. 1.1.0. The initial geometry of **4-6a** was optimized under MMFF force field, and the conformer distribution were searched under MMFF force field. The results of found conformers were described in **Tables 4-4**. Similar simulations were performed for **4-6b**, but same results to **4-6a** were obtained as they were interconvertible. Similar simulations were also performed for **4-6c** and **4-6d**, and the results were summarized in **Table 4-5**.

**Table 4-4.** Stable conformers of intermediate **4-6a** and **4-6b** suggested by molecular mechanics (MMFF) calculation.

| Entry | Model | Energy [kJ/mol] | ∠ ⊖ - C/C-Br [°] | Entry | Model | Energy [kJ/mol] | ∠ ⊖ - C/C-Br [°] |
|---|---|---|---|---|---|---|---|
| 1 | 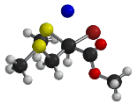 | -933.41 | 62.10 | 11 | 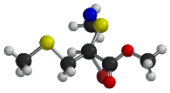 | -904.88 | 146.17 |
| 2 | 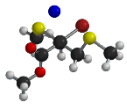 | -932.98 | 63.27 | 12 | 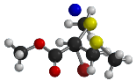 **8a** | -904.30 | 158.56 |
| 3 | 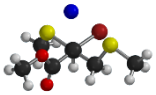 | -932.81 | 59.49 | 13 | 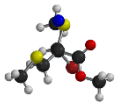 | -902.79 | 140.64 |
| 4 | 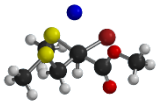 | -932.74 | 64.55 | 14 | 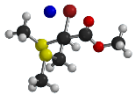 | -899.88 | 38.13 |
| 5 | 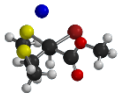 | -926.76 | 68.48 | 15 | 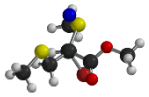 | -899.78 | 144.91 |
| 6 | 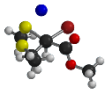 | -926.63 | 65.39 | 16 | 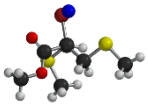 | -894.80 | -12.61 |
| 7 | 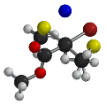 | -924.21 | 59.30 | 17 | 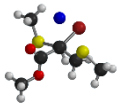 | -894.63 | 43.30 |
| 8 | 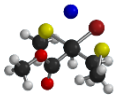 | -924.12 | 55.82 | 18 | 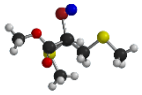 | -894.10 | -15.73 |
| 9 | 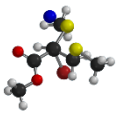 **8b** | -908.60 | 162.87 | 19 | 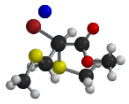 | -893.96 | -37.62 |
| 10 | 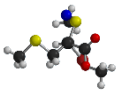 | -906.94 | 142.91 | 20 | 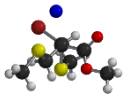 | -892.07 | -46.26 |

**Table 4-5.** Stable conformers of intermediate **4-6c** and **4-6d** suggested by molecular mechanics (MMFF) calculation.

| Entry | Model | Energy [kJ/mol] | ∠ ⊖ - C/C-Br [°] | Entry | Model | Energy [kJ/mol] | ∠ ⊖ - C/C-Br [°] |
|---|---|---|---|---|---|---|---|
| 1 | 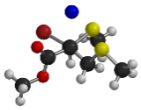 | -933.41 | -62.10 | 11 | 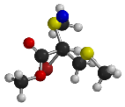 | -902.79 | -140.64 |
| 2 | 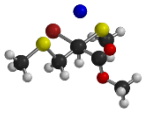 | -932.98 | -63.27 | 12 | 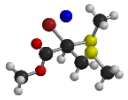 | -899.88 | -38.13 |
| 3 | 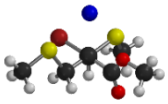 | -932.81 | -59.49 | 13 | 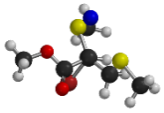 | -899.78 | -144.91 |
| 4 | 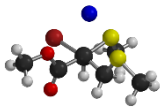 | -932.74 | -64.55 | 14 | 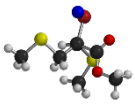 | -894.80 | 12.61 |
| 5 | 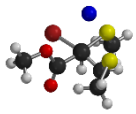 | -926.76 | -68.48 | 15 | 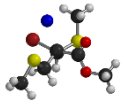 | -894.63 | -43.30 |
| 6 | 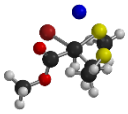 | -926.63 | -65.39 | 16 | 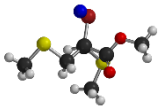 | -894.10 | 15.73 |
| 7 | 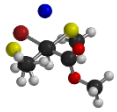 | -924.21 | -59.30 | 17 | 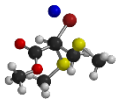 | -893.96 | 37.62 |
| 8 | 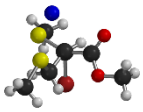 **8c** | **-908.60** | **-162.87** | 18 | 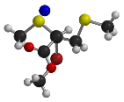 | -893.77 | -156.83 |
| 9 | 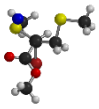 **8d** | -906.94 | **-142.91** | 19 | 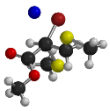 | -892.07 | 46.26 |
| 10 | 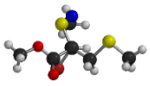 | -904.88 | -146.17 | | | | |

***Synthesis***

**Methyl 2,3-dibromopropionate (4-6):**[1] A liquid of bromine (80 g, 0.50 mol) was added dropwise via an addition funnel to a solution of methyl methacrylate (**4-5**) (50.16 g, 0.50 mol) in $CH_2Cl_2$ (200 mL) at 0 °C. The reaction mixture was stirred at 0 °C for 3 h and at room temperature for additional 3 h. *Sat.* $Na_2S_2O_3$ aq. (150 mL) was added to the reaction mixture and stirred at room temperature for 15 min. The layers were separated, and the

aqueous layer was extracted with $CH_2Cl_2$ (20 mL × 3). The organic layers were combined and washed with $H_2O$ (150 mL) and brine (150 mL). The combined organic layer was dried over $Na_2SO_4$ and concentrated to yield crude **4-6** (182 g, yield: >99%). The crude **4-6** was used in the next reaction without further purification.

**Methyl β-bromo-methacrylate (4-7):**[4a] A solution of 1,8-diazabicyclo[5.4.0]undec-7-ene (DBU) (83.84 g,0.55 mol) in THF (150 mL) was added dropwise to a solution of **4-6** (182.71 g) in THF (150 mL) at room temperature. The reaction mixture was refluxed for 2 h. After cooling to room temperature, $H_2O$ (150 mL) was added and the aqueous layer was extracted with EtOAc (50 mL × 3). The organic layers were combined and washed with 1 M HCl aq. (100 mL), $H_2O$ (100 mL) and brine (100 mL). The combined organic layer was dried over $Na_2SO_4$ and concentrated. The residue oil was purified by distillation under reduced pressure (b.p.: 47.0 °C / 10 mmHg) to yield **4-7** as colorless oil (33.92 g, Yield: 37.6%). $^1$H NMR spectrum (400 MHz, $CDCl_3$, 26 °C): δ/ppm 7.46 (1H, s, =C*H*Br), 3.72 (3H, s, OC$H_3$), 1.98 (2H, s, C$H_2$).

**Methyl β-bromo-α-(bromomethyl)acrylate (4-1):**[4b] A solution of *N*-bromosuccinimide (16.98 g, 95.4 mmol) in $CCl_4$ (20.0 mL) was added to a solution of **4-7** (15.0 g, 83.8 mmol) in $CCl_4$ (80.0 mL). The reaction mixture was refluxed for overnight. The precipitate was removed by filtration, and the filtrate was concentrated and distilled under reduced pressure (bp: 52.2 °C / 0.66 mmHg) to yielded **4-1** as colorless oil (18.49 g, Yield: 85.6%). $^1$H NMR spectrum (400 MHz, $CDCl_3$, 26 °C): δ/ppm 7.70 (1H, s, =C*H*Br),4.28 (2H, s, C$H_2$Br), 3.82 (3H, s, OC$H_3$).

**Model Reaction with Monothiols:** A solution of benzyl mercaptan (0.187 g, 1.506 mmol) in DMF (0.45 mL) was added to a solution of **4-4** (0.193 g, 0.750 mmol) and $K_2CO_3$ (0.218 g, 1.575 mmol) in DMF (0.30 mL). The reaction mixture was stirred at room temperature for 4 h. Then, $CHCl_3$ (4.0 mL) was added and the organic layer was washed with 0.5 M HClaq. (6.0 mL). The organic layer was collected and washed again with brine (3.0 mL). Then, the organic layer was concentrated under reduced pressure to

afford the **4-9** (0.373 g, >99%)

**Polymerization:** Typical procedure is shown. A solution of **4-1** (0.194 g, 0.752 mmol) in $CH_3CN$ (0.45 mL) was added dropwise to a solution of **4-4** (0.155 g, 0.751 mmol) and $K_2CO_3$ (0.215 g, 1.56 mmol) in $CH_3CN$ (0.30 mL). The reaction mixture was stirred at room temperature for 24h. Then, $CHCl_3$ (3.0 mL) was added and the organic layer was washed with 0.5 M HClaq. (4.5 mL). The organic layer was collected and washed again with 0.14 M HClaq. (3.5 mL). The aqueous layer was extracted again with $CHCl_3$ (3.0 mL). The combined organic layers were washed with brine (5.0 mL) and concentrated under reduced pressure. Then, the concentrated solution was dried in vacuo to afford the polymer (0.236g, >99%)

**References**

(1) (a) T. Kitayama and K. Hatada, *Polym. Int.*, **2000**, 49, 11. (b) K. Ute, N. Miyatake, K. Hatada, *Polymer*, **1995**, 36, 1415.

(2) T. kodaira, *Prog, Polym. Sci.*, **2000**, 25, 627.

(3) (a) G. B. Butler, *J. Polym. Sci. Part A: Polym. Chem.*, **2000**, 38, 3451. (b) X. Tang, M. Hong, L. Falivene, L. Caporaso, L. Cavallo, E. Y.-X. Chen, *J. Am. Chem. Soc.*, **2016**. 138, 14326. (c) A. E. Peterson, E. Kokkoli, M. A. Hilmyer, *ACS Macro. Lett.*, **2014**, 3, 1156.

(4) (a) A. Jolit, P. M. Walleser, G. P. A. Yap, M. A. Tius, *Angew. Chem., Int. Ed.*, **2014**, 53, 6180. (b) D. Gopel, K. Rajagoparan, *Tetrahedron Lett.*, **1987**, 28, 5327.

(5) C. Kalidas, G. Hefter, Y. Marcus, *Chem. Rev.*, **2000**, 100, 819.

*Chapter 5*

# Side-group-induced Ring-opening Polymerization of Lactones by Conjugate Substitution

## 1. Introduction

Ring-opening polymerization (ROP) is composed of ring-open reaction of cyclic monomers with active species such as radicals, cations and anions to generate a new active species.[1] The polymerizability of cyclic monomers are generally dependent on ring strains, because typical ROP is driven by enthalpy gain in the release of strain energy. For example, ROPs of lactones with four-, six- and seven-membered rings proceed in cationic or anionic mechanism, but that with a five-membered ring does not proceed due to the low ring strain. On the other hand, conversion of functional groups to thermodynamically stable structures, *e.g.* from an enol ether to carbonyl and alkyl groups, also can drive ROPs.[2] Such ROPs are accessible by sophisticated monomer designs; for example, cationic ROP of cyclic imino ethers accompanies with the isomerization from imino ether to thermodynamically stable amide group (**Scheme 5-1a**).[2a-d] The cationic and radical ROPs of the cyclic ketene acetals also proceeds with the isomerization from acetal to ester groups (**Scheme 5-1b**).[2e-k] Such conversions of functional groups are attractive to design ROPs for inactive cyclic compounds and to improve ROP under harsh conditions due to the low reactivity of monomers.

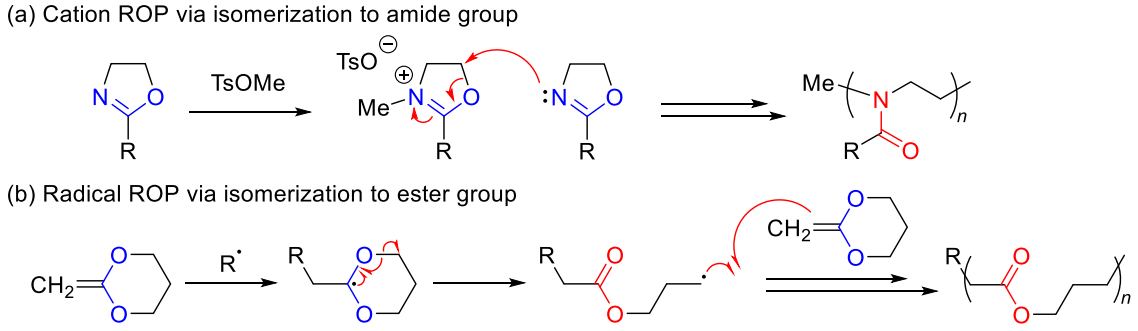


**Scheme 5-1.** Ring-opening polymerizations via isomerization to stable structures.

In the conclusion of Chapter 2, the author has pointed out that polymerization by $S_N2$' reaction has a potential to develop ROP accessible toward unprecedented polymers. In Chapter 2, the synthetic strategy was polycondensation by $S_N2$' and Michael addition. On the other hand, in this chapter, $S_N2$' reaction is applied as an elemental reaction of ROP (**Scheme 5-2**). Inspired from ROP driven by the conversion of functional groups

described in **Scheme 5-1**, $S_N2$' acceptor, *i.e.* α-(acyloxymethyl)acrylate moieties is allocated outside of the lactone ring sharing ester linkage each other. The $S_N2$' reaction at α-(acyloxymethyl)acrylate moiety induces the ring-opening of lactone with releasing carboxylate anion, which lead to further $S_N2$' reaction to another monomer. Then, unsaturated polyester is formed. Importantly, the unsaturated structure is converted from the *exo*-olefin to *endo*-olefin stable thermodynamically. Thus, the ROP is driven not only by the release of ring strain but also by the enthalpy gain through the rearrangement of double bond.

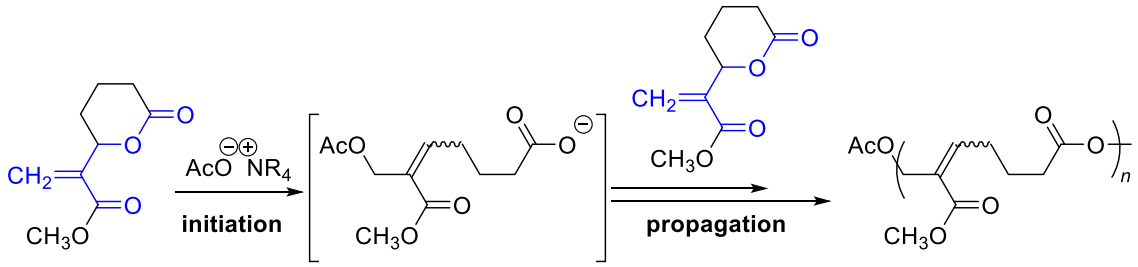


**Scheme 5-2.** Ring-opening polymerization induced by $S_N2$' reaction of side-group.

## 2. Results and Discussion

### 2.1 Monomer Synthesis

The cyclic monomer, methyl 2-(6-oxotetrahydro-2*H*-pyran-2-yl)acrylate (**5-5**), was synthesized through 4 steps from δ-valerolactone (**5-1**) according to the literature (**Scheme 5-3**).[3] Methyl 5-hydroxylentaoate (**5-2**) was prepared by transesterification between **5-1** and methanol. Then, the primary alcohol was oxidized with pyridinium chlorochromate (PCC) to yield methyl 5-oxopentanoate (**5-3**). Subsequently, Morita-Baylis-Hillman reaction with **5-3** and methyl acrylate was conducted to afford dimethyl 3-hydroxy-2-methyleneheptanedioate (**5-4**). Finally, the cyclization reaction was conducted to yield cyclic monomer **5-5**. Resulted **5-5** was purified by silica gel column chromatography, and the isolated product was characterized by $^1$H NMR spectrum (**Figure 5-1**).

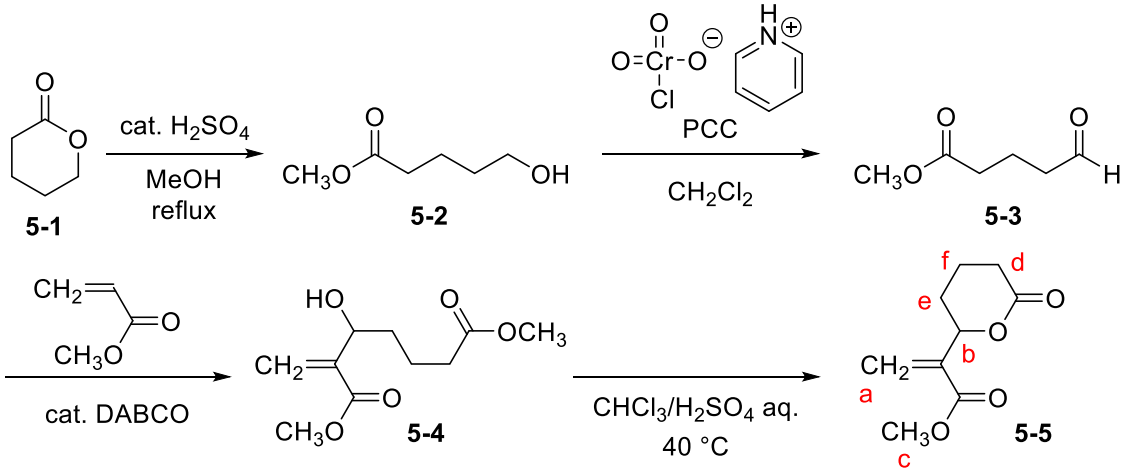


**Scheme 5-3.** Monomer synthesis via 4 steps from δ-valerolactone (**5-1**).

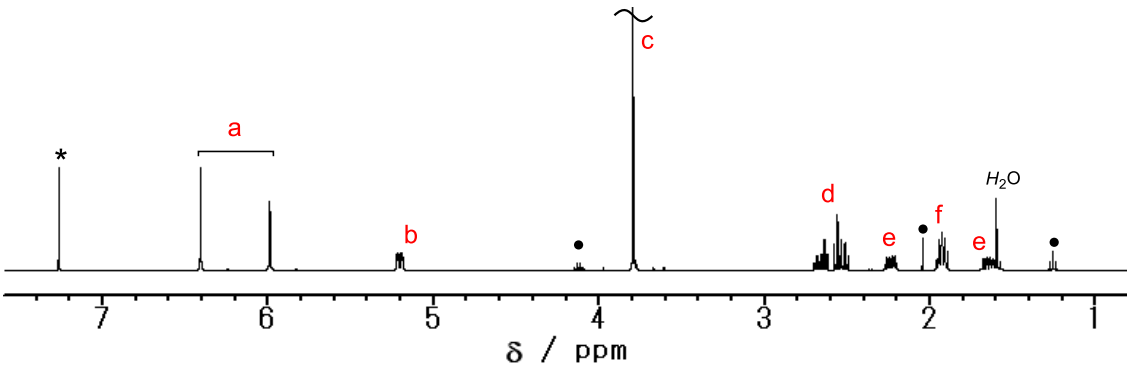


**Figure 5-1.** $^1$H NMR spectrum of **5-5**. (400 MHz, $CDCl_3$, 25 °C. *: $CHCl_3$, ●: EtOAc)

## 2.2 Optimization of Ring-opening Polymerization by $S_N2$' reaction

Conjugate substitution ($S_N2$') reaction can be carried out under the ambient conditions in common organic solvents. Therefore, ROP of **5-5** was expected to be applicable under air, whereas typical ROP of lactone is moisture-sensitive to require $N_2$ atmosphere or high-vacuum condition. Since no reports on ROP by conjugate substitution were available, the optimization of reaction conditions was attempted first; the characters of this polymerization, e.g. livingness, will be discussed later.

As a first attempt, ROP of **5-5** was initiated with tetrabutylammonium acetate at room temperature in bulk (**Table 5-1**, Entry 1). The initiator, an organic carboxylate salt, was selected as the expected active species in this ROP was a carboxylate anion. As discussed later, the terminal end of the propagating chain was a still living carboxylate anion. Then, ethyl α-(bromomethyl)acrylate (**5-7**), a terminator of anionic polymerization,[4] was added. The ROP for 48 h afforded a polymer ($M_{n,\,SEC}$ = 3100, $Đ$ =

**Table 5-1.** Ring-opening polymerization of **5-5** in bulk.

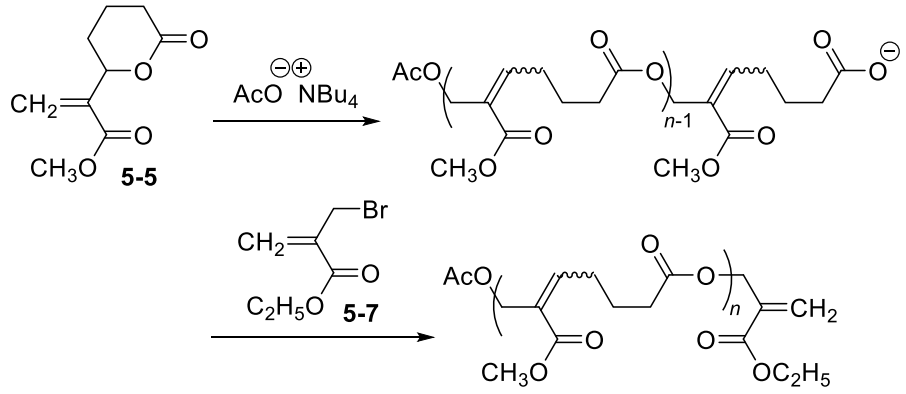


| Entry[a] | [**5-5**] /[I] | Additive | Temp. [°C] | Time [h] | Yield[b] [%] | Conv.[c] [%] | $M_{n,theo}$[d] | $M_{n,NMR}$[c] | $M_{n,SEC}$[e] | $Đ$[e] | $F$[f] (%) | $T$[g] (%) |
|---|---|---|---|---|---|---|---|---|---|---|---|---|
| 1 | 25 | – | 25 | 48 | 17 | 63 | 2020 | 5470 | 3100 | 1.18 | 37 | 31 |
| 2 | 25 | – | 50 | 24 | >99[h] | 71 | 2250 | 2280 | 1900[h] | 1.32[h] | 98 | 43 |
| 3 | 25 | – | 80 | 24 | >99[h] | 85 | 2640 | 4300 | 600[h] | 2.26[h] | 61 | 98 |
| 4 | 25 | $K_2CO_3$ | 25 | 24 | 46 | 95 | 2930 | 3550 | 2700 | 1.33 | 83 | >99 |
| 5 | 50 | $K_2CO_3$ | 25 | 48 | 75 | 85 | 5050 | 7670 | 3700 | 1.28 | 66 | 94 |
| 6[i] | 80 | $K_2CO_3$ | 25 | 120 | 63 | 72 | 6750 | 13100 | 3800 | 1.31 | 52 | – |
| 7 | 25 | DPP[j] | 25 | 24 | 0 | 0 | – | – | – | – | – | – |
| 8 | 25 | $Zn(CF_3SO_3)_2$ | 25 | 24 | 0 | 0 | – | – | – | – | – | – |

[a] $AcONBu_4$: $1.2 \times 10^{-2}$ mmol, additive: $6.0 \times 10^{-2}$ mmol, **5-7**: $1.8 \times 10^{-2}$ mmol. [b] Isolated yield. [c] Determined by $^1$H NMR spectrometry. [d] $M_{n,thero}$ = ([**5-5**]/[I] × conversion) × (unit molecular weight) + (molecular weights of end structures). [e] Determined by SEC (polystyrene standard, THF, 40 °C). [f] Initiator efficiency as a ratio of $M_{n,theory}/M_{n,NMR}$. [g] Termination efficiency. [h] Crude yield. [i] Without terminator. [j] Diphenyl phosphate.

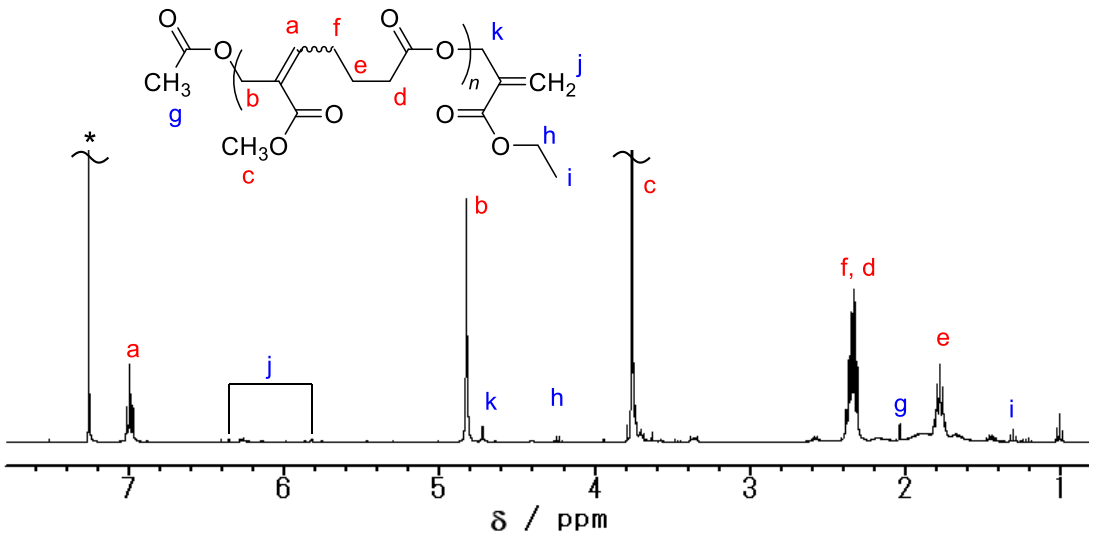


**Figure 5-2.** $^{1}$H NMR spectrum of the product (Entry 5) (400 MHz, 26 °C, $CDCl_3$) *: $CHCl_3$

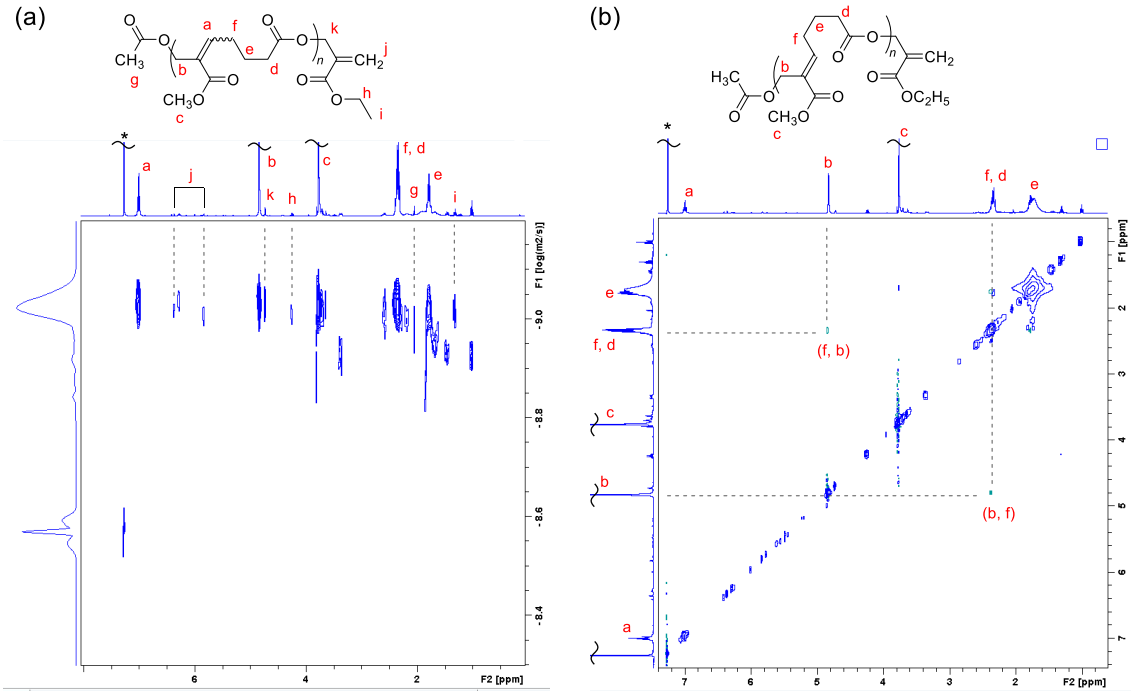


**Figure 5-3.** (a) DOSY spectrum of the product in the Entry 5, (b) NOESY spectrum of the product in the Entry 4. (400 MHz, 26°C, $CDCl_3$) *: $CHCl_3$

1.18). The $^{1}$H NMR spectrum of the product is shown in **Figure 5-2** (Note: for high-resolution, the spectrum for the product in Entry 5 is shown.). The signals a-f corresponding to the protons of the polymer backbone were clearly observed. This result suggested that the polymerization proceeded as expected. In addition, the DOSY and NOESY spectra were measured to characterize chain-ends and stereochemistry of the

repeating units (**Figure 5-3**). In the DOSY spectrum, signals g–j exhibited similar diffusion coefficients to the polymer backbone, suggesting that the expected chain-ends by the initiator and terminator (**Figure 5-3a**). The NOESY spectrum showed the correlations between the signals b and f, suggesting that majority of the resulted polymer units were composed of (*E*)-isomeric structure (**Figure 5-3b**).

The incomplete conversion in Entry 1 (63%) and low termination efficiency (10%) suggested low reactivity of the propagation chain-end. Thus, the ROP was conducted at 50 °C and 80 °C (Entries 2 and 3). In both cases, the conversions were increased to 71 and 85%, respectively. Nevertheless, the resulted $M_{n,SEC}$s were decreased, particularly in entry 3, probably due to the chain-transfer reaction by back-biting mechanism (**Scheme 5-4**). Thus, the ROP should be employed at 25 °C.

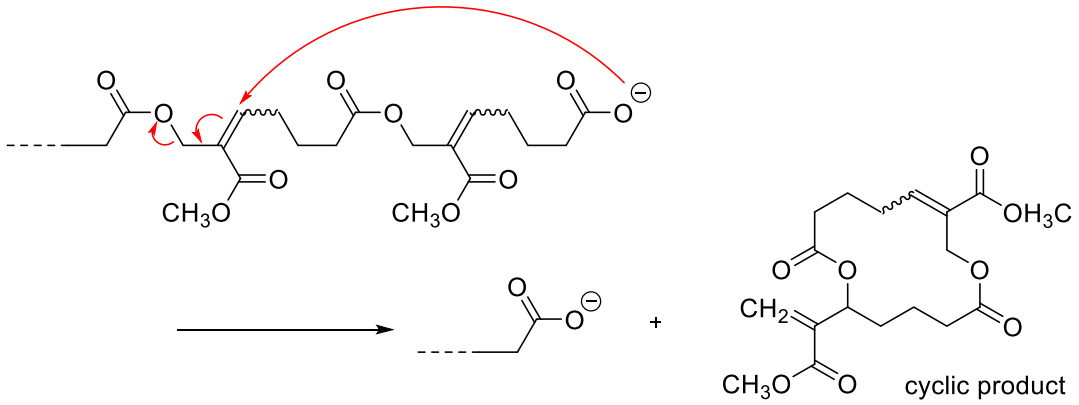


**Scheme 5-4.** Possible back-biting reaction.

In anionic polymerization, counter anion often affects the reactivity of propagating chain-end. For example, anionic polymerization of acrylates proceeds faster with alkali metal cation than that with ammonium cation.[5] Then, the ROP was conducted in the presence of excess $K_2CO_3$ in order to attempt counter cation exchange (Entry 4,5). The ROP resulted in increasing conversion up to 95% even at room temperature (Entry 4, $M_{n,SEC}$ = 2700, $Đ$ = 1.33). In addition, the incorporation of terminal end was achieved almost quantitatively ($T$ > 99%). Increasing feed ratios of the monomer to the initiator resulted in higher $M_n$ (Entry 5: $M_{n,SEC}$ = 3700, $Đ$ = 1.28, Entry 6: $M_{n,SEC}$ = 3800, $Đ$ = 1.31). As Lewis/Brønsted acids that actives the carbonyl bond of ester bond was expected to

catalyze the ROP, the polymerizations with diphenyl phosphate (DPP) and zinc trifluoromethanesulfonate [$Zn(CF_3SO_3)_2$] were conducted. However, they did not afford polymers (Entry 7, 8).

Next, ROP of **5-5** in solution was also investigated (Table 5-2). The polymerization in $CH_3CN$ resulted in the similar result to bulk conditions (Entry 9, $M_{n,\,SEC}$ = 2300, $Đ$ = 1.36). On the other hand, in *N,N*-dimethylformamide (DMF) and dimethyl sulfoxide (DMSO), the resulted in decreased $M_{n,SEC}$s (Entries 10 and 11). The complex $^1$H NMR spectra of the products in Entries 10 and 11 implied some side reactions such as hydrolysis of the lactone ring and back-biting reaction, although the details were not detected. In contrast, ROP in toluene proceeded without any problems (Entries 12 and 13).

**Table 5-2.** Ring-opening polymerization of **5-5** in solution in the presence of $K_2CO_3$.

| Entry[a] | Solvent | (mL) | Time [h] | Yield[b] [%] | Conv.[c] [%] | $M_{n,theory}$[d] | $M_{n,NMR}$[c] | $M_{n,SEC}$[e] | $Đ$[e] | $F$[f] |
|---|---|---|---|---|---|---|---|---|---|---|
| 9 | $CH_3CN$ | (0.1) | 24 | 47 | 72 | 6800 | 7480 | 2300 | 1.36 | 89 |
| 10 | DMF | (0.1) | 24 | 19 | n.d. | − | − | 1100 | 1.64 | − |
| 11 | DMSO | (0.1) | 24 | 36 | n.d. | − | − | 500 | 2.25 | − |
| 12 | Toluene | (0.1) | 24 | 75 | 72 | 6800 | 9060 | 3000 | 1.37 | 75 |
| 13 | Toluene | (0.3) | 48 | 78 | 90 | 8460 | 9560 | 3000 | 1.51 | 88 |

[a] [M]/[I] = 50, $AcONBu_4$: $1.2 \times 10^{-2}$ mmol, $K_2CO_3$: $6.0 \times 10^{-2}$ mmol, **5-7**: $1.8 \times 10^{-2}$ mmol. [b] Isolated yield. [c] Determined by $^1$H NMR spectrometry. [d] $M_{n,thero}$ = ([**5-5**]/[I] × conversion) × (unit molecular weight) + (molecular weights of end structures). [e] Determined by SEC (polystyrene standard, THF, 40 °C). [f] Initiator efficiency as a ratio of $M_{n,theory}/M_{n,NMR}$.

### 2.3 Livingness of the ROP by Conjugate Substitution

To investigate the livingness of ROP of **5-5**, the plots of time vs. monomer conversion (**Figure 5-4a**) and conversions vs. $M_n$ (**Figure 5-4b**) were observed. The ROPs of **5-5** were conducted in the presence of $K_2CO_3$ at room temperature in bulk and toluene solution. The conversion under bulk condition slowed down and saturated 80% at 48 h (**Figure 5-4a**, red square), while the ROP in toluene reached 90% after 48 h (**Figure 5-4a**, blue circle). Although the initial rate of polymerization in bulk was faster than that in toluene, the increased high viscosity in late stage would lead to slow propagation. In both cases, linear relationship between monomer conversions and $M_{n,SEC}$s

were observed, suggesting living polymerization. Generally speaking, living ROPs of lactones are moisture-sensitive and must be conducted under $N_2$ or argon atmosphere. Therefore, it was remarkable that the current ROP that kept livingness even in an 'open' system to air.

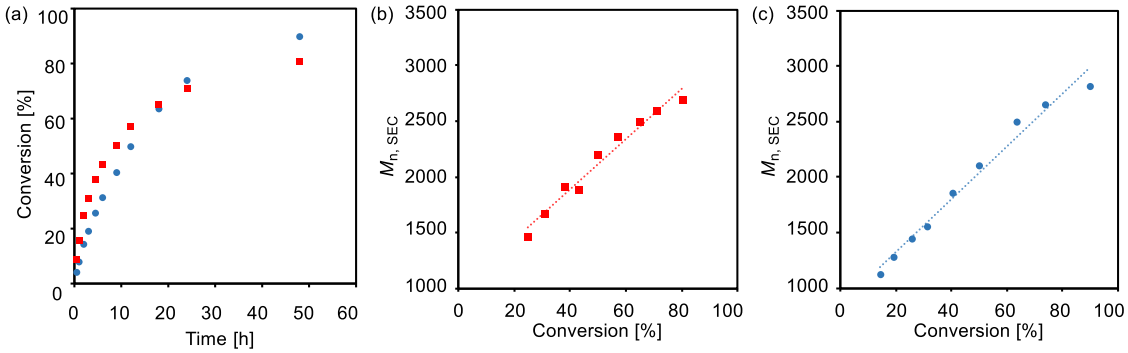


**Figure 5-4.** (a) Plot of monomer conversion vs time ([M]/[I] = 50, red square: in bulk, blue circle: in toluene), (b) Plot of $M_{n, SEC}$ vs monomer conversion in bulk, (c) Plot of $M_{n, SEC}$ vs monomer conversion in toluene.

## 2.4 Immortality of the ROPs

As aforementioned, typical living ROPs are moisture-sensitive to be terminated by water in air. The exception is immortal polymerization, defined as polymerization that keep active species even after isolation of resulting polymer.[6] In the current case, *i.e.* the ROP of **5-5** without adding terminator kept the carboxylate chain ends. Therefore, the re-initiation of polymerization seems possible by adding a monomer to the isolated polymer again (**Scheme 5-5**). $K_2CO_3$ and **5-5** were added to the non-terminated polymer ($M_{n,SEC}$ = 3800, $Đ$ = 1.36, $M_p$ = 5400) which obtained in Entry 3, and the polymerization was re-initiated. After 24 hours and 48 hours, small portion of reaction mixtures were sampled to monitor the growths of molecular weights. The SEC curve after 24 hours (**Figure 5-5**) exhibited the shifted $M_p$ to the high molecular weight region with keeping unimodal peak ($M_{n,SEC}$ = 4300, $Đ$ = 1.42, $M_p$ = 6300), indicating that the terminal structure remained active. In other words, ROP of **5-5** is immortal polymerization. After 48 hours, $M_p$ did not significantly increased; the time vs. conversion plots in **Figure 5-4a** suggests the almost consumption of monomers after 24 h, and thus the increase of molecular weight was small in this stage.

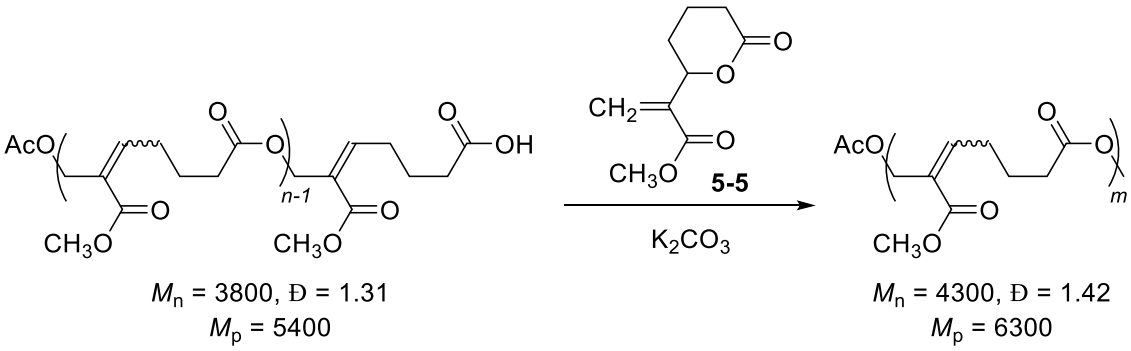


**Scheme 5-5**. Re-initiation of ROP from the purified polymer.

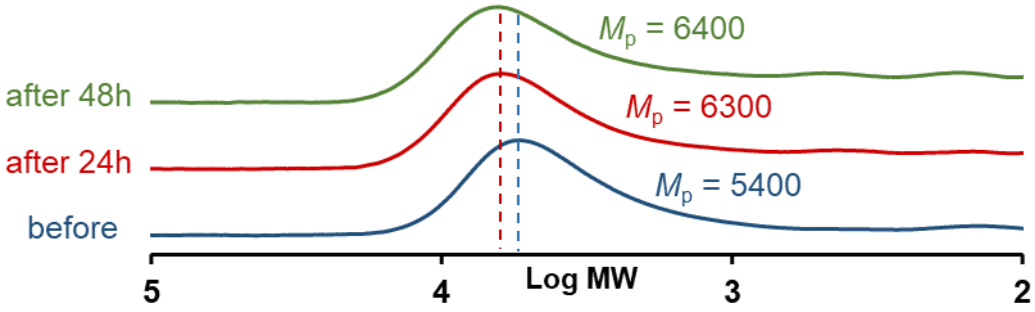


**Figure 5-5.** SEC curves of before and after re-initiation of ROP.

## 3. Conclusion

Conjugate substitution reaction was effective as an elemental reaction of ROP of lactones. The ROPs were living and immortal polymerization even under ambient condition; this is a sharp contrast to conventional ROPs operatable only under inactive gas atmosphere.

From a viewpoint of classical ROP, similar polyester can be prepared from **5-8** (**Scheme 5-6**). However, in addition to the difficulty of the synthesis of **5-8**, the ROP seems not easy due to the unsaturated eight-membered ring with low ring-strain. Therefore, the ROP of **5-5** is more effective to access the unsaturated polyester. In other words, the eight-membered ring of **5-8** can be resolved to six-membered ring and two vinylidene atoms (8 = 6 + 2). Since the ROP is driven by the conversion of *exo*-olefin to *endo*-olefin, the contribution of ring-strain is not so far. Therefore, similar strategy can be operated to other types of lactones, particularly macrolactones that cannot polymerize due to the small ring-strains.

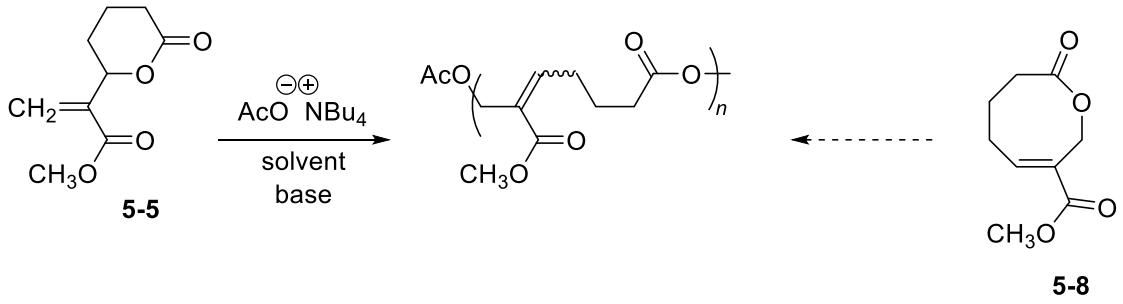


**Scheme 5-6.** Comparison of the current and conventional ROPs.

## 4. Experimental section

***Instruments.***

$^{1}H$ and $^{13}C$ NMR spectra were recorded in $CDCl_3$ (Kanto Chemical) on AVANCE NEO (Bruker) spectrometer. Chemical shifts in $^{1}H$ and $^{13}C$ NMR spectra were referred to the signal of tetramethylsilane (TMS) and solvent ($CDCl_3$), respectively. Molecular weight and its distributions were determined at 40 °C by size-exclusion chromatography (SEC) on an EXTREMA chromatograph (JASCO) equipped with two SEC columns [Shodex HK-404L], using tetrahydrofuran (THF, Wako Pure Chemical Industries, for HPLC grade, flow rate = 0.6 mL $min^{-1}$), and calibrated against standard polystyrene (PS) samples (TSK-gel oligomer kit, Tosoh, $M_n$: $1.03 \times 10^6$, $3.89 \times 10^5$, $1.82 \times 10^5$, $3.68 \times 10^4$, $1.36 \times 10^4$, $5.32 \times 10^3$, $3.03 \times 10^3$, $8.73 \times 10^2$) and detected with UV (UV-4070, JASCO) and RI (RI-4035, JASCO) detectors.

***Materials***

Methyl methacrylate, δ-varelolactone, 1,4-diazabicyclo[2.2.2]octane (DABCO), deuterochloroform ($CDCl_3$), tetrabutylammonium acetate were purchased from Tokyo Chemical Industry Co., Ltd. Sulfonic acid ($H_2SO_4$ aq.), potassium carbonate ($K_2CO_3$) sodium sulfate ($Na_2SO_4$), hexane, ethyl acetate (EtOAc), chloroform ($CHCl_3$), dichloromethane ($CH_2Cl_2$), tetrahydrofuran (THF), acetonitrile ($CH_3CN$), toluene, *N,N*-dimethylformamide (DMF), methanol (MeOH), hydrochromic acid (HCl aq.), zinc trifluoromethanesulfonate [$Zn(CF_3SO_3)_2$], celite were purchased from Wako Pure Chemical Industries, Ltd. Pyridinium chlorochromate (PCC), diphenyl phosphate (DPP) were purchased from Sigma-Aldrich Co. LLC.

***Synthesis***

**Methyl 5-hydroxypentanoate (5-2):**[5a-c] Conc. $H_2SO_4$ aq. (1.8 mL) was added dropwise to the solution of δ-valerolactone (**5-1**) (30.4 g, 303 mmol) in methanol (600 mL). The mixture was refluxed for 20 h. After cooling to room temperature, $Na_2CO_3$ (8.88 g, 83.8 mmol) was added and stirred for 20 min. Then, $H_2O$ (400 mL) was added to the mixture, and the mixture was extracted with EtOAc (300 mL). The aqueous layer was extracted with EtOAc (100 mL × 4). The organic layers were combined and washed with $H_2O$ (100

mL × 2) and brine (100 mL). The combined organic layer was dried over $Na_2SO_4$ and concentrated to yield crude **5-2** (31.3 g, yield: 78.9 %). The crude **5-2** was used in the next reaction without further purification. $^1$H NMR spectrum (400 MHz, $CDCl_3$, 25 °C): δ/ppm 3.68 (3H, s, $OCH_3$), 3.654 (2H, m, $\underline{CH_2}OH$) 2.37 (2H, t, *J* = 7.12 Hz, $COCH_2$), 1.78-1.69 (2H, m, $\underline{CH_2}CH_2CH_2OH$), 1.64-1.57 (2H, m, $CH_2\underline{CH_2}CH_2OH$), 1.49 (1H, t, *J* = 5.12 Hz, $CH_2\underline{OH}$).

**Methyl 5-oxopentanoate (5-3):**[5d-e] Celite (30 g) was added to the solution of pyridinium chlorochromate (31.9 g, 148 mmol) in $CH_2Cl_2$ (300 mL). The solution of **5-2** (16.3 g, 123 mmol) in $CH_2Cl_2$ (100 mL) was added to the mixture at room temperature for 2.5 h. The reaction mixture was filtered through pad of silica gel and washed with $Et_2O$. The filtration was concentrated to yield crude **5-3** (15.5 g, yield: 96.8%). The crude **5-3** was used in the next reaction without further purification. $^1$H NMR spectrum (400 MHz, $CDCl_3$, 25 °C): δ/ppm 9.98 (1H, t, *J* = 1.26 Hz, CHO), 3.68 (3H, s, $OCH_3$), 2.54 (2H, dt, $J_1$ = 7.23 Hz, $J_2$ = 1.26 Hz, $\underline{CH_2}CHO$), 2.38 (2H, t, *J* = 7.23, $CO\underline{CH_2}$), 1.96 (2H, quin, *J* = 7.23 Hz, $\underline{CH_2}CH_2CHO$).

**Dimethyl 3-hydroxy-2-methyleneheptanedioate (5-4):** Methyl acrylate (20.59 g, 239 mmol) and DABCO (2.67 g, 23.8 mmol) was added to **5-3** (15.15 g, 116 mmol). The mixture was stirred for 5 days. Then, $CH_2Cl_2$ (150 mL) were added to the mixture. The solution was washed with 0.25 M HCl aq. (100 mL). The aqueous layer was extracted with $CH_2Cl_2$ (20 mL × 2). The organic layers were combined and washed with 0.25 M HCl aq. (100 mL) and brine (150 mL). The combined organic layer was dried over $Na_2SO_4$ and concentrated to yield crude **5-4** (20.26 g, yield: 80.8%). $^1$H NMR spectrum (400 MHz, $CDCl_3$, 25 °C): δ/ppm 6.25 (1H, s, $CH_2$=), 5.83 (1H, t, *J* = 1.04 Hz, $CH_2$=), 4.41 (1H, t, *J* = 6.80 Hz, $\underline{CH}OH$), 3.78 (3H, s, $OCH_3$), 3.67 (3H, s, $CH_2COO\underline{CH_3}$), 2.37 (2H, m,$\underline{CH_2}COOCH_3$), 2.00-1.59 (4H, m, $CH\underline{CH_2CH_2}$).

**Methyl 2-(6-oxotetrahydro-2*H*-pyran-2-yl)acrylate (5-5):** 0.1 M $H_2SO_4$ aq. (600 mL) was added to the solution of **5-4** (20.26 g, 93.7 mmol) in $CHCl_3$ (600 mL). The mixture was stirred at 40 °C for 2 weeks. Then, the organic and aqueous layers were separated and the aqueous layer was washed with $CHCl_3$ (50 mL × 2). The organic layers were combined and washed with brine (150 mL). The combined organic layer was dried over

$Na_2SO_4$ and concentrated to yield crude **5-5** (19.06 g). The crude **5-5** was purified by silica gel column chromatography using Wakogel C-400HG (Wako pure Chemical Industry, 400g) and co-solvent hexane–EtOAc (v/v = 3/2) to afford **5-5** (3.66 g, yield: 21.2 %, $R_f$ = 0.28). $^1$H NMR spectrum (400 MHz, $CDCl_3$, 25 °C): δ/ppm 6.41 (1H, t, $J$ = 0.73 Hz, $CH_2$=), 5.99 (1H, q, $J$ = 0.73 Hz, $CH_2$=), 5.21 (2H, dd, $J_1$ = 9.96 Hz, $J_2$ = 3.44 Hz, CH), 3.80 (3H, s, $OCH_3$), 2.62-2.70 (1H, m, $\underline{CH_2}CO$), 2.50-2.58 (1H, m, $\underline{CH_2}CO$), 2.27-2.20 (1H, m, $CH\underline{CH_2}$), 1.96-1.90 (2H, m, $\underline{CH_2}CH_2CO$), 1.68-1.58 (1H, m, $CH\underline{CH_2}$).

**Ring-opening polymerization of 5-5:** Typical procedure is shown. The 0.5 M solution of tetrabutylammonium acetate (20 μL, 0.010 mmol) was added to the **5-5** (55.3 mg, 0.300 mmol). The mixture was stirred for 24 h, and the solution of ethyl α-(bromomethyl) acrylate (2.5 μL, 0.018 mmol). After 30 min, the mixture was concentrated and reprecipitated to $Et_2O$ (20.0 mL). The precipitate was collected by centrifugation and dried in vacuo to afford the polymer (9.6 mg, 16.6 %).

**Reinitiation of ring-opening polymerization:** $K_2CO_3$ (3.2 mg, 0.02 mmol) and **5-5** (42.2 mg, 0.229 mmol) were added to the non-terminated polymer (22.4 mg, $M_{n,SEC}$ = 3800, $Đ$ = 1.36, $M_p$ = 5400) which obtained in Entry 3, and the polymerization was re-initiated. After 24 hours and 48 hours, small portion of reaction mixtures were sampled to monitor the growths of molecular weights. (after 24 h: $M_{n,SEC}$ = 4300, $Đ$ = 1.42, $M_p$ = 6300, after 48 h: $M_{n,SEC}$ = 4200, $Đ$ = 1.42, $M_p$ = 6400)

**References**

(1) O. Nuyken, S. D. Pask, *Polymers*, **2013**, 5, 361.

(2) (a) T. Saegusa, Y. Chujo, *Makromol. Chem. Macromol. Symp*., **1991**, 51, 1. (b) S. Kobayashi, H. Uyama, H. Shirasaka, *Makromol. Chem., Rapid. Commun.*, **1990**, 11, 11. (c) M. Miyamoto, H. Amii, K. Aoi, T. Saegusa, *Macromolecules*, **1993**, 26, 1474. (d) E. R. Lavagnino, R. R. Chauvette, W. N. Cannon, E. C. Kornfield, *J. Am. Chem. Soc.*, **1960**, 82, 2609. (e) W. J. Bailey, Z. Ni, S.-R. Wu, *J. Polym. Chem. Chem. Ed.*, **1982**, 20, 3021. (f) W. J. Bailey, S.-R. Wu, Z. Ni, *Makromol, Chem,*, **1982**, 183, 1913. (g) I. Cho, M. S. Gong, *J. Polym. Sci., Polym. Lett. Ed.*, **1982**, 20, 361. (h) T. Schulze, E. Klemm, *Angew. Makromol. Chem.*, **1995**, 229, 123. (i) W. J. Bailey, Z. Ni, S.-R. Wu, *Macromolecules*, **1982**, 15, 711. (j) J.-Y. Yuan, C.-Y. Pan, B. Z. Tang, *Macromolecules*, **2001**, 34, 211. (k) T. Endo, N. Yoko, K. Azuma, K. Nate, *Makromol. Chem.*, **1985**, 186, 1543. (l) P. Feng, *Chin. J. Polym. Sci.*, **1993**, 11, 153. (m) W. J. Bailey, P.-Z. Feng, *Polym. Prepr.*, **1987**, 28, 154. (n) I. S. Chung, K. Matyjaszewski, *Macromolecules*, **2003**, 36, 2995. (o) R. A. Evans, G. Moad, E. Rizzardo, S. H. Thang, *Macromolecules*, **1994**, 27, 7935.

(3) (a) K. Lehr, R. Mariz, L. Leseurre, B. Gabor, A. Fürstner, *Angew. Chem. Int. Ed.*, **2011**, 50, 11373. (b) A. Díaz-Rodríguez, W. Borzęck, I, Lavandera, V. Gotor, *ACS Catal.*, **2014**, 4, 386. (c) X.-H. Yang, K. Wang, S.-F. Zhu, J.-H. Xie, Q.-L. Zhou, *J. Am. Chem. Soc.*, **2014**, 136, 17426. (d) V. Hickmann, A. Kondoh, B. Gabor, M. Alcarazo, A. Fürstner, *J. Am. Chem. Soc.*, **2011**, 133, 13471. (e) A. Matsumoto, S. Lee, H. Okamura, *J. Polym. Chem. Sci., Part A: Polym. Chem.*, **2015**, 53, 1000.

(4) Y. Kohsaka, T. Kurata, K. Yamamoto, S. Ishihara, T. Kitayama, *Polym. Chem.*, **2015**, 6, 1078.

(5) Y. Kataoka, Y. Kohsaka, T. Kitaura, S. Domae, S. Ishihara, T. Kitayama, Polym. Chem. **2017**, 8, 3858–3861.

(6) T. Aida, Y. Maekawa, S. Asano, S. Inoue, *Macromolecules*, **1988**, 21, 5, 1195–1202.

*Chapter 6*

# Conclusion

This chapter will summarize the results obtained in each chapter and describes future prospects.

In Chapter 1, the background of this thesis, *i.e.* elemental reactions in step-growth polymerization and conjugate substitution reaction, were presented in order to introduce the concept and purpose of this research. The demands for the design of monomers and elemental reactions were described from the viewpoint of classical Flory-Carothers theory. Hence, the author mentioned that the classical chemistry in step-growth polymerization have not covered the polymerization style from a single monomer (pair) to a variety of resulting polymers, which is common in nature.

Recently, new polymerization design has been proposed such as polycondensation by multi-component reactions. These achievements clearly suggested that the keys for the frontier of polymerization chemistry are monomer designs. α-(Substituted methyl)acrylates is attractive for this purpose, as it undergo nucleophilic conjugate substitution ($S_N2'$) reaction in a quantitative yield under ambient condition, which has a potential to afford a library of substitution products by tuning substituents of an acrylate skeleton and a base catalyst. Moreover, the substitution products can be applied to further reaction such as Michael addition. Thus, in this thesis, monomer design leading to $S_N2'$ reaction was studied.

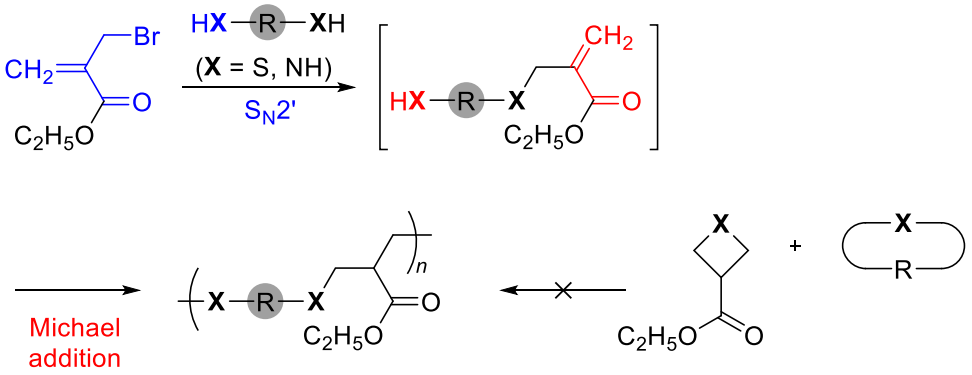


**Scheme 6-1.** Tandem polymerization based on $S_N2'$ and Michael addition reactions described in Chapter 2.

In Chapter 2, the author aimed a novel polycondensation, consisting of $S_N2'$ reaction

of α-(bromomethyl)acrylates with dithiols/diamines and subsequential Michael addition reaction (**Scheme 6-1**). Since both reactions have robustness, the polycondensation was expected to be operated under any conditions. However, contrary to the expectation, the optimization of reaction conditions was required to achieve a high degree of polymerization; the byproducts, hydrobromide and its salt in the $S_N2$' reaction, prevented the second step of the polymerization, *i.e.* Michael addition. Nevertheless, the polycondensations of mono-electrophile (acryloyl group) and di-nucleophiles were successful after the optimization. The polymerization afforded poly(thioether)s with high density of sulfur atoms in the backbone; this reaction design thus would contribute to reduce carbon atoms in polymer engineering. Moreover, the resulting structure in this polymerization can be regarded as the alternating copolymer of two heterocycles that cannot undergo alternating ring-opening copolymerization. Then, the polymerization is also attractive to access such untouched polymers.

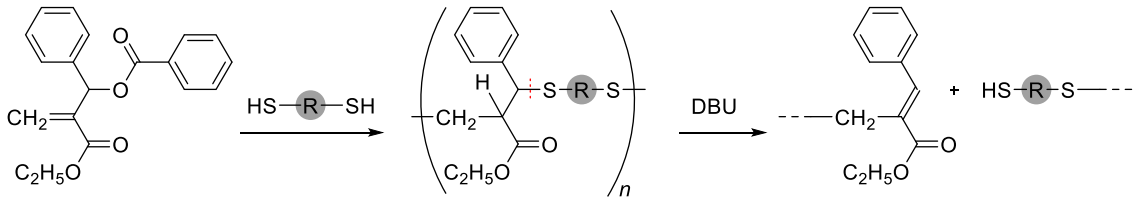


**Scheme 6-2.** Polycondensation affording poly(thioether)s that undergo irreversible main chain scission by $E_1$cB reaction.

In Chapter 3, the polycondensation described in chapter 2 was improved to afford poly(thioether)s that irreversibly decomposed (**Scheme 6-2**). The resulting polymer in Chapter 2 was degradable by retro-Michael addition (E1cB reaction), but the reaction was reversible; thus, deactivation of the decomposed chain-ends of acrylates was required by end-capping with excess monothiol. In this chapter, a substituent was newly introduced to the allylic position of α-(bromomethyl)acrylate; the existence of substituent afforded poly(thioether)s composed of asymmetric repeating units degradable to more stable *endo*-olefins by E1cB reaction, leading to irreversible main chain scission by E1cB reaction.

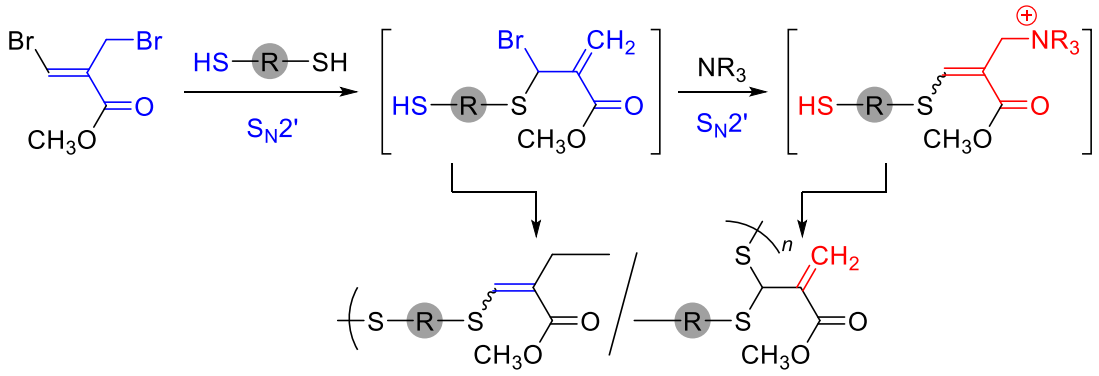

**Scheme 6-3.** Tandem polymerization based on sequential $S_N2$' reactions.

In Chapter 4, the author aimed the tandem polycondensation which constituted on only sequential $S_N2$' reactions onto β-bromo-α-(bromomethyl)acrylates (**Scheme 6-3**). The results in Chapter 2 implied that the combination of two reactions with different characters was not efficient to achieve high degree of polymerization, even if each reaction has high efficiency. Therefore, similar polymerization but composed of only $S_N2$' reaction was designed. That is to say, the polycondensation of β-bromo-α-(bromomethyl)acrylate and dithiols was examined. A low nucleophilic bases such as $K_2CO_3$ resulted in high content of *endo*-olefin, while bases with strong nucleophilicity, e.g. DBU, yielded *exo*-olefin units in an almost complete selectivity. In addition, the isomeric structure in *endo*-olefin units was influenced by the alkali metal cation through the template effect. Notably, the controls of microstructure were allowed tuning of thermal properties of the resulting polymers. In this chapter, the author proposed the novel concept on polymer chemistry that a diversity of polymer structures in step-growth polymerization from a single pair of monomers.

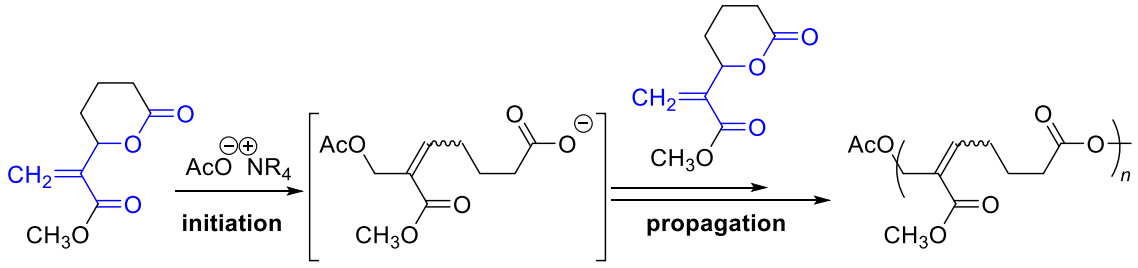

**Scheme 6-4.** Ring-opening polymerization induced by $S_N2$' reaction of side-group.

In Chapter 5, the $S_N2$' reaction of α-(substituted methyl)acylates, was applied to ring-

opening polymerizations (ROPs) of lactones based on a novel mechanism induced from the outside of the rings (**Scheme 6-4**). Generally speaking, ROPs of lactones are based on transesterification with hydroxy-chain end. Thus, the ROP requires a catalyst to activate the ester bond and, for classical metal catalyst, high temperature over 250 °C under vacuum. The current polymerization was based on $S_N2'$ reaction so that the reaction did not require catalysts and harsh condition. The ROP was achieved only with an initiator of carboxylate salts under ambient condition. Notably, the ROP was living polymerization. More importantly, it could be re-initiated after the isolation of resulting polymer, suggesting immortal polymerization.

In conclusion, the author has presented the diverse polymerization designs utilizing $S_N2'$ reaction. The $S_N2'$ reaction have potentials to access various reaction designs with robustness, leading to the developments of the novel polymerization systems involved not only polycondensations but also ROPs. In addition, the resulting polymers had the significance on synthetic strategy to provide polymers inaccessible by classical polymerizations. That is to say, these achievements presented a potential to break limitation of synthetic polymers. Therefore, the author believe that this study gives an opportunity to review the conventional polymerization chemistry in drastic and to break limitation of the polymer chemistry.

## Acknowledgements

This thesis presents the research that the author carried out from 2015 to 2021 at the Department of Science and Technology, Graduate School of Medicine, Science and Technology, Shinshu University under the Associate Professor Yasuhiro Kohsaka.

First of all, the author would like to express his sincere gratitude to Associate Professor Yasuhiro Kohsaka for his continuous guidance, support and encouragement through this work.

The author also acknowledges his appreciation to Professor Masahiro Suzuki (Shinshu University), Associate Professor Tetsuya Fujimoto (Shinshu University), Professor Masami Kamigaito (Nagoya University) and Associate Professor Yasuhito Koyama (Toyama Prefectural University) for careful reviews of this thesis and valuable comments.

Ethyl α-(bromomethyl)acrylate *in Chapter 2* was a kind gift from Chemicrea Inc. The research in *Chapter 4* was financially supported by the Sasasgawa Scientific Research Grant from The Japan Science Society (2018-3022). The DSC measurements in *Chapter 4* were supported by Professor Toshikazu Takata (Tokyo Tech, Hiroshima University). The author would like to express his appreciation to all those who cooperated in carrying out the research.

Finally, the author would like to express his deep appreciation to his parents for their constant care and encouragement.

*March 2021,*

*Keito Hagiwara*

*Department of Science and Technology*
*Graduate School of Medicine, Science and Technology*
*Shinshu University*